

Abstract

Applications for the new generations of Global Navigation Satellite Systems (GNSS) are developing rapidly and attract a great interest. Both US Global Positioning System (GPS) and European Galileo signals use Direct Sequence-Code Division Multiple Access (DS-CDMA) technology, where code and frequency synchronization are important stages at the receiver. The GNSS receivers estimate jointly the code phase and the Doppler spread through a two-dimensional searching process in time-frequency plane. Since both GPS and Galileo systems will send several signals on the same carriers, a new modulation type - the Binary Offset Carrier (BOC) modulation, has been selected. The main target of this modulation is to provide a better spectral separation with the existing BPSK-modulated GPS signals, while allowing optimal usage of the available bandwidth for different GNSS signals. The BOC modulation family includes several BOC variants, such as sine BOC (SinBOC), cosine BOC (CosBOC), alternate BOC (AltBOC), multiplexed BOC (MBOC), double BOC (DBOC) etc. The BOC-modulation triggers new challenges in the acquisition and tracking processes, since the receiver can acquire and lock incorrectly on a side-lobe peak around the maximum peak of the correlation envelope. Reliable receiver positioning requires accurate estimation of Line-of-Sight (LOS) propagation delays from different satellites to the receiver. The propagation over wireless channel suffers adverse effects, such as the environmental effects, the presence of multipath propagation, high level of noise, partial or full or obstruction of LOS component, especially in indoor environments. The synchronization process becomes even more challenging in such conditions.

The research results presented in this thesis focus on acquisition and tracking algorithms for Galileo and modernized GPS signals, analyzed in the context of BOC modulations, for various static and fading multipath profiles. Also, the effect of bandwidth limitation at various stages of the receiver was considered.

First, the performance at signal acquisition stage was analyzed, by considering the impact of different receiver constraints and acquisition parameters. A comprehensive analysis of the choice of detection and false alarm probabilities at each stage of a double-dwell structure, for a realistic Galileo signal was performed, and the conditions under which a double-dwell structure is better than a single-dwell structure were discussed. The design of bandwidth-limiting receiver filters and the effect of the transition band, in the context of signal acquisition, were studied. It was shown that the performance (in terms of root mean square error) can be improved by using an asymmetric transition band between the passband and stopband frequencies. Also the effects of over-sampling on BOC-modulated pseudo-random codes during the code acquisition process were analyzed and it was proven that sufficient performance can be achieved if the code-Doppler bin

size is designed properly.

The next results presented in this thesis concentrate on eliminating the BOC-generated ambiguities by removing the effect of sub-carrier modulation using one or a pair of single-sideband correlators. These techniques have the advantage that they allow the use of a higher step of searching the timing hypotheses compared with the ambiguous situation. Compared to other existing similar approaches, the three methods proposed in this thesis provide a less complex implementation and they can be generalized to every even and odd BOC modulation order. Also, the complexity of different unambiguous BOC processing methods was studied, taking into account both correlation and sideband selection in the receiver, when different filtering structures are considered.

Another part of this work focus on the tracking stage, where a new unambiguous approach, the Sidelobes Cancellation Method (SCM) was introduced. In order to remove or diminish the side-peaks threat, the SCM technique can be applied alone or in conjunction with other various tracking structures. This technique removes the threat brought by the side-peak ambiguities, while keeping the same sharp correlation of the main peak and, thus, it allows for better tracking performance. Moreover, if the search step of time uncertainty is kept sufficiently small, the SCM approach was also proved to be beneficial at acquisition stage. In contrast to other methods already introduced in literature for the same purpose, the SCM has the advantage that it can be used with any BOC-modulated signal. In order to cope with the side-peak ambiguities, a separate correlation function is computed and stored in the receiver and the delay estimation is done according to this stored correlation function.

The last part of this thesis includes a collection of nine original publications that contain the main results of the author's research work. New algorithms and architectures for the code acquisition and tracking in static and multipath fading channels were introduced and their performance was studied under various scenarios.

Acknowledgements

The work presented in this thesis has been carried out at the Department of Communications Engineering from Tampere University of Technology, Finland, as part of the wider research projects "Advanced Techniques for Mobile Positioning" (MOT), "Advanced Techniques for Personal Navigation" (ATENA) and "Future GNSS Applications and Techniques" (FUGAT).

First and foremost, my sincere gratitude goes to my supervisor, DrTech Doc. Elena Simona Lohan, for her constant encouragement, fruitful discussions and invaluable guidance throughout my research years. I am also grateful to Prof. Markku Renfors for giving me the opportunity to work on a stimulating research topic and for his support and patience during the course of this work.

I would like to thank Prof. David Akopian and Prof. A. Dempster for their time and effort spent in reviewing this thesis and for the constructive comments. Distinguished thanks are due to Prof. Olivier Julien for agreeing to act as the opponent in the public defense of the dissertation.

I express my appreciation to all my colleagues at Department of Communications Engineering for creating such a pleasant and friendly working atmosphere. I would like to say a special word of thanks to my work roommates DrTech Toni Huovinen, Elina Laitinen and to my colleagues Vesa Lehtinen, DrTech Abdelmonaem Lakhzouri, Mohammad Zahidul Hasan Bhuiyan, Md. Farzan Samad, Antonia Kalaitzi, Hu Xuan and Danai Skournetou. I am also very grateful to Zahid and Farzan for helping with the language revision of the manuscript. Warm thanks are also due to Prof. Jarmo Takala, Tobias Hidalgo Stitz, Tero Ihalainen, Tero Isotalo and DrTech Mikko Valkama.

For over two years, I have had the privilege to work at Atheros Technology Finland (former u-NAV Microelectronics), as part of a very competitive professional team. I would like to express my deepest gratitude to Juha Röström, manager of Atheros Technology Finland, to Ilkka Saastamoinen, to Peter Benschop and to all my colleagues from Atheros.

Warm thanks go to Ulla Siltaloppi, Tarja Erälaukko, Sari Kinnari, Elina Orava, Marianna Jokila, Saara Kallio and Leena Lintusaari for their always kind help with practical matters, friendly support and kind advices.

I wish to thank to the whole Romanian community in Tampere for the enjoyable moments spent together in our gatherings and parties. My gratitude also goes to my mother Sita, my brother Dan, my sisters-in-law Cornelia and Eliza, my nephew Bogdan, my niece and goddaughter Sofie and my father-in-law Vasile for their support and for being near to me, despite the physical distance that has separated us most of the time during these years. I am profoundly indebted to my mother-in-law Maria, who is such a great grandmother and who greatly helped me during some critical periods of my life. Special thanks go to my husband Adrian.

I thank also to my beloved children Vlad and Alex, for all the joy they bring in my life and for reminding me what life is truly about. Last but not least, I would like to thank to my father, who during his life taught me the value of education and showed me the worth of knowledge. I dedicate this work to him.

Tampere, July 2009

Contents

List of publications	vii
List of abbreviations and symbols	ix
List of figures	xiv
List of tables	xvi
1 Introduction	1
1.1 Background and motivation	2
1.2 Scope and contribution of the thesis	6
1.3 Outline of the thesis	9
2 Overview of Global Navigation Satellite Systems	10
2.1 Satellite-based positioning technology	10
2.2 Global and Local Navigation Satellite Systems	11
2.3 Global Positioning System	13
2.4 European Galileo System	14
2.4.1 Galileo Services	16
2.4.2 Galileo Spectrum Allocation	17
3 Modulation families and signal model for Galileo and modernized GPS signals	19
3.1 Binary Offset Carrier (BOC) modulated signal	19
3.2 Baseband signal model in multipath-fading channels	24
4 Acquisition of Galileo and GPS signals	32
4.1 Signal searching stage	32
4.2 Serial search versus hybrid or parallel search	34
4.3 Classical acquisition model	36
4.4 Signal detection	37
4.5 Differential correlation methods	41
4.6 Unambiguous acquisition of BOC-modulated signals	42

4.6.1	'Sideband correlation' or 'BPSK-like' techniques	43
4.6.2	Filter Bank-Based approaches	47
5	Tracking of Galileo and GPS signals	52
5.1	DLL-based methods	53
5.2	Enhanced feedback tracking algorithms	55
5.3	Feedforward-based methods	60
5.4	State-of-art unambiguous tracking algorithms	61
5.5	Sidelobes Cancelation Method	63
6	Filter design consideration in context of BOC-modulated signals	66
6.1	Bandlimiting constraints in GNSS	66
6.1.1	IIR versus FIR filters	69
6.1.2	Effect of the transition band	71
6.2	Filtering in the context of unambiguous acquisition approaches . .	72
7	Summary of publications	76
7.1	Overview of the publication results	76
7.2	Author's contribution to the publications	78
8	Conclusions	81
	APPENDIX	85
	Bibliography	87

List of Publications

- [P1] A. Burian, E.S. Lohan, and M. Renfors. Oversampling Limits for Binary Offset Carrier Modulation for the Acquisition of Galileo Signals. In *Proc. of Nordic Radio Symposium and Finnish Wireless Communication Workshop (NRS/FWCW)*, Aug. 2004, Oulu, Finland.
- [P2] E.S. Lohan, A. Burian, and M. Renfors. Acquisition of Galileo Signals in Hybrid Double-Dwell Approaches. In CDROM *Proc. of the 2nd European Space Agency (ESA) Workshop on Satellite Navigation User Equipment Technologies (ESA NAVITEC 2004)*, Dec. 2004, Noordwijk, The Netherlands.
- [P3] A. Burian, E.S. Lohan, and M. Renfors. Filter Design Considerations for Acquisition of BOC-modulated Galileo Signals. In *Proc. of 16th Annual IEEE International Symposium on Personal Indoor and Mobile Radio Communications (PIMRC 2005)*, volume 3, pages 1520–1524, Sep. 2005, Berlin, Germany.
- [P4] A. Burian, E.S. Lohan, and M. Renfors. BPSK-like Methods for Hybrid-Search Acquisition of Galileo Signals. In *Proc. of IEEE International Conference on Communications (ICC 2006)*, volume 11, pages 5211–5216, Jun. 2006, Istanbul, Turkey.
- [P5] A. Burian, E.S. Lohan, V. Lehtinen, and M. Renfors. Complexity Considerations for Unambiguous Acquisition of Galileo Signals. In *Proc. of 3rd Workshop on Positioning, Navigation and Communication 2006 (WPNC 2006)*, pages 65–73, Mar. 2006, Hannover, Germany.
- [P6] E.S. Lohan, A. Burian, and M. Renfors. Low-Complexity Acquisition Methods for Split-Spectrum CDMA Signals. In *Wiley International Journal of Satellite Communications and Networking*, Vol. 26, Issue 6 (Nov./Dec. 2008), DOI: 10.1002/sat.922, pages 503–522.
- [P7] A. Burian, E.S. Lohan, M. Renfors. Sidelobe Cancellation Method for Unambiguous Tracking of Binary-Offset-Carrier-modulated Signals. In CDROM

Proc. of 3rd European Space Agency (ESA) Workshop on Satellite Navigation User Equipment Technologies (ESA NAVITEC 2006), Dec. 2006, Noordwijk, The Netherlands.

- [P8] A. Burian, E.S. Lohan, and M. Renfors. Efficient Delay Tracking Methods with Sidelobes Cancellation for BOC-Modulated Signals. In *EURASIP Journal on Wireless Communications and Networking*, Vol. 2007, Article ID 72626, 20 pages, 2007.
- [P9] A. Burian, E. Laitinen, E.S. Lohan, M. Renfors. Acquisition of BOC Modulated Signals Using Enhanced Sidelobes Cancellation Method. In *Proc. of European Navigation Conference ENC-GNSS*, Apr. 2008, Toulouse, France.

List of abbreviations and symbols

ABBREVIATIONS

C/A	Coarse/Acquisition
N/A	Not Applicable
ACF	Auto-Correlation Function (sometimes ACF refers to the absolute value of correlation function, as it is explained in the text, or made obvious from the plots)
ADC	Analog-to-Digital Converter
AltBOC	Alternate Binary Offset Carrier
AWGN	Additive White Gaussian Noise
B&F	Betz and Fishman acquisition method
BEIDOU	China's Navigation Satellite System
BPF	Bandpass Filter
BOC	Binary Offset Carrier modulation
BPSK	Binary Phase Shift Keying modulation
CBOC	Composite Binary Offset Carrier modulation
CDBOC	Complex Double Binary Offset Carrier modulation
CDMA	Code Division Multiple Access
CDF	Cumulative Distribution Function
CNR	Carrier-to-Noise-Ratio
Compass	China's stand-alone Satellite Navigation System
CosBOC	Cosine Binary Offset Carrier
COSPAS	Cosmicheskaya Sistyema Poiska Avariynich Sudov
CS	Commercial Service
DBOC	Double-BOC modulation
DC	Differential Correlation
DLL	Delay Locked Loop
DoD	Department of Defense
DP	Dot Product
DSB	Double Sideband Processing
DS-CDMA	Direct Sequence-Code Division Multiple Access
DSP	Digital Signal Processing
DS-SS	Direct Sequence Spread Spectrum
EC	European Commission

EGNOS	European Geostationary Navigation Overlay System
EML	Early Minus Late
ESA	European Space Agency
FBB	Filter-Bank-Based
FDMA	Frequency Division Multiple Access
FFT	Fast Fourier Transform
FIC	Full-band Independent Code acquisition method
FIR	Finite Impulse Response
FPGA	Field-Programmable Gate Array
GAGAN	India's GPS-Aided GEO-Augmented Navigation
GIOVE	Galileo In-Orbit Validation Element
GJU	Galileo Joint Undertaking
GLONASS	Global Orbiting Navigation Satellite System (Globalnaya Navigatsionnaya Sputnikovaya Sistema)
GNSS	Global Navigation Satellite System
GPS	Global Positioning System
GSM	Global System for Mobile communications
HRC	High Resolution Correlator
IC	Interference Cancellation
I	In-phase
I&D	Integrate and Dump
IF	Intermediate Frequency
IFFT	Inverse Fast Fourier Transform
IFIR	Interpolated Finite Impulse Response filter
IIR	Infinite Impulse Response
INMARSAT	INternational MARitime convention on communication by SATellite
IRNSS	India's Regional Navigational Satellite System
LOS	Line-Of-Sight
LPF	Low Pass Filter
M&H	Martin and Heiries acquisition method
MAT	Mean Acquisition Time
MBOC	Multiplexed Binary Offset Carrier
MEDLL	Multipath Estimating Delay Lock Loop
MEE	Multipath Error Envelope
MF	Matched Filter
MGD	Multiple Gate Delay
ML	Maximum-Like
ms	millisecond
MSAS	Multi-Functional Satellite Augmentation System
MTLL	Mean Time to Lose Lock
NC	Narrow Correlator
NCO	Numerically Controlled Oscillator

NEML	Narrow Early Minus Late
NLOS	Non Line-Of-Sight
NRZ	Non-Return to Zero
OS	Open Service
P(Y)	Precision (Encrypted)
PAC	Pulse Aperture Correlator
PDF	Probability Density Function
PDP	Power Delay Profile
PPS	Precise Positioning Service
PRN	Pseudo-Random Noise
PRS	Public Regulated Service
PSD	Power Spectral Density
Q	Quadrature-phase
QZSS	Japan's Quasi-Zenith Satellite System
RF	Radio Frequency
RMSE	Root Mean Square Error
RNSS	Radio Navigation Satellite Service
SAR	Search-And-Rescue service
SARSAT	Search And Rescue Satellite-Aided Tracking
SBAS	Satellite-Based Augmentation Systems
SCM	Sidelobes Cancellation Method
SCPC	SubCarrier Phase Cancellation acquisition method
SinBOC	Sine Binary Offset Carrier
SNR	Signal-to-Noise-Ratio
SoL	Safety of Life
SPS	Standard Positioning Service
SSB	Single Sideband Processing
s	second
TOA	Time-of-Arrival
TK	Teager Kaiser operator
TMBOC	Time-Multiplexed Binary Offset Carrier modulation
UAL	Unsuppressed Adjacent Lobes acquisition method
UMTS	Universal Mobile Telecommunications System
US	United States
WAAS	Wide Area Augmentation System

SYMBOLS

α_l	complex time-varying coefficient of the l th path during the n th code epoch
α_1	roll-off parameter of passband edge frequency
α_2	roll-off parameter of stopband edge frequency
$\delta(t)$	Dirac pulse

Δ	early-late chip spacing
$(\Delta f)_D$	residual Doppler error
$(\Delta f)_{bin}$	frequency-bin step
$(\Delta t)_{bin}$	time-bin step
$(\Delta f)_{max}$	maximum Doppler uncertainty in Hz
$(\Delta t)_{max}$	maximum code uncertainty in chips
ε	power containment factor
$\eta(t)$	additive white Gaussian noise
$\tilde{\eta}(\tau)$	filtered noise
γ	decision threshold
$\Lambda(t)$	triangular pulse
τ_l	path delay
$\hat{\tau}_l$	estimated code delay
BW	code epoch bandwidth
$c_{k,n}$	k th chip corresponding to n th symbol
$d(t)$	data modulated sequence
d_n	complex data symbol
\hat{d}_n	estimated data bits
$\mathbf{E}(\cdot)$	expectation operator
E_b	bit energy
FBB_{efw}	FBB with equal width frequency bandwidths
FBB_{ep}	FBB with equal power bandwidths
f_c	chip rate
f_D	Doppler shift introduced by channel
\hat{f}_D	estimated Doppler frequency
f_{pass}	passband edge frequency
f_{ref}	reference frequency
f_s	sampling rate
f_{sc}	sub-carrier frequency
f_{stop}	stopband edge frequency
$G_s(f)$	power spectral density
k	Boltzmann constant ($1.3806503 \times 10^{-23}$ J/K)
K_p	penalty factor, which represents the time lost if a false alarm occur
L	number of channel paths
m	code epoch index
m_1, m_2	BOC modulation parameters
N_0	two-sided PSD of the additive Gaussian noise
N_{1bins}	the number of correct bins in the correct window
N_{BOC_1}	BOC modulation order
N_{BOC_2}	second BOC modulation order, to differentiate between SinBOC and CosBOC
N_{bins}	the number of bins over a single decision variable is formed
N_c	coherent integration time, expressed in code epochs or ms

N_{corr}	number of complex correlators
N_{FIR}	filter order for FIR filter
N_{fb}	the total number of filters used in the filter bank-based method
N_{IFIR}	filter order for interpolated FIR filter
N_{IIR}	filter order for IIR filter
N_{nc}	non-coherent integration time, expressed in blocks
N_{pieces}	the number of filters per sideband used in the filter bank-based method
N_s	oversampling factor
N_{sh}	shifting factor applied at sample level
$p_{TB}(t)$	rectangular pulse shaping
$P_{DBOC}(f)$	power spectral density for DBOC-modulated signals
P_d	probability of detection
P_{fa}	probability of false alarm
r_p	passband ripple
r_s	stopband attenuation
$r(t)$	received signal
$\mathcal{R}(t)$	code epoch-by-epoch correlation
\mathcal{R}_{DBOC}	autocorrelation function of a DBOC waveform
$\bar{\mathcal{R}}$	averaged non-coherent correlation function
$Q_{N_{nc}}(\cdot)$	the generalized Marcum Q-function of order N_{nc}
Q_{win}	number of time-frequency windows
$s_{DBOC}(t)$	DBOC-modulated waveform
$s_{SinBOC}(t)$	sine BOC-modulated waveform
$s_{CosBOC}(t)$	cosine BOC-modulated waveform
$s_{ref}(t)$	reference code at the receiver
S_F	spreading factor
sps	symbols per second
T_0	room temperature in Kelvin $\approx 290K$
T_B	pulse duration
T_c	chip period
T_{sym}	code symbol period
x_{max}	maximum separation between successive paths
x_t	DBOC-modulated signal
W_t	time-window length
W_f	frequency-window length
w	weighting factor for Sidelobe Cancellation Method

List of Figures

2.1	Galileo frequency plan GJU 2005 [67].	17
3.1	Examples of time-domain waveforms for SinBOC- and CosBOC-modulated signals.	21
3.2	Examples of power spectral densities for BOC-modulated signals.	23
3.3	Examples of absolute value of ACF for BPSK and BOC-modulated signals.	24
3.4	Illustration of multipath effect on BOC-modulated correlation function, 2-paths Rayleigh fading channel (upper plots) and no multipath (lower plots). Left plots: SinBOC(1,1). Right plots: CosBOC(10,5).	28
3.5	Basic block diagram of a Galileo/GPS receiver.	29
4.1	Examples of correlation outputs, single-path static channel.	34
4.2	Example of correct time-frequency window, in the presence of fading multipath.	34
4.3	Simplified block diagram of an acquisition model.	36
4.4	Block diagram of the multiple-dwell acquisition structure.	40
4.5	Block diagram of 'sideband correlation method' (B&F).	44
4.6	Block diagram of 'BPSK-like method' (M&H).	44
4.7	Block diagrams of proposed unambiguous acquisition methods.	45
4.8	Illustration of normalized envelope of correlation functions after processing with the proposed low-complexity unambiguous methods.	46
4.9	Block diagram of the Filter-Bank-Based acquisition method.	48
4.10	Illustration of division into frequency bands for the equal-frequency-width, respectively equal-power FBB acquisition techniques.	49
4.11	Averaged correlation functions after FBB processing. Left plot: un-normalized; Right plot: normalized by the maximum signal amplitude.	49

4.12	Time-step bins needed to achieve a target detection probability, for FBB and B&F unambiguous acquisition methods, average (left plot) and worst (right plot) cases.	50
5.1	DLL block diagram.	53
5.2	Code tracking exemplification for EML discriminator.	54
5.3	S-curves for non-coherent EML, single-path channel.	56
5.4	S-curves for non-coherent EML with SinBOC(1,1) modulation, in presence of distant paths (left plot) and in presence of closely-spaced paths (right plot).	57
5.5	Multipath error envelopes for non-coherent wide EML, narrow EML and HRC code tracking algorithms.	59
5.6	Exemplification of SCM technique, single-path static channel. Left: SinBOC(1,1) case. Right: CosBOC(10,5) case. Upper plots: BOC-modulated signal and reference subtraction pulse. Lower plots: the correlation function after SCM.	64
6.1	ACF for bandlimited SinBOC(1,1) signal.	67
6.2	Power containment for BPSK, SinBOC(1,1) and CosBOC(15,2.5)-modulated signals.	70
6.3	Frequency responses for FIR and IIR filtering, with different transition bands.	72
6.4	Performance of dual-sideband FBB methods using FIR filtering. Left plot: Detection probability. Right plot: Mean acquisition time.	74
6.5	Complexity comparison of DSB FBB and DSB B&F methods. Left plot: $N_{pieces}=2$. Right plot: $N_{pieces}=4$	75
8.1	Performance in terms of detection probability (left plot) and mean acquisition time (right plot), for a SinBOC(1,1) modulated signal, transmitted over a Rayleigh channel with 2 paths.	86
8.2	Performance in terms of detection probability (left plot) and mean acquisition time (right plot), for a CosBOC(10,5) modulated signal, transmitted over a Rayleigh channel with 3 paths.	86

List of Tables

2.1	SPS Positioning and Timing Accuracy Standard (95 % Probability)	14
2.2	Galileo services performance	16
2.3	Galileo signal structures (as of 2005).	18
6.1	GPS and Galileo receiver bandwidths	68
6.2	Number of filters needed for the ambiguous and unambiguous acquisition methods)	73
6.3	Number of operations for 1 ms receiver processing, per real filter	73

Chapter 1

Introduction

For centuries, explorers and navigators have craved for a system that would allow locating their position on the globe with the accuracy necessary to reach their intended destinations. About two thousand years ago, the first lighthouses were erected for navigational aid. Columbus and his contemporary sailors navigated using an ancestor of the modern inertial navigation systems, by measuring the course and distance from some known points.

In the early 1970s the Global satellite-based Positioning and navigation System (GPS) started to be developed by the United States Department of Defense, initially for military purposes, but later made it also available to civilian users [99], [149], [132]. The US GPS, the best-known and currently the only fully operational Global Navigation Satellite System (GNSS), provides autonomous and continuous geo-spatial positioning and timing information, anywhere in the world [114]. The current GPS system is military operated, it has only a few signals for civil users, and it does not offer any guarantee of integrity and quality of service. Over the last decade, several improvements to the GPS service have been implemented, including new signals for civil use and increased accuracy and integrity for all users [192], [48], [76]. GPS is a billion-worth industry, saving lives and helping society in countless ways, and nowadays most of the satellite positioning applications are based on it. By the time the GPS became fully operational, the predicting rise and advantages of such technology gave the the initiative to other countries to pursue their own GNSS development. Russia runs its own GNSS, called GLONASS, which is currently in the process of being restored to full operation [39]. China has also indicated expansion of its regional Beidou navigation system into a global system Compass, and India and Japan are developing their own regional satellite navigation systems. The European countries aimed, in the first phase, to provide an augmentation to the existing GPS/GLONASS constellation, via the European Geostationary Navigation Overlay System (EGNOS) program, while the next step will be to build a civilian owned and controlled system that meets the requirements of all modes of transport. This system, referred to as

the Galileo positioning system, is the next generation GNSS, still in the initial deployment phase, and it is scheduled to be operational by 2013, according to [191] and [51]. The Galileo services are primarily intended for civil users and should be interoperable and compatible with civil GPS and with its augmentations [32], [45], [49], [50], [67].

The combined use of both GNSS will improve the accuracy, integrity, availability and reliability through the use of a single common receiver design, especially in urban environments and it will provide system certification, liability and guarantee of service [157], [80], [48]. The benefits of more satellites in conjunction with improved modernized signals will provide the potential for sub-meter positioning in a standard handset and enhanced accuracy with shorter initialization time. The users accessing data from multiple satellite systems can continue to operate if one of the systems fails and will benefit from a more reliable signal tracking, also designed for Safety-of-Life applications [67], [77], [69], [49]. In the next decade considerable growth is expected in the use of GNSS, as the increased positioning accuracy and system reliability provide cost savings and other benefits for a wide range of economic and social activities that rely on location. With such a wide variety of new signals and satellite systems, receiver designers discover the fact that there are still many new design challenges from one end of the receiver (the antenna) to the other (the software providing the user with position). An overview of these challenges is well-discussed in [36], [34]. In this context, there is always a continuous demand for efficient Digital Signal Processing (DSP) algorithms at the GNSS receiver, in order to fulfill the required quality of service.

1.1 Background and motivation

The Galileo and GPS interoperability is realized by a partial frequency overlap with different signal structures and/or different code sequences. Thus, in order to accommodate several signals on the same carrier, a new modulation type, the Binary Offset Carrier (BOC) modulation, has been proposed in [15]. Its split spectrum property allows moving the signal energy away from the band center, thus achieving a higher degree of spectral separation between the BOC-modulated signals and other GPS legacy signals, such as the Coarse/Acquisition (C/A) code [18], [19], [21]. Since its introduction, several BOC families have been considered, with characteristics defined by the spectral shaping and the width of the side lobes [5], [180], [7], [79], [126]. The BOC modulation enables combined GNSS receivers to outperform an equivalent Binary Phase Shift Keying (BPSK) modulation and to track the GPS and Galileo signals with higher accuracy, even in challenging environments that include multipath, noise and narrow-band interference [78], [77], [169]. Despite these advantages, BOC modulation triggers new challenges in the delay estimation process, since the Auto-Correlation Function

(ACF) of BOC-modulated signals is characterized by multiple side-peaks with non-negligible magnitudes within the range of two chips around the maximum peak [116]. Since locking on a false lock point produces a biased measurement and thus an erroneous navigation solution, the receiver should employ efficient solutions in order to deal with these ambiguities.

At the receiver the incoming signal is first amplified and after a series of Intermediate Frequency (IF) mixers, filters and down-conversion operations it is brought to (or near) baseband for subsequent processing. While the GLONASS system uses the Frequency Division Multiple Access (FDMA) scheme and carrier frequencies different from GPS [39], the GPS and Galileo receivers will use direct-Code Division Multiple Access (CDMA) [137], [52], [77], [67]. In this context, signal acquisition and tracking at the receiver play a crucial role in the accuracy of the position solution [179], [199], [151]. The acquisition stage is a searching process over the code-frequency search space. By performing correlations of the received signal with the replica spreading code, the incoming code phase and the Doppler frequency shift of a particular satellite are detected. Each correlation calculation corresponds to a code-Doppler bin, which defines the resolution of scanning the searching space [99]. The acquisition performance is determined to a great extent by the size of the search space. Since one of the main features of the Galileo system is the introduction of longer codes than those used for GPS C/A signals, with an increased code uncertainty region, the fully serial search would lead to high acquisition times values [153], [154], [155], [95], while the parallel search will increase the implementation complexity [179], [181], [184]. A scheme which can offer a successful trade-off between the low complexity (the serial search) and the low acquisition time (parallel search), is a hybrid serial-parallel approach [156], [12], [209] in which the full length code is divided into several partial codes and the correlation is performed on each partial code. Also, detector structures based on Fast Fourier Transform (FFT) have been introduced for fast code acquisition [2], [23], [183], [204], [205], [211]. Such a structure performs correlation in the frequency domain and provides better performance over the wider correlation bandwidth of Doppler frequencies, in terms of mean acquisition time, when compared to the time-domain correlators.

Besides the issues brought by BOC modulation, there are other challenges which should be accounted at the receiver. In low Carrier-to-Noise Ratio (CNR) environments (e.g. urban areas, indoors) the performance is deteriorated, since the receiver gets the satellite signal via multiple paths and processes the combined signal as if only the direct path were present [14], [178], [11]. A particularly challenging problem is the situation of closely-spaced paths or short multipath spacing, where different replicas of the transmitted signal arrive at the receiver at sub-chip intervals [64], [106], [118]. The receiver performance is also affected by pre-correlation band-limitation and by the resolution due to the sampling process, since in time domain, the ACF becomes smoother around the peaks, and it is

no longer piecewise linear, as in the case of infinite bandwidth [17], [26], [38]. This smoothing of the ACF produces a loss in resolution in a similar fashion with lowering the sample rate and it is prone to increase the delay errors [29], [30]. One solution to enhance the timing accuracy and to lower the correlation losses due to time quantization is to use oversampling at the chip or sub-chip interval (for BOC-modulated signals) [149]. Also, intuitively, the performance also depends on the spacing between the timing hypotheses or the time-bin step. If the grid of scanning the possible code phases becomes less dense, the detection probability is decreased. In a conventional hardware, the correlator spacing can be seen as the resolution at which the correlation function is sampled [38]. Therefore the time-bin step should be chosen in such a way to avoid to lock on additional peaks which appear in the ACF within two-chip interval due to BOC-modulation and it should be small enough in order to acquire the main lobe. However, on the other hand, by reducing the time-bin step, the computational load and the acquisition time are increasing [63].

In order to deal with these two conflicting situations, unambiguous acquisition techniques were introduced, which attempt to reconstruct the 'BPSK-like' shape of the ACF envelope and therefore can enable the use of a higher time-bin step. These so-called 'BPSK-like techniques' [129], [81], [82] or 'sideband techniques' [10], [63], [20], [62], [113], [122] use sideband selection filters and modified reference Pseudo-Random Noise (PRN) code at the receiver. The effect of sub-carrier modulation is removed by using a pair or a single sideband correlator since the BOC-modulated signal can be obtained as one or the sum of two BPSK modulated signals, located at positive and negative sub-carrier frequencies. These methods tend to degrade the signal amplitude, due to filtering and correlation losses. Moreover, they have been previously tested only for sine BOC (SinBOC) cases and even BOC modulation orders. In this thesis we tested them also for odd-BOC modulation orders, where we showed that the 'BPSK-like' techniques [129], [81] fail to work for odd-BOC modulation orders. A generalized class of frequency-based unambiguous acquisition methods, namely the Filter Bank-Based (FBB) approaches, have been proposed and analyzed in [123], [128]. This approach decreases the signal bandwidths before the correlation stage, in order to increase the main lobe width of the correlation function, and thus, to allow the use of time-bin steps higher than one chip.

Following the search stage, the correlation output is coherently and possibly further non-coherently averaged in order to detect the presence or absence of signal, and thus to decide if the received signal and the locally generated code are synchronized or not [99]. The detection probability can be improved and the side-peak ambiguities can be decreased if, instead of using the conventional non-coherent integration, each current pre-detection sample is multiplied with the complex conjugate of the previous one and these products are then accumulated [173], [47], [88] [170], [91], [208]. This differential combining or differential

correlation method diminishes the interference effects and can decrease the acquisition time [142].

Based on the observations that most of the acquisition time is spent in testing non-synchronous positions and that different approaches based on repeated observation of the same region may decrease the acquisition time, the idea of multiple integration times (multiple-dwells) was introduced in [41]. A double-dwell structure has a first stage with a short integration time, followed by a verification stage of previous decision with a longer integration time, which should give a smaller global false alarm probability than a single-dwell structure. Different multiple-dwell schemes are compared in [42]. Also, the detector can use either a fixed or a variable dwell length from one position to another [99], [165].

After the signal acquisition, the code phase and Doppler shift need to be tracked for (selected) visible satellites long enough in order to obtain accurate estimates of the parameters. If the tracking module fails to track the code-phase changes that occur over required time, the signal needs to be re-acquired. Since the estimate of the Line-Of-Sight (LOS) code delay is used to calculate the pseudorange, it consequently affects on the accuracy of the position solution. Therefore the code-tracking stage is very critical in the context of GNSS receiver design. The main algorithms used for GPS and Galileo code tracking (provided a sufficiently small Doppler shift) are based on so-called feedback delay estimators, which are implemented based on a feedback loop. The most known feedback delay estimators are the Delay-Locked Loops (DLL) [9], [22], [61], [64], [110].

However, since the classical DLLs fail to deal with multipath propagation [179], more efficient algorithms are needed, especially in the case of closely-spaced multipath scenario. One class of these enhanced DLL techniques is based on the idea of narrowing the spacing between early and late correlators (i.e., narrow correlator class) [193], [90], [130]. Another class of enhanced DLL structures uses a modified reference waveform for the correlation at the receiver, which narrows the main lobe of the cross-correlation function, at the expense of a deterioration of the signal power. Examples belonging to this class are the gated correlator [130], the strobe correlators [65], [90], the pulse aperture correlator [60], and the modified correlator reference waveform [90], [202]. Another category of improved DLL techniques performs multipath interference cancelation by estimating not only the delay of the LOS path, but also the delays, phases, and amplitudes of the Non-LOS (NLOS) paths [195], [197], [64], [110]. There are also another categories of feedback delay estimators, as for instance those based on the extended Kalman filters, which suffer from high complexity and high sensitivity during the initialization phase [124]. An alternative to the above-mentioned feedback approach is based on the open-loop (or feedforward) solution, which makes the delay estimation in a single step, without requiring a feedback loop. There are several well-known alternatives for open-loop solutions, namely, the deconvolution algorithms, the Teager-Kaiser (TK) based algorithms, the subspace-based

approaches, the algorithms based on quadratic programming or the suboptimal Maximum-Likelihood (ML) based algorithms [124].

Due to the narrow shape of the main peak, the innovation brought by the use of BOC modulation leads to substantial improvement in tracking. However, a false lock produces biased measurements and therefore will affect the accuracy of the navigation solution. Various solutions have been found which minimize tracking ambiguity, for example in [61], [116], [201]. Most of these methods try to resolve the tracking ambiguity problem in the same fashion for all BOC families. A recent tracking technique, dedicated to SinBOC(1,1) signals, is presented in [74]. Also, an innovative tracking approach, which completely removes the sidelobe ambiguities of SinBOC(n,n) signals and offers an improved resistance to long-delay multipath, has been introduced in [96], [97]. However, this method employs two correlation channels instead of one, as the used DLL discriminators are a combination of BOC autocorrelation function and of BOC/PRN correlation function [97]. In this context, low-complexity tracking algorithms, which have both multipath mitigation as well as side-peaks reduction capabilities, are of high demand.

To summarize, this thesis was motivated by the various challenges in acquisition and tracking of GNSS signals, such as the ambiguities introduced by the BOC modulation, the transmission of signal over multipath channels and at low signal conditions, the usage of higher code lengths in Galileo or various constraints at the receiver front-end, such as bandwidth limitation or correlation resolution. The algorithms introduced in this work aimed at achieving low errors and improved performance (i.e., good detection probabilities, low false alarm rates and low acquisition times), also in low CNR conditions.

1.2 Scope and contribution of the thesis

The core of this thesis is the design and analysis of signal processing algorithms suitable for acquisition and tracking of European Galileo and modernized GPS signals. As emphasized in the previous section, new proposals such as BOC-modulated signals or longer spreading codes, as well as the continuous demand for positioning in difficult environments trigger new challenges in the synchronization process. The aim of this thesis is to analyze various receiver parameters in the context of BOC-modulated signals and to introduce efficient methods for acquiring and tracking these types of signals. The performance of the proposed algorithms has been tested and validated through extensive simulations, performed in various static and fading multipath channels.

Since the proposed code lengths for new GNSS systems are higher, the searching strategy is of utmost concern for fast signal acquisition [67]. Typically, the double-dwell serial search strategies have been preferred to single-dwell architec-

tures for CDMA signal acquisition [27], [42], and until now, only few papers have addressed the problem associated to hybrid or parallel search strategies. Comparisons between the double-dwell and single-dwell architectures are hard to find in existing literature, especially for hybrid-search approaches [104], [119]. Also, little is known about how to design the detection and false alarm probabilities at each dwell stage, in order to attain the minimum acquisition time and under which conditions the double dwell-structure is indeed better than a single-dwell one. We have performed a comprehensive analysis about the choice of detection and false alarm probabilities, as well as about the design of various parameters to be used at each stage of a double-dwell structure. We also presented the conditions under which a double-dwell architecture provides a lower acquisition time compared with a single-dwell structure, for a realistically modeled Galileo signal [P2].

Since the absolute value of the autocorrelation function of a BOC-modulated signal presents additional peaks, the acquisition and tracking of these signals pose additional challenges, due to increased complexity and longer acquisition time. An important part of this thesis is dedicated to analyzing and proposing improved techniques for unambiguous acquisition and tracking of BOC-modulated signals. First, we have investigated and developed further the unambiguous acquisition algorithms, which allow the use of a higher search step compared with the ambiguous solution [P4], [P5], [P6]. The effect of sub-carrier modulation is removed by using a single or a pair of sideband correlators, thus reconstructing the BPSK-like shape of autocorrelation function at the expense of signal power degradation. Compared with the earlier works [129], [81], the proposed unambiguous methods are significantly less complex and are also valid for both even and odd BOC-modulation orders. Two of the proposed methods in this thesis are extensions of the 'BPSK-like' [129], [81] or 'sideband correlation' [10], [20], [63] mentioned techniques, while the third one, the Unsuppressed Adjacent Lobes technique, is first introduced in the publication [P6]. These algorithms have been tested using both serial and hybrid search strategies, for various BOC-modulation orders proposed in Galileo and modernized GPS specifications. In the previously introduced unambiguous acquisition methods, the effect of different filtering structures for sideband selection is not considered. We have also analyzed the filter design issue and the implementation complexities of different unambiguous BOC acquisition methods. We considered the impact of both the correlation and sideband selection parts, for which different Finite Impulse Response (FIR) and Infinite Impulse Response (IIR) filtering structures were used [P5], [P6].

The second class of unambiguous algorithms introduced and analyzed in publications [P7], [P8], [P9], namely the Sidelobes Cancellation Method (SCM), removes or diminishes the sidelobe ambiguities. In contrast with other methods introduced in the literature [96], [97], [13], [54], [201], this technique has the advantage that it can be extended to any sine or cosine, odd or even BOC-modulation case, while maintaining a sharp and narrow main lobe, which is beneficial to the

tracking process. Also it provides a lower complexity solution than other unambiguous methods [96], [97], since it uses ideal reference correlation functions, which are generated only once and can be stored at the receiver side. This technique relies on subtracting the ideal reference correlation function from the ambiguous one, and, if provided with the correct estimated delay, there is no decrease in the signal power as in the case of the other unambiguous acquisition or tracking methods. After removing the sidelobe ambiguities through the SCM algorithm, other tracking-loop structures can be used to alleviate the multipath effect [193], [65], [130], [93], [195]. In contrast with the BPSK-like methods, the SCM was mainly targeted to be used at the tracking stage, because it maintains the narrow width of the main lobe. This approach was tested also during acquisition process, since the re-use of some hardware blocks from the acquisition stage might be desirable in the tracking stage [P9]. The SCM technique used in conjunction with two differential correlation methods [142], enhanced also the performance at the acquisition stage, if the search step of time uncertainty was kept sufficiently small [P9].

In most of the earlier research studies, the effects of bandwidth limitation at various stages of the receiver or the sampling process are not considered. The sampling resolution is usually dictated by hardware constraints and various designs are possible, either using sampling at the IF stage or close to the Radio Frequency (RF) stage [4], [145]. In order to enhance the timing resolution of the received signal, oversampling or interpolation may be used [149], [30]. We have analyzed the effect of oversampling on BOC-modulated signals, considering both integer and non-integer oversampling factors and we have shown the condition that should be fulfilled by the time-bin step size in order to achieve good performance [P1]. Since in context of GNSS systems, the frequency spectrum represents the most important resource, spectrum shaping of received signal is of utmost importance [77], [78]. In general, the ideal rectangular filtering is considered at the receiver and the effect of real filtering for bandwidth limitation is ignored. However, real filtering depends on the filter design parameters and can skew and delay the symmetrical correlation function, and thus, the signal suffers additional performance degradation when compared with the case of rectangular shaping [31], [29]. Therefore efficient filtering structures are needed when the receiver bandwidth is limited. In this context, we have analyzed and compared the impact of both FIR- and IIR filter structures, for target applications such as Galileo or modernized GPS satellite systems and we have shown that the performance can be improved by using an asymmetric transition band between the passband and stopband frequencies [P3].

1.3 Outline of the thesis

The core of this thesis is in the area of BOC-modulated signal acquisition and tracking for the Galileo and modernized GPS systems. It is composed of eight chapters, an appendix and a compendium of nine publications referred in text as [P1], [P2], ..., [P9]. These include six articles published in international conferences, one article published in a national conference and two articles published in international journals. The structure of the thesis has been chosen with the intention to provide a comprehensive and unified framework of the challenges in signal synchronization in GNSS systems and to point out the main contribution of the author. The new algorithms and the main results of the thesis have been originally presented in [P1]-[P9] and they are briefly referred in the text. In this thesis, the presented acquisition and tracking algorithms are analyzed in static and fading environments for BOC-modulated signals.

This introductory part has defined the challenges addressed in this work and has illustrated the scope of the thesis including its motivations, objectives and contributions, followed by the overall thesis outline. Chapter 2 gives an overview of the satellite-based navigation technology and introduces briefly the GPS and Galileo systems. Signal characteristics, services and spectrum allocation are presented based on the current public knowledge on standard developments. The signal model of Galileo and modernized GPS signals is presented in Chapter 3. The BOC modulation is discussed first, followed by a brief description on propagation aspects and fading channel characteristics of wireless systems. A short overview of the fading channels models with different fading types and distributions is provided. Also the impact on performance of different receiver architecture parameters is discussed. Chapter 4 introduces the code acquisition task, presenting several search strategies and detection structures. Various unambiguous acquisition methods for processing the BOC-modulated signals are presented next. Chapter 5 is dedicated to the tracking of modernized GPS and Galileo signals, presenting the classical DLL-based methods, as well as various feedforward-based structures. Unambiguous tracking approaches, such as the SCM algorithm, are provided next. Chapter 6 presents the bandlimiting constraints and describes different filter structures in the context of GNSS signals. An overview of the thesis publications [P1]-[P9] is presented in Chapter 7, as well as the author's contribution to them. The conclusions and remaining open issues are drawn in Chapter 8. More simulation results regarding the SCM techniques, in context of signal acquisition, are presented in Appendix. Finally, the results of this work are given in the attached publications.

Chapter 2

Overview of Global Navigation Satellite Systems

This chapter presents briefly the principles of satellite-based positioning and gives an overview of two main GNSS, the Navstar GPS and the new European Galileo system. The structures of GPS and Galileo signals are introduced, based on standardization documents, as well as the main differences between them, from signal processing point of view.

2.1 Satellite-based positioning technology

The position location services have progressed remarkably during the last decade. These services can use either satellite-based or network-based positioning technology. The scope of this thesis is limited to the satellite-based technology, e.g., GPS and Galileo, which computes the receiver position in time and space using the Time Of Arrival (TOA) ranging broadcasted by a constellation of satellites. Even if its implementation is complex, the principle behind TOA ranging is simple and is based on the measurements of the time interval of the signal transmitted by an emitter (i.e., satellite) at a known location to arrive at the receiver. The receiver determines the time required for the transmitted signal to propagate from satellite to receiver and determines the distance from emitter by multiplying this time by the speed of light (approximately 3×10^8 m/s). The instant time of transmission of the satellite signal is embedded in the navigation signals and, in order to achieve the true time difference, the receiver and satellite clocks have to be synchronized. In order to fix the receiver position in the three-dimensional space, the trilateration concept is used, which simultaneously performs three range measurements. By intersecting three uncertainty spheres of the three satellites, the receiver narrows its possible locations down to two points, from which one of these points is actually on the surface of the Earth. A GNSS receiver requires computing the

distance to the fourth satellite in order to correct the receiver clock bias. However, the receivers generally look for more than four satellites, in order to improve the accuracy. The receiver determines the satellite position by extracting the satellite orbital parameters (i.e., satellite ephemeris) from the navigation signal [99].

The time offset between the GPS system time and the receiver clock induces error which corrupts the ranging measurements. In addition to this timing error, the measurements are also corrupted by incorrect or outdated values of satellite ephemeris, tropospheric and ionospheric signal delays, receiver noise and multipath signal propagation [132]. Due to these error sources, the range measurement is an estimate of the true distance between the satellite and the receiver (i.e., a *pseudorange* measurement).

2.2 Global and Local Navigation Satellite Systems

Nowadays, most of the satellite positioning applications are based on Navstar GPS, which was initially meant for military purposes, but, later, it has been ensured for the maximum civilian use [137], [192]. In mid of 70's, the former Soviet Union began the development of its own GNSS, called GLONASS, which was declared operational in 1993 [39]. In contrast to all other CDMA-based satellite navigation systems, GLONASS uses FDMA-based multiple access technique. The system was never brought to completion, but its significance as an element of the national security issue was recognized and is currently being updated and modernized. The GLONASS modernization directive, issued at 18 January 2006, stated a constellation of 18 satellites by the end of 2007, full constellation capability of 24 satellites by the end of 2009, and a comparable performance with that of GPS and Galileo by 2010 [168].

In order to improve the performance of standalone GPS, besides the GPS modernization program itself, several Satellite-Based Augmentation Systems (SBAS) have been or are in process to be developed in order to meet the demanding requirements. These systems support wide-area or regional augmentation through the use of additional satellite-broadcast messages and provide better position accuracy, integrity and reliability by correcting ephemeris errors. The EGNOS program is the precursor of Galileo which has been intended to provide a European augmentation to the GPS and GLONASS systems. It consists of three geostationary satellites and a network of ground stations. Its open service and commercial data distribution service are currently available. The EGNOS system started its initial operation in July 2005. The EGNOS Safety-of-Life service is intended to be available upon certification of the service provider and final system qualification in 2009 [50], [89]. The Wide Area Augmentation System (WAAS) is a system that improves the precision and accuracy of GPS and is the US counterpart of EGNOS. The WAAS is mainly available in North America. A Canadian WAAS sys-

tem is also currently developed. The Japanese Satellite-Based Augmentation System (SBAS) is a Multi-functional Satellite Augmentation System (MSAS) which is designed to supplement the GPS system, by improving the reliability and accuracy of the provided solution. Similar service is provided by the Chinese SBAS, named BEIDOU. India develops its own GPS-Aided GEO-Augmented Navigation (GAGAN) system, with up to three satellites planned initially, which will be compatible with NAVSTAR GPS and with the upcoming Indian Regional Navigational Satellite System (IRNSS). It is expected to be fully operational by 2012 [89].

Nowadays, also stand-alone satellite navigation systems are developed, such as Galileo (the future European satellite system) and Compass (in China).

The Chinese GNSS system was initially started as BEIDOU navigation system (made up of 4 satellites) with limited coverage and application. China has decided to upgrade its current BEIDOU system to a truly global navigation system, named as Compass, which was originally meant as military system. Compass is intended to offer open service with 10 meters location-tracking accuracy [89]. It is planned to work with at least 35 satellites, with both local and global coverage. The Compass operational concept is based on the '2-way active' system, which can institute user charges and limit the number of users. Japan also plans a CDMA-based system, the regional Quasi-Zenith Satellite System (QZSS). The QZSS is a proposed regional time transfer system and enhancement for the GPS, which would be receivable within the Asia-Pacific region. The first satellite is currently scheduled to be launched in 2010. The QZSS system has initially started with three satellites, with possibility of more extensive constellation afterwards. QZSS can only provide limited accuracy on its own and is not currently required in its specifications to work in a stand-alone mode [102].

The European Commission (EC) in a joint initiative with the European Space Agency (ESA) aims to build its own independent global civilian controlled satellite navigation system, referred as Galileo [32], [45], [49], [52]. The largest space project to date, Galileo will be an autonomous system, interoperable with GPS and globally available. It is based on the CDMA technology, as the GPS, and it is meant to provide similar or higher degree of precision and to guarantee the continuity of public service provision for specific applications [50]. In order to manage the development phases of the Galileo Programme, the EC and ESA have jointly set up the Galileo Joint Undertaking (GJU) in 2003 - the European Programme for Global Navigation Services [67]. Galileo has been designed to be interoperable with other navigation systems (GPS, GLONASS, SBAS) or non-GNSS systems (GSM, UMTS, INMARSAT, motion sensors, etc.), in order to meet the demand for high-precision user applications [72], [78], [80], [35], [157].

The following sections provide detailed information about GPS and Galileo systems from signal processing perspective, focusing on signal structures and on the most relevant characteristics for the algorithms presented in this thesis.

2.3 Global Positioning System

GPS is a complex system, which from architectural point of view, consists of three elements. The first element is the space segment, which consists of a constellation of 24 satellites in six orbital planes. The second GPS component is the control segment, which monitors the satellites through checking their operational health and determining their position in space. It consists of the master control station, monitor stations and ground antenna for uploading information to the GPS satellites. The master control station receives GPS observations from the monitor stations and processes them in order to estimate navigation data parameters, such as satellite orbits and clock errors. The third component is the user segment, which comprises the GPS receiver equipment [99], [114]. The user position is determined using the method of trilateration, by solving the four pseudorange equations, as explained in the previous section.

The Direct Sequence - Spread Spectrum (DS-SS) technique, based on CDMA scheme, allows the user to receive multiple signals on the same frequency band, with minimum mutual interference. The transmitted signal is modulated by its own PRN code and has a spectrum much wider than the bandwidth of the modulating data message. As a consequence, better resistance to interference and jamming is achieved, as well as rejection of detection for unauthorized users. Each satellite broadcasts continuously the navigation message over two L-band carriers, L1 with center frequency at 1575.42 MHz, and L2 at 1227.60 MHz. The L1 frequency is Binary Phase Shift Keying (BPSK) modulated by the C/A code and in quadrature by the Precision Encrypted P(Y) code. The L2 frequency is only BPSK-modulated by the P(Y) code. The C/A code is freely available for civilian use and is the basis for the Standard Positioning Service (SPS). The C/A code has a length of 1023 chips, with a transmission code rate (chip rate) of 1.023 Mchips/s, resulting in a code duration of 1 ms. Each satellite is identified by a unique PRN code, which is a Gold code chosen in such a way to reduce cross-correlation among signals. On the other hand, the P(Y) codes are permitted only to US Department of Defense (DoD) authorized users, which have access to the encoded Precise Positioning Service (PPS) [192]. The P(Y) code adopts very long sequences, with chip rate ten times higher than the C/A code chip rate, and has a code length of 6.1871×10^{12} chips [99].

Each transmitted signal is composed of the carrier (L1 or L2), the PRN code (C/A or P(Y)) that serves as ranging codes, and of navigation message, transmitted at a bit rate of 50 bps. The navigation message includes precise satellite ephemeris as a function of time, atmospheric and almanac data [157]. The GPS system performance is mainly reported in terms of accuracy, which implies the conformance between the measured and true positioning, velocity and timing information. The last SPS accuracy specification standard defined by DoD on October 4, 2001 [192] is shown in Table 2.1.

Table 2.1: SPS Positioning and Timing Accuracy Standard (95 % Probability)

	Horizontal Error	Vertical Error	Time Transfer Error
Global average positioning domain accuracy	≤ 13 m	≤ 22 m	≤ 40 ns
Worst site positioning domain accuracy	≤ 36 m	≤ 77 m	≤ 40 ns

The limitations of current GPS and the new range of GNSS applications trigger the design of new modernized GPS signals, which will provide an improvement in system accuracy, availability and integrity. The GPS modernization implies new signal structures, new modulation types, use of longer codes, introduction of forward error correction scheme on signals, faster transmission rates and availability of data-free components [157], [211]. One of the first announcements was the addition of a new civilian signal to be transmitted on a frequency other than the L1 frequency. This new civilian signal is known as L2C signal as it is broadcasted on the L2 frequency (1227.6 MHz). The L2C signal is meant to improve the navigation accuracy, providing an easy-to-track signal and acting as a redundant signal in case of localized interference. In order to comply with safety-critical applications, a new civilian L5 signal was introduced in the aeronautical radio-navigation services at 1176.45 MHz. It has higher transmission power than L1 or L2C signal and improves the signal structure for enhanced performance. Another new signal, the L1C signal, targeted for civilian use, will be available from the year 2013, at the time when GPS III block is scheduled to launch. Its implementation will provide backward compatibility with the C/A signal and will enable greater civil interoperability with Galileo L1 signal.

A major component of the modernization process is the new military signal, called M-code, which was designed for further improvement of the anti-jamming and secure access of the military GPS signals. The M-code is transmitted in the same L1 and L2 frequencies, already in use by the P(Y) code. It is modulated by a BOC modulation, with a sub-carrier frequency of 10.23 MHz and spreading code rate of 5.115 Mchips/s, also referred as sine BOC(10,5) [10], [48]. The new BOC modulation scheme allows compatibility with existing C/A and P(Y) signals, without producing interference problems. More details about the BOC modulation will be provided in Section 3.1.

2.4 European Galileo System

The upcoming European GNSS system, Galileo will provide high accuracy and guaranteed global positioning service under civilian control. It is designed to be

interoperable with GPS and GLONASS systems [67]. When fully deployed, the Galileo system will use a constellation of 30 satellites, positioned in three circular Medium Earth Orbit planes at an altitude around 23000 km with an inclination of 56 degree relative to the equatorial plane. The Galileo ground segment will consist of a Navigation System Control Center, a network of stations monitoring Galileo satellite orbits and synchronization, and several tracking, telemetry and command ground stations. The Galileo Control Centers, which will be located in Europe, will receive data from a global network of Galileo Sensor Stations. This will allow to synchronize the time signals of satellites with the ground station clocks and to calculate data for system integrity. The five S-band (2-4 GHz) and ten C-band (4-8 GHz) uplink stations around the globe will manage the flow of data between the satellites and the Galileo Control Centers. The first spacecraft in the system, GIOVE-A was launched in 2005 and a second one, named GIOVE-B was sent to the orbit in Spring 2008 (GIOVE stands for "Galileo In-Orbit Validation Element"). The two satellites in together test and verify the atomic clocks, navigation signals and other technologies needed to run the positioning system in orbit. As test satellites, GIOVE-A and GIOVE-B broadcast the first Galileo signals from space, but they will not be part of the final Galileo system. In order to complete the testing phase, two more GIOVE satellites will be launched by 2010 and four satellites should be in the orbit for the system, in order to deliver an exact position anywhere on Earth. The Galileo service to the general public is expected to start around the end of 2012, when 12 satellites will be in orbit [50].

Compared to the traditional GPS, the Galileo system will offer a series of advantages, which will be highlighted next. While it will provide the same security features as GPS, Galileo will offer a guarantee of quality and a high level of continuity, which are essential for many sensitive applications, such as aviation, railway transportation or rescue operations. It will provide a similar (or possibly higher) degree of precision and will be more reliable, since it will include a signal integrity message, informing users immediately of any errors. In addition, the Galileo and GPS systems will be complementary to each other, since the users could benefit from two independent infrastructures in a coordinated manner, which will ensure improved availability and security. Thus Galileo should be compatible and interoperable with GPS and it should not cause any degradation for GPS users. A combined GPS-Galileo receiver should be able to achieve position, navigation and timing solutions equal or better than those achieved by either system alone. Ideally, the goal is to get benefit from a larger number of satellites and to use the satellites interchangeably, in order to derive an optimal position solution [157]. Thus, Galileo can be considered as an evolution of the navigation systems, which pays more attention to the user needs.

2.4.1 Galileo Services

Some of the Galileo services will be provided independently by the Galileo system, while the other services will result from the combination with the other systems. The first category, referring to Galileo satellite-only services, has been grouped into the following five service levels [67], [157].

The *Open Service* (OS) is dedicated to consumer applications and will provide positioning, velocity and timing information that can be accessed free of charge. The *Safety of Life Service* (SoL) is meant to increase safety of professional applications. It will be offered openly and will have the capability of authenticating the received signal as being an actual Galileo signal. The main characteristic of SoL service as compared to the OS is the provision of integrity information at global level. The *Commercial Service* (CS) is a restricted-access service for commercial and professional applications. The CS service has guaranteed service and it is based on adding to the open access signals two signals protected by commercial encryption. It will allow for a higher data throughput rate, and thus, improved accuracy. The *Public Regulated Service* (PRS), another restricted service, will be devoted to government-regulated applications which require high continuity and availability. Through the use of appropriate interference mitigation techniques and controlled access, the PRS will provide a higher level of protection against the interfering threats to the Galileo signal-in-space.

Table 2.2: Galileo services performance

	Open Services (OS)	Commercial Services (CS)		Public Regulated Services (PS)		Safety-of-Life Services (SoL)
	Global	Global	Local	Global	Local	Global
Coverage	Global	Global	Local	Global	Local	Global
Accuracy	DF: H: 4 m V: 8 m SF: H: 15 m V: 35 m	DF: ≤1 m	≤10 cm locally augmented signals	H: 6.5 m V: 12 m	1 m locally augmented signals	DF: 4-6 m
- horizontal(H) - vertical(V) - dual frequency(DF) - single frequency(SF)						
Availability	99.8 %	99.8 %		99-99.9 %		99.8 %
Integrity	No	Value-added service		Yes		Yes

The *Search and Rescue* (SAR) service will support the humanitarian search and rescue activities, by accurately pinpointing the distress messages from anywhere across the Earth. The SAR will be backward compatible and will improve the existing COSPAS-SARSAT (Search And Rescue Satellite-Aided Tracking) system, by becoming near real time and more precise, and by improving the average waiting time of distress messages [33]. In addition, the Galileo SAR service will have the return link feasibility from the SAR operator to the distress emitting source, thus helping in identification of false alarms [157]. The Galileo system is

expected to provide an accuracy of less than 1 meter for some services, as shown in Table 2.2 [49], [157]. Other Galileo-related services are locally assisted services which use some local elements to improve performance, e.g., differential encoding, more carriers or additional pilot tones.

2.4.2 Galileo Spectrum Allocation

As proposed in the standardization document from 2005 [67], [167], the Galileo Navigation Signals are to be transmitted in the four frequency bands, illustrated in Fig. 2.1. These four frequency bands are the E5a band (with frequency ranges of 1164 - 1191.795 MHz), the E5b band (1191.795 - 1214 MHz), the E6 band (1260 - 1300 MHz) and the E2-L1-E1 band (1559 - 1591 MHz). They provide a wide bandwidth for the transmission of the Galileo Signals. The frequency bands have been selected in the allocated spectrum for Radio Navigation Satellite Services (RNSS) and in addition to that, E5a, E5b and L1 bands were included in the allocated spectrum for Aeronautical Radio Navigation Services (ARNS), employed by Civil-Aviation users [67]. Some Galileo frequencies are overlapping with GPS in E5/L5 and L1 bands [72], [77], thus attaining the interoperability between the two systems [78].

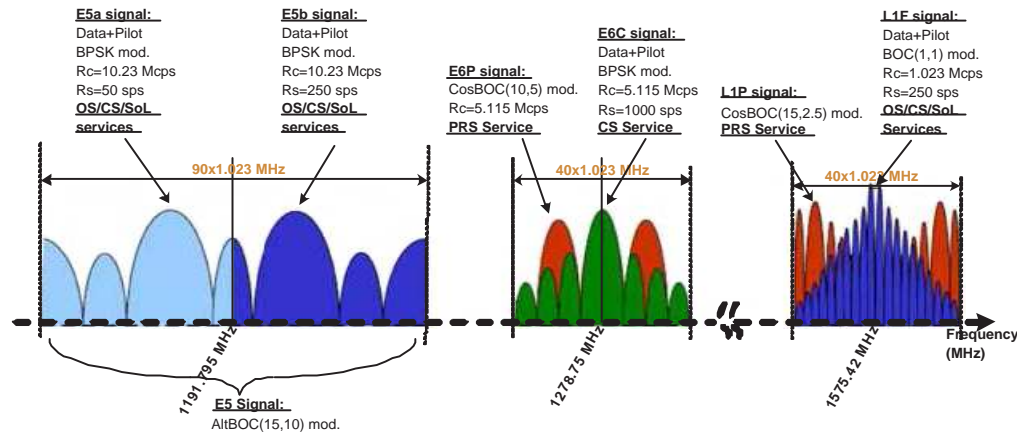


Figure 2.1: Galileo frequency plan GJU 2005 [67].

Table 2.3 shows a summary of Galileo signal specifications, as proposed in 2005 and specified in Galileo Joint Undertaking documents [68], such as the modulation types, chip rates, possible availability of pilot signals, data symbol rates and the code length for each Galileo signal. Compared to GPS, the code length for the OS signal was chosen as 4092 chips (i.e., four times longer than the GPS C/A code length), while for the E5 signals, the code length was proposed to be 10230 chips. Also, higher data symbol rates have been specified for Galileo (i.e.,

Table 2.3: Galileo signal structures (as of 2005).

Galileo signals	RF	Modulation type	Chip rate [MHz]	Pilot availab.	Data symb. rate	Code length [chips]
L1F (OS/CS/SoL)	L1	SinBOC (1,1)	1.023	Yes	250 sps	4092
L1P (PRS)	L1	CosBOC (15,2.5)	2.5575	N/A	N/A	N/A
E6C (CS)	E6	BPSK (5)	5.115	Yes	1000 sps	N/A
E6P (PRS)	E6	CosBOC (10,5)	5.115	N/A	250 sps	N/A
E5A (OS/CS/PRS)	E5	BPSK (10)	10.23	Yes	50 sps	10230
E5B (OS/CS/PRS)	E5	BPSK (10)	10.23	Yes	250 sps	10230

between 50 and 1000 sps) and the presence of data-less signals (pilot signals). A new multiplexing scheme (which represents the modulation type by which two signals are combined), the Alternate BOC (AltBOC) multiplexing, was proposed for E5 signals [67]. The modulation type proposed for L1F OS signal (as of 2005) was the SinBOC(1,1) [68]. For L1P PRS signals the cosine BOC(15,2.5) (denoted as CosBOC(15,2.5)) was chosen.

In accordance with the July 2007 agreement between the EU and the US, a Multiplexed Binary Offset Carrier (MBOC) waveform was selected as the candidate for Galileo OS signal and the future GPS L1C signal [70], [89]. The MBOC modulation ensures a better spectral separation with C/A codes and increases the tracking abilities of Galileo OS and GPS L1 civil signals [69], [79], [44], [127]. The MBOC modulation outperforms the SinBOC(1,1)-modulation on the L1 (data + pilot channels) frequency in mitigating the effects of multipath or reflected signals [89]. The MBOC is implemented either as a Composite BOC (CBOC) modulation (in the case of Galileo), with a superposition of BOC(1,1) and BOC(6,1), or as Time-Multiplexed BOC (TMBOC) modulation, as is planned for the GPS L1C signal [89]. Various characteristics of MBOC signal are described in [5], [7], [79]. According to the new standardization proposals [70], the MBOC modulation has been proposed to replace the SinBOC(1,1) modulation for OS signal.

The algorithms presented in this thesis focus on the sine- and cosine-types of BOC modulations, chosen as representative according to the current standardization documents at the time when the research was done [68]. These modulation types are illustrated in the next chapter.

Chapter 3

Modulation families and signal model for Galileo and modernized GPS signals

In this chapter, the BOC modulation concept is explained and exemplified, and the challenges brought in the synchronization process by this modulation are highlighted. An overview of received baseband signal model for Galileo and GPS signals is briefly presented, in context of transmission over multipath fading channels.

3.1 Binary Offset Carrier (BOC) modulated signal

The BOC modulation was introduced by Betz [15], [16] for the modernized GPS system. Since then, other variants of BOC modulation have also been considered, including SinBOC and CosBOC modulations types [15], [19], AltBOC modulation [78], Complex Double BOC modulation (CDBOC) [126] and Multiplexed BOC (MBOC) modulation [7], [79]. The negotiations for Galileo system structure under the terms of US/EC agreement in 2005 [68], proposed the use of SinBOC(1,1) for the L1 OS signal, which was one of the BOC modulations considered during this work.

A BOC-modulated signal is the product of a Non-Return-to-Zero (NRZ) spreading code [83] with a synchronized square wave subcarrier, which can be either sine or cosine phased. The typical notation of a BOC-modulated signal is $\text{BOC}(f_{sc}, f_c)$, where f_{sc} is the subcarrier frequency in MHz and f_c is the chip rate in MHz [15]. For Galileo signals, the $\text{BOC}(m_1, m_2)$ notation is also used, where m_1 and m_2 are two parameters computed from f_{sc} and f_c with respect to the reference frequency $f_{ref} = 1.023$ MHz, $m_1 = \frac{f_{sc}}{f_{ref}}$ and $m_2 = \frac{f_c}{f_{ref}}$.

The ratio $N_{BOC_1} = \frac{2m_1}{m_2} = \frac{2f_{sc}}{f_c}$ denotes the BOC modulation order and is a

positive integer [125]. For example, $N_{BOC_1} = 2$ represents BOC(1,1) modulation case, while $N_{BOC_1} = 12$ represents BOC(15,2.5) modulation. A special case of BOC modulation is the BPSK modulation with $N_{BOC_1} = 1$. In order to consider the CosBOC modulation case, a second BOC modulation order N_{BOC_2} has been introduced, such that the SinBOC modulation corresponds to $N_{BOC_2} = 1$ and CosBOC modulation corresponds to $N_{BOC_2} = 2$ [125].

According to its original definition from [15] the SinBOC $s_{SinBOC}(t)$ waveform is defined as:

$$s_{SinBOC}(t) \triangleq \text{sign}\left(\sin\left(\frac{N_{BOC_1}\pi t}{T_c}\right)\right), 0 \leq t < T_c \quad (3.1)$$

where $\text{sign}(\cdot)$ is the signum operator and $T_c = 1/f_c$ is the chip period. Since the above waveform is a sequence of +1 and -1, the eq. (3.1) can be also re-written as in eq. (3.2), as explained in [125].

$$s_{SinBOC}(t) = p_{T_{B_1}}(t) \otimes \sum_{i=0}^{N_{BOC_1}-1} (-1)^i \delta(t - iT_{B_1}), \quad (3.2)$$

where $\delta(\cdot)$ is the Dirac pulse, \otimes is the convolution operator and $p_{T_{B_1}}(\cdot)$ is the rectangular pulse of amplitude 1 and support $T_{B_1} = T_c/N_{BOC_1}$.

The CosBOC-modulated signal can be expressed similarly, as the convolution between the modulating signal and the $s_{CosBOC}(t)$ waveform [125]:

$$s_{CosBOC}(t) \triangleq \text{sign}\left(\cos\left(\frac{N_{BOC_1}\pi t}{T_c}\right)\right), 0 \leq t < T_c \quad (3.3)$$

This can be re-written, equivalently:

$$\begin{aligned} s_{CosBOC}(t) &= p_{T_{B_1}}(t) \otimes \sum_{k=0}^1 \sum_{i=0}^{N_{BOC_1}-1} (-1)^{i+k} \\ &\times \delta\left(t - iT_{B_1} - \frac{kT_{B_1}}{2}\right), \end{aligned} \quad (3.4)$$

As follows from eq. (3.4), the CosBOC modulation acts as a two-stage BOC modulation, in which the signal is first SinBOC modulated, and then, the sub-chip is further split into two parts. The following generation can be straightforwardly inferred [125], [126]:

$$\begin{aligned}
s_{DBOC}(t) &\triangleq p_{T_B}(t) \otimes \sum_{k=0}^{N_{BOC_2}-1} \sum_{i=0}^{N_{BOC_1}-1} (-1)^{i+k} \\
&\times \delta(t - iT_{B_1} - kT_B),
\end{aligned} \tag{3.5}$$

where DBOC stands for Double-BOC modulation [125] and $p_{T_B}(\cdot)$ is the rectangular pulse of amplitude 1 and support $T_B = T_c/(N_{BOC_1}N_{BOC_2})$, expressed as:

$$p_{T_B} \triangleq \begin{cases} 1, & \text{if } 0 \leq t < \frac{T_c}{N_{BOC_1}N_{BOC_2}} \\ 0, & \text{otherwise} \end{cases} \tag{3.6}$$

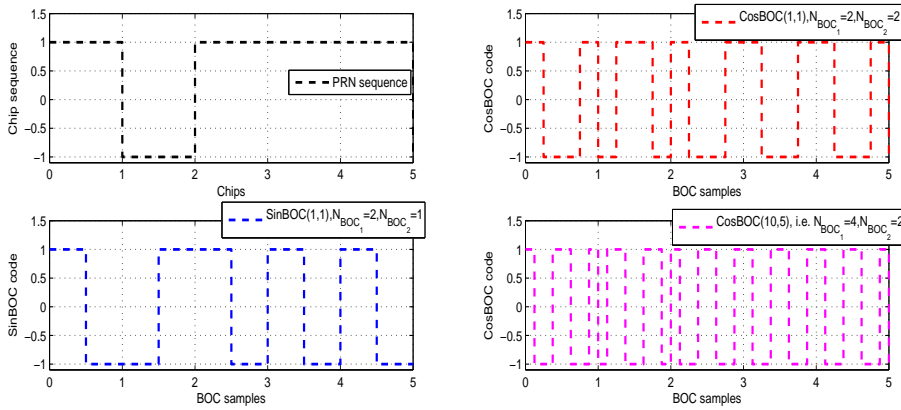


Figure 3.1: Examples of time-domain waveforms for SinBOC- and CosBOC-modulated signals.

The DBOC concept covers both SinBOC and CosBOC modulations, which are particular cases of eq. (3.5), where $N_{BOC_2}=1$ represents the SinBOC case and $N_{BOC_2}=2$ represents the CosBOC case. Thus the N_{BOC_2} can be seen as the BOC-modulation order of the second stage, which, together with N_{BOC_1} and f_c parameters generalizes the DBOC modulation for both SinBOC and CosBOC cases [125]:

$$\begin{cases} N_{BOC_1} = 1, N_{BOC_2} = 1, & \Rightarrow DBOC \equiv BPSK \\ N_{BOC_1} > 1, N_{BOC_2} = 1, & \Rightarrow DBOC \equiv SinBOC \\ N_{BOC_1} > 1, N_{BOC_2} = 2, & \Rightarrow DBOC \equiv CosBOC \end{cases} \tag{3.7}$$

Examples of time-domain waveforms for SinBOC ($N_{BOC_2}=1$) and CosBOC-modulated signals ($N_{BOC_2}=2$) are shown in Fig. 3.1.

A DBOC-modulated signal $x(t)$ can thus be seen as the convolution between a DBOC waveform $s_{DBOC}(t)$ and a spread data modulated sequence $d(t)$ as in eq. (3.8) [126].

$$\begin{aligned}
x(t) &= \sum_{n=-\infty}^{+\infty} b_n \sum_{k=1}^{S_F} c_{k,n} s_{DBOC}(t - nT_{sym} - kT_c) \\
&= s_{DBOC}(t) \otimes \sum_{n=-\infty}^{+\infty} \sum_{k=1}^{S_F} b_n c_{k,n} \delta(t - nT_{sym} - kT_c) \\
&\triangleq s_{DBOC}(t) \otimes d(t),
\end{aligned} \tag{3.8}$$

where b_n is the complex data symbol corresponding to the n -th code symbol, T_{sym} is the symbol period, $c_{k,n}$ is the k -th chip corresponding to the n -th symbol, S_F is the spreading factor ($S_F = T_{sym}/T_c$), $\delta(t)$ is the Dirac pulse and s_{DBOC} is the DBOC waveform defined in eq. (3.5).

A generic way to express the normalized Power Spectral Density (PSD) for BPSK, SinBOC and CosBOC cases is provided in [125]. The PSDs $P_{DBOC}(f)$ of DBOC-modulation family are computed, using eq. (3.5), as follows:

1. If $N_{BOC_1} = \text{even}$ and $N_{BOC_2} = \text{odd}$:

$$P_{DBOC}(f) = \left(\frac{\sin(\pi f T_B) \sin(\pi f T_c)}{\pi f \cos(\pi f T_B)} \right)^2 \tag{3.9}$$

2. If $N_{BOC_1} = \text{even}$ and $N_{BOC_2} = \text{even}$:

$$P_{DBOC}(f) = \left(\frac{\sin(\pi f T_B) \sin(\pi f T_{B_1}) \sin(\pi f T_c)}{\pi f \cos(\pi f T_B) \cos(\pi f T_{B_1})} \right)^2 \tag{3.10}$$

3. If $N_{BOC_1} = \text{odd}$ and $N_{BOC_2} = \text{odd}$:

$$P_{DBOC}(f) = \left(\frac{\sin(\pi f T_B) \cos(\pi f T_c)}{\pi f \cos(\pi f T_B)} \right)^2 \tag{3.11}$$

4. If $N_{BOC_1} = \text{odd}$ and $N_{BOC_2} = \text{even}$:

$$P_{DBOC}(f) = \left(\frac{\sin(\pi f T_B) \sin(\pi f T_{B_1}) \cos(\pi f T_c)}{\pi f \cos(\pi f T_B) \cos(\pi f T_{B_1})} \right)^2 \tag{3.12}$$

where $T_B = \frac{T_c}{N_{BOC_1} N_{BOC_2}}$ and $T_{B_1} = \frac{T_c}{N_{BOC_1}}$.

An alternative way of defining PSD (instead of $P_{DBOC}(f)$) is to normalize it with the chip period (or, equivalently, the signal power over infinite bandwidth), similar with [78], [15], [16]:

$$P_{DBOC,norm}(f) = \frac{P_{DBOC}(f)}{T_c} \quad (3.13)$$

Using the normalized expression of eq. (3.13), for $N_{BOC_2} = 1$, the same expressions as reported in [78], [15] are obtained for SinBOC modulation.

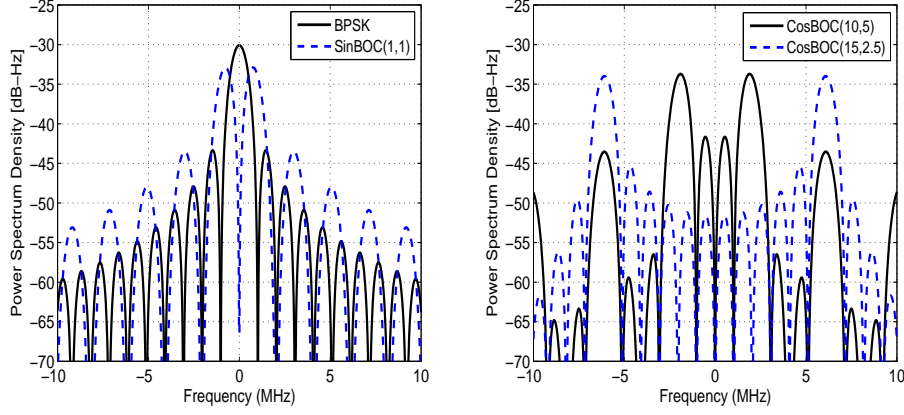


Figure 3.2: Examples of power spectral densities for BOC-modulated signals.

Fig. 3.2 illustrates some examples of the normalized PSD, computed according to [125]. It can be observed that for even N_{BOC_1} modulation orders, the spectrum is symmetrically split into two parts, thus the signal energy is moved away from the band center. Therefore, there is less interference with the C/A GPS band (i.e., BPSK case) and the desired spectral separation is obtained [166]. Also, it should be mentioned here that in case of odd BOC modulations, the interference around DC frequency is not completely suppressed.

The ACF of a DBOC waveform can be derived based on eq. (3.5) [121]:

$$\begin{aligned} \mathcal{R}_{DBOC} &\triangleq s_{DBOC}(t) \otimes s_{DBOC}(t) \\ &= \Lambda_{T_B}(t) \otimes \sum_{k=0}^{N_{BOC_2}-1} \sum_{j=0}^{N_{BOC_2}-1} \sum_{i=0}^{N_{BOC_1}-1} \sum_{l=0}^{N_{BOC_1}-1} (-1)^{k+j+i+l} \\ &\quad \times \delta(t - iT_{B_1} + lT_{B_1} - kT_B + jT_B), \end{aligned} \quad (3.14)$$

where $\Lambda_{T_B}(t)$ is the triangular pulse of support $2T_B$ (i.e., the ACF of a rectangular pulse of support T_B).

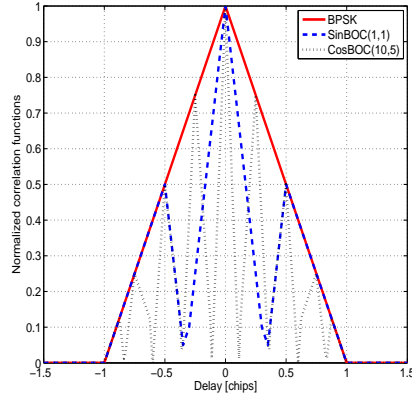


Figure 3.3: Examples of absolute value of ACF for BPSK and BOC-modulated signals.

Illustration of absolute values of the ideal ACF (i.e., without noise and multipath), for several BOC-modulated PRN sequences, together with the BPSK case, are shown in Fig. 3.3. As illustrated, for any BOC-modulated signal, there are multiple peaks with significant magnitudes compared with the magnitude of the central peak. For example, the sidelobes of a SinBOC-modulated signal appear at the delays given by $\tau_{sidelobes} = \arg \max_{\tau} (s_{DBOC}(\tau))$, where $s_{DBOC}(\tau)$ is defined as in eq. (3.5). Compared to the BPSK situation, the envelope of a SinBOC(1,1)-modulated signal possesses two additional peaks at about ± 0.5 chips apart from the maximum peak, as it can be observed from Fig. 3.3. In general, there are $2N_{BOC_1} - 1$ sidelobes in the correlation function for SinBOC-modulated signals and $2N_{BOC_1} + 1$ for CosBOC-modulated signals. These sidelobes interfere with the channel paths and may create ambiguities, the most significant ones being those with the smallest delay relative to the global maximum [124]. The additional peaks which appear in ACF envelope within the two-chip interval may induce a missed detection due to a zero (or very low sampling point) and may thus lead to a longer acquisition time.

3.2 Baseband signal model in multipath-fading channels

Besides the challenges introduced by BOC modulation and the thermal noise added at the receiver front end, the transmission through the wireless channel adds other impairments, which should be accounted [158]. In an optimal transmission channel, without any reflections, there is one direct LOS path between the receiver

and transmitter. However, due to various obstacles encountered in the propagation environment, the components of transmitted signal reach the receiver's antenna through different paths. Thus, the received signal is the superposition of multiple copies of the transmitted signal. Each signal copy will experience differences in attenuation, delay and phase shift and this can result in either constructive or destructive interference, amplifying or attenuating the signal power seen at the receiver [178], [75], [150], [174]. The fluctuations in the envelope of a transmitted radio signal are referred either as small-scale or as large-scale fading. The large-scale fading propagation models refer mainly to path loss and shadowing. The path loss is the difference between the transmitted power and the average received power and it represents the signal level attenuation caused by free space propagation, reflection, diffraction and scattering [163]. Shadowing or slow shadow fading is a result of obscuration by i.e., buildings, hills or trees, which weaken or even block the transmitted signal [163]. The small-scale fading, often referred as fading, is used to describe the rapid fluctuations of the amplitude of a radio signal over a short period of time or travel distance, so that large-scale path loss effects may be ignored. The fading is affected by multipath propagation, since the instantaneous received signal strength is a sum of many contributions coming from different directions due to many reflections of the transmitted signal reaching the receiver. Also the movement of the satellite in comparison with the GNSS receiver creates some frequency or Doppler shift to the code and carrier frequencies of the received signal [99]. Another factor which influences over fading is the transmission bandwidth of the signal. If the transmitted signal bandwidth is greater than the bandwidth of the multipath channel, the received signal will be distorted, but the fast fading in the received signal strength is not significant. The bandwidth of the multipath channel is characterized by the coherence bandwidth, which is a measure of the maximum frequency difference for which signals are still strongly correlated in amplitude. For example, if the transmitted signal has a narrower bandwidth as compared to the channel, the amplitude of the signal might change rapidly but the signal will not be distorted in time. Thus, in addition to the bandwidth of the transmitted signal, the statistics of fast fading are very much related to the specific amplitudes and delays of multipath channels.

In this work, the discrete linear time-variant model for the channel impulse response is used. The motivation came from the fact that linear models are much simpler to simulate and analyze than the non-linear ones. Moreover, the channel modeling with a finite number of taps is more convenient and natural for computer simulations and has been proved to cover a multitude of wireless propagation scenarios [139], [133]. Fading phenomenon can be modeled via the so-called fading channel coefficients for linear time-variant model, which reflect the severity of the fading phenomenon. Depending on the environment of the signal propagation, these coefficients follow different distribution models. In the case of at least one strong LOS signal path and possible weaker NLOS paths, the fading channel

distribution is typically assumed to be Rician [178]. However, in case of NLOS propagation paths, the received signal fading typically follows a Rayleigh distribution [139]. This distribution has deeper fading fluctuation than Rician fading and is used to characterize dense urban area or indoor environments. A generic model of fade statistics used in the study of mobile radio communications is the Nakagami or m-distribution [136]. This fading distribution often gives the best fit to land-mobile and indoor mobile multipath propagation as well as scintillating ionospheric radio links [178]. More recent studies showed that Nakagami-m distribution gives the best fit for satellite-to-indoor radio wave propagation [107], [108].

If one of the reflected signals components is added constructively to one of the sidelobes peaks, which are due to BOC modulation, the amplitude of this sum might be larger than the LOS component and might be wrongly detected instead of the peak at the correct delay. Also, the arriving paths may overlap or be closely-spaced (i.e., at less than one chip apart), thus more strain is imposed on the acquisition process, since a resolution less than half of a chip is needed in order to locate correctly the mobile receiver.

The baseband equivalent model of a signal received over a static or fading multipath channel, assuming a single-user model, can be expressed as:

$$r(t) = \sum_{l=1}^L \alpha_l x(t - \tau_l) e^{-j2\pi f_D t} + \eta(t), \quad (3.15)$$

where f_D is the Doppler shift introduced by channel, L is the number of channel paths, α_l is the complex time-varying coefficient of the l -th path during n -th code epoch, τ_l is the corresponding path delay, assumed to be constant or slowly varying during the observation interval and $x(\cdot)$ is the DBOC-modulated data sequence (given in eq. 3.8). One symbol is equivalent with a code epoch and typically has a duration of 1 ms. For Galileo signals, a separate pilot channel with data bits is transmitted, thus the modulation data is known at the receiver [67]. Due to both satellite and user dynamics, the incoming signal is distorted by a Doppler shift. The variation of ranging code chip rate due to this code phase error produces an additional error in the pseudorange and carrier phase measurements. The degradation of the code phase measurements due to this code Doppler offset is not considered in this model. All interference sources, except the multipath, are incorporated into the Additive White Gaussian Noise (AWGN) term $\eta(t)$. Usually, in GNSS applications the Signal-to-Noise Ratios (SNR) are expressed using the Carrier-to-Noise Ratios (CNR) term [24], which is used to report the signal quality and can be expressed in dB-Hz units (eq. 3.16) or in dBm units (eq. 3.17):

$$CNR[dB - Hz] = \frac{E_b}{N_0} + 10 \log_{10}(BW), \quad (3.16)$$

$$CNR[dBm] = \frac{E_b}{N_0} + 20\log_{10}(BW) + 10\log_{10}(kT_0), \quad (3.17)$$

where E_b represents the bit energy or signal power, N_0 is the two-sided PSD of the additive Gaussian noise, BW is the signal bandwidth after despreading, k is the Boltzmann constant ($k = 1.3806503 \times 10^{-23}$ Joule/Kelvin) and T_0 is the room temperature in Kelvin ($T \approx 290K$).

The SNR is usually defined as the SNR at the receiver's antenna input. In this thesis we consider the SNR after integration of 1 ms (in narrowband domain, i.e. at a rate of 1 kHz). Normalizing double-sided noise bandwidth to 1 Hz, we get a $10\log_{10}(1000)=30$ dB offset. Therefore, the relationship between the CNR (in dB-Hz) and narrowband PSD N_0 is:

$$CNR[dB - Hz] = \frac{E_b}{N_0} + 30dB, \quad (3.18)$$

At the receiver, both acquisition and delay tracking stages are based on code epoch-by-epoch correlation $\mathcal{R}(\cdot)$ of received signal with a reference BOC-modulated PRN code $s_{ref}(\cdot)$, with a certain candidate of Doppler frequency \hat{f}_D and code delay $\hat{\tau}_l$:

$$\mathcal{R}(\hat{\tau}_l, \hat{f}_D, m) = \mathbf{E} \left(\frac{1}{T_{sym}} \int_{(m-1)T_{sym}}^{mT_{sym}} r(t) s_{ref}(\hat{\tau}_l, \hat{f}_D) dt \right), \quad (3.19)$$

where m is the code epoch index, T_{sym} is the code symbol period, $\mathbf{E}(\cdot)$ is the expectation operator with respect to the PRN code and the reference code $s_{ref}(\cdot)$ is given as:

$$\begin{aligned} s_{ref}(\hat{\tau}_l, \hat{f}_D) &= \left(s_{DBOC}(t) \otimes \sum_{n=-\infty}^{+\infty} \sum_{k=1}^{S_F} \hat{b}_n c_{k,n} \delta(t - nT_{sym}) \right. \\ &\quad \left. - kT_c \right) \otimes p_{T_B}(t) e^{+j2\pi\hat{f}_D t}, \end{aligned} \quad (3.20)$$

where \hat{b}_n are the estimated data bits. The noise level can be further reduced by typically performing coherent and non-coherent integrations. The averaged non-coherent correlation function $\bar{\mathcal{R}}(\cdot)$ can be expressed as:

$$\bar{\mathcal{R}}(\hat{\tau}_l, \hat{f}_D) = \frac{1}{N_{nc}} \sum_{N_{nc}} \left| \frac{1}{N_c} \sum_{m=1}^{N_c} \mathcal{R}(\hat{\tau}_l, \hat{f}_D, m) \right|^2, \quad (3.21)$$

where N_c is the coherent integration time (expressed in code epochs or ms for GPS/Galileo signals) and N_{nc} is the non-coherent integration time, expressed in blocks of length N_c ms.

Two examples of averaged correlation function as expressed by eq. (3.21), for two BOC-modulated signals (SinBOC(1,1), left plot, and CosBOC(10,5), right plot) are shown in Fig. 3.4. In the upper figures, the signal is sent through a 2-paths Rayleigh channel with average path powers 0 and -1 dB, and assuming infinite bandwidth. The successive channel path delays have a random spacing with respect to the precedent delay, with the separation between the two successive paths fixed at 0.5 chips in the left plot and at 0.25 chips in the right plot, respectively. The same signals, not affected by multipath, are shown for reference in the lower plots. As it can be observed, besides the sidelobe ambiguities brought by BOC modulation process, the estimation delay is also strained by the multipath effect which may skew the triangular shape of the ACF pulse.

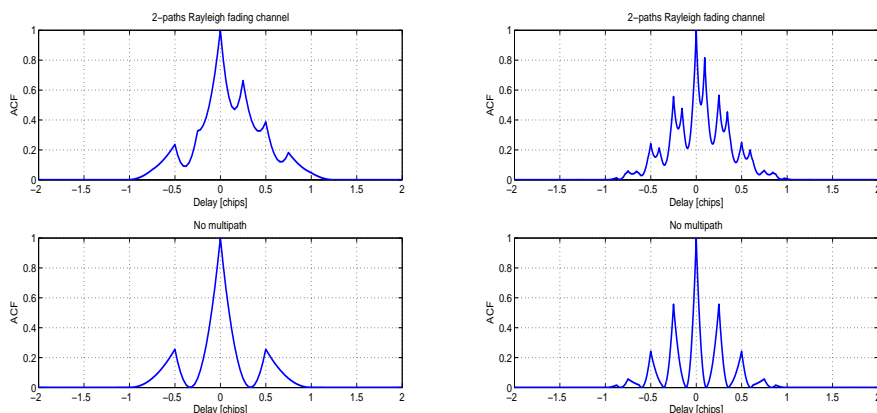


Figure 3.4: Illustration of multipath effect on BOC-modulated correlation function, 2-paths Rayleigh fading channel (upper plots) and no multipath (lower plots). Left plots: SinBOC(1,1). Right plots: CosBOC(10,5).

A basic Galileo or GPS receiver block diagram is shown in Fig. 3.5. The antenna receives the satellite signal and passes it to the RF chain, where a combination of amplifiers, mixers and filters is used to condition the incident voltage of the antenna and to perform the desired frequency translation. The final component in the front-end path is the Analog-to-Digital Converter (ADC), which is used to convert the analog signal to digital samples. Although not depicted, many GNSS front-end designs use an automatic gain control, which is a feedback monitoring of sampled data stream in order to minimize the impact of narrow-band interference [23]. In order to preserve transmitted information, the sampling

process is of crucial importance, since the sampling resolution affects further the timing accuracy. Sampling the received signal using low-pass sampling, the usual interpretation of Nyquist sampling theorem, requires a sampling rate of twice the maximum frequency of interest. When designing the frequency plan of the receiver, the sampling rate is restricted by the maximum IF frequency that can be generated by the carrier Numeric Controlled Oscillator (NCO) in order to mix the incoming signal to baseband and by the maximum signal bandwidth [23].

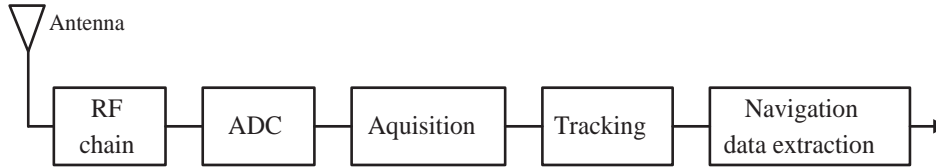


Figure 3.5: Basic block diagram of a Galileo/GPS receiver.

In order to capture the necessary signal power, the minimal signal plus noise bandwidth should contain at least the main lobes, where the most signal energy is concentrated. As it can be seen in Fig. 3.2, for higher BOC orders, the signal needs extremely large bandwidths. This leads to a more complex design, the goal being to minimize the number of intermediate stages, therefore minimizing the required RF and IF local oscillators [26], [34]. In advanced software receiver designs, the ADC should be placed as near as possible to antenna, being a key component of any architecture which uses direct digitization of RF signal, or after an initial down-conversion to an intermediate frequency. Since the ADC will operate at high frequencies, it consumes a great deal of power and it has limited real-time performance. More efficient conversion methods have been employed, such as bandpass sampling, which intentionally alias the information bandwidth of RF signal to a desired intermediate frequency [4]. A direct RF sampling front-end design for multiple frequency receiver is presented in [187], which intentionally uses aliasing, instead of frequency down conversion. In [144], [145], [146] it is shown that the Nyquist criterion does not need to be fulfilled when tracking the navigation signals. Instead, it is sufficient to reconstruct the signal autocorrelation function, at the cost of a higher tracking error due to thermal noise. In this work, the translation of RF carrier to lower IF is not considered and instead of the bandpass signal model, a baseband-equivalent signal is assumed. For this simplified receiver structure, the sampling process is considered to take place at baseband.

Even if, due to a lower computational complexity, low sample rates are often used, lowering the sample rate to the Nyquist rate will increase the additional multipath error, which is inversely proportional to the sample rate [29]. Besides the BOC modulation and multipath, the frequency bandwidth limitation also affects the shape of correlation function, by smoothing or flattening it around peaks. This

smoothing is prone to increase the delay errors in a similar way as lowering the sampling rate [29]. A low sampling frequency receiver would be more likely to have serious ACF distortion (due to low resolution in time domain) and higher background noise that will eventually pass into the tracking loop [203]. Also, the application of minimum-phase-type filters can impact on ACF shape, by skewing and delaying it [31]. The bandlimiting filtering effects and filter's design for BOC-modulated signals are described in detail in Chapter 6.

Since not all samples would fall on the peak of correlation function, correlation losses will occur due to time quantization of the correlation function [38]. If the time quantization effects are not eliminated, the introduced self-interference time errors will degrade the receiver's final positioning performance [30]. Therefore, one important parameter, which affects the timing accuracy and hence the receiver performance, is the sampling resolution of correlation function. In order to achieve the desired delay accuracy in acquisition and tracking processes, oversampling may be used. One alternative solution to oversampling is interpolation [30]. Oversampling improves the time domain resolution of the amplitude and phase of the sampled signal. The continuous-time signal model approximates the equivalent discrete-time model fairly well when the signal is oversampled [149]. For a GPS receiver (which typically uses a time-bin step of half of chip), in the best case, the signal is sampled at minus one-half chip error, at no error and at plus one-half chip error. Since one sample is on the peak (zero error), there is no loss in this case. However, the worst case is when the signal is sampled at minus one-fourth chip error and plus one-fourth chip error and in this case there is a loss of the two samples of 2.5 dB, when an unfiltered correlation curve is considered [38].

The sample rate can be expressed in terms of samples-per-chip. For a DBOC-modulated signal, one chip consists of $N_{BOC_1} N_{BOC_2} N_s$ samples [126], where N_s denotes the oversampling factor or the number of sub-samples per BOC sub-chip interval, which can be an integer or fractional number and BOC sub-chip interval has a duration $T_c / (N_{BOC_1} N_{BOC_2})$. The normalized sampling rate corresponds to $N_{BOC_1} N_{BOC_2} N_s f_c$ bandwidth. As stated in [29], the least multipath error contribution situation will originate when the highest possible oversampling is applied, while using a receiver filter that lets to pass only the signal-in-space spectrum. The acquisition speed and performance depend on the step of scanning all possible code phases (i.e., the time-bin step). In a conventional hardware implementation the correlation spacing can also be seen as the resolution at which the correlation function is sampled [38]. The behavior of BOC-modulated signals in the presence of oversampling has been analyzed in [P1], where it was shown that the performance is deteriorated if non-integers factors are used. In the presence of BOC modulation, there are always periodical deep gaps in the ACF at certain delay-lags, which depends on the time-bin step and on BOC modulation order. Sufficient performance can be obtained if these parameters are chosen ac-

cordingly.

The next two chapters will address the challenges triggered by the BOC modulation and by transmission over multipath fading channels, considering the signal acquisition and tracking stages, respectively.

Chapter 4

Acquisition of Galileo and GPS signals

In order to determine the difference between the transmission time from the satellite and the signal reception time, a GNSS receiver has to synchronize a locally generated reference code with the received signal. Thus, in any spread spectrum system, such as GPS or Galileo, in order to despread and demodulate the sent data, it is necessary to estimate the timing and frequency shift of the received signal. The synchronization process consists of two steps: acquisition and tracking [71], [179]. The purpose of signal acquisition process is to determine visible satellites and to achieve coarse values of the carrier frequency and code phase of the satellite signals. Similar with any CDMA-based receiver, the essential operations of signal acquisition are: achieving the acquisition state (this phase is also known as *search strategy*) and identifying the presence or absence of the signal, known also as *detection stage*.

This chapter provides an overview of the acquisition process in context of Galileo BOC-modulated signals and presents novel acquisition algorithms which deal with the BOC modulation ambiguities. Different search methods and detector structures are presented and the novel acquisition algorithms proposed in the papers [P4], [P5] and [P6] are then summarized.

4.1 Signal searching stage

The satellites are differentiated by different PRN sequences and the reference PRN code should be aligned with the incoming signal in order to determine the correct time alignment (i.e., the code phase) of PRN code. The PRN codes have high correlations near zero delay error. Therefore, the searching process is done through correlations, which measure the similarity of the code and its delayed replica. In an ideal case, without interference and noise, the correlation function would ap-

pear just as an impulse at the correct delay and would have zero values elsewhere. However, in practice, signal obstructions (buildings, trees, ice on antenna etc.), RF interference, and antenna gain roll-off affect significantly on the correlation output. The minimum expected CNR can be predicted if the receiver is equipped to measure the input signal noise and the RF interference, and the antenna gain pattern is stored in its memory [99].

The LOS velocity of the satellite with respect to the receiver causes a Doppler effect on transmitted signal. In the worst case, the frequency of a GPS receiver, moving at high speed, can deviate up to ± 10 KHz [23] from the carrier frequency f_c . Therefore, the search process is two-dimensional, and both the time shift (code phase) $\hat{\tau}_l$ of the transmitted signal and the Doppler frequency \hat{f}_D should be determined [99]. The search space is given by the length of the spreading code and by the Doppler frequencies uncertainties. Each tentative code phase is denoted as a code (or time) bin, each tentative frequency shift is referred to as a Doppler (or frequency) bin, and the combination of one code and frequency bin forms one cell. Depending on the searching methods, the whole code-frequency uncertainty space can be divided into several search windows and each window can contain several time-frequency bins. The time-frequency search window defines the decision region, over which the decision statistics are calculated [99]. A correct time-frequency window contains at least one correct bin, given that the reference code is aligned with less than one chip error to the incoming signal [153]. The search process starts with a certain tentative Doppler frequency and tentative delay, and all delays and frequencies of the search windows are covered, with a predefined search step. From the correlation output, it can be determined whether the search window is correct via a correlation peak, which appears for the correct $\hat{\tau}_l$ and \hat{f}_D [71]. Fig. 4.1 illustrates the two-dimensional correlation function for incorrect (i.e., signal not present, left plot) and correct (i.e., signal is present, right plot) search windows, for a static, single-path channel and a CNR of 30 dB-Hz.

The correlation output is tested in the detection stage, via a threshold comparison, in order to determine if a correct code-frequency combination is found. In noisy scenarios, the correlation peak may be lost in background noise. Another challenge in the acquisition process is given by the multipath propagation phenomenon. As explained in Section 3.2, due to different lengths of the propagation paths, the components of the same signal arrive at the receiver with different delays. The correlation output for a correct window and for a two-path Rayleigh fading channel is illustrated in Fig. 4.2, where a CNR of 30 dB-Hz was considered.

The acquisition is referred to as "cold start", if the receiver does not rely on any stored information and starts to search the satellites from scratch. If there is information regarding the almanac data, the last computed position and the current time, the acquisition is referred as "warm start". In this case, if the almanac data is outdated and the found satellites do not match the actual visible satellites, the

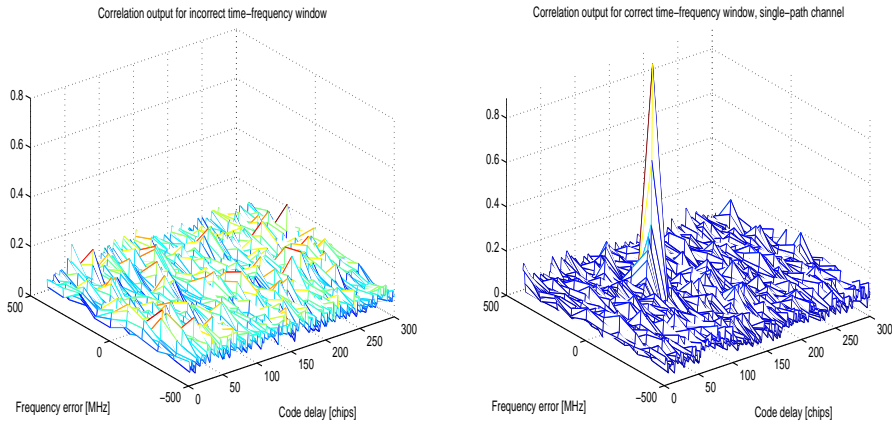


Figure 4.1: Examples of correlation outputs, single-path static channel.

receiver has to make a cold start [23].

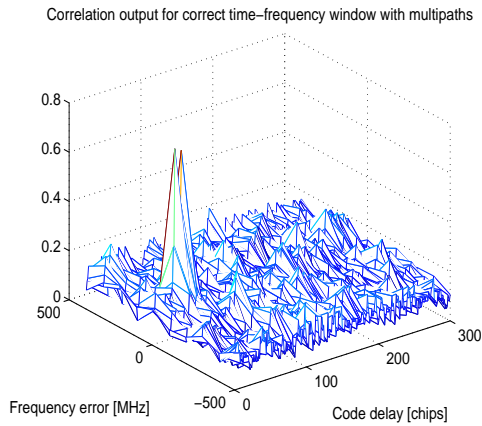


Figure 4.2: Example of correct time-frequency window, in the presence of fading multipath.

4.2 Serial search versus hybrid or parallel search

As mentioned in Chapter 2, the proposed PRN codes for Galileo system have higher lengths than those used by GPS C/A signals (i.e., 4092 chips for L1F signal). The use of longer codes leads to an increase in the uncertainty space, thus the search process becomes more time consuming. In order to obtain a more efficient

and faster signal acquisition in time-domain, various search methods have been developed, which can be classified as serial search, parallel search or combined (hybrid) serial/parallel search techniques.

The *serial search* explores in a sequential fashion all the possible values of frequency and time bins, to check if there is an alignment or not, by using a single correlating element at a time. Thus, this search method can take a long time if the uncertainty region is large and it is mostly used when there is some assistance information about the expected Doppler frequency and code delay [100]. A structured classification of serial strategies of CDMA signals and their analysis can be found, for example, in [143], [95], [153], [154] and [155]. Serial acquisition methods were also proposed in [129], which were specifically designed for BOC-modulated signals. Also, in [124], fast serial acquisition methods were introduced, which employed FFB processing.

In *parallel search* techniques based on parallel matched-filter (MF) implementation, more than one correlating element is used to explore simultaneously different regions and in an extreme case, there is one correlating element for every searching position (fully parallel search). A bank of matched filters is used, each matched to a different waveform pattern of PRN code, for all possible code phases and Doppler uncertainties [46]. The decision statistic is based on all outputs from all filters. Obviously, this approach will reduce largely the acquisition time, but it will increase the implementation complexity. Parallel code acquisition with MF in static channels and frequency non-selective or selective fading channels was studied in [181], [182], [184], [38].

More recent research studies have focused on the *hybrid search* strategies, as a better trade-off between the parallel and serial search strategies. The choice of a hybrid search structure is self imposing for CDMA systems with high code lengths, since it allows to achieve a proper balance between the acquisition speed and the hardware complexity, and it covers the serial- and parallel-search situations as two extreme cases [141], [156], [209]. In fully parallel search, there is only one window in the whole uncertainty space, while in serial search only one bin is used per window. Therefore, in case of maximum searching uncertainty (i.e., cold case), the fully serial-search would be too slow, while a fully parallel-search would be prohibitively expensive. In hybrid-search, it is assumed that the whole code-Doppler uncertainty space $(\Delta t)_{max} \times (\Delta f)_{max}$ is divided in several time-frequency windows, each containing N_{bins} . Here $(\Delta t)_{max}$ denotes the maximum code uncertainty in chips and $(\Delta f)_{max}$ represents the Doppler uncertainty in Hz. The number of time-frequency windows is given by $Q_{win} = \frac{(\Delta t)_{max} \times (\Delta f)_{max}}{W_t \times W_f}$, where W_t and W_f are the time and frequency window lengths. The window size is a trade-off between the mean acquisition time and the available number of correlators. In the hybrid search strategy, the number of bins per window is still limited by the available number of correlators that may be used to form the decision statistic [12]. Assuming that each correlator is used

once to form a decision statistic, the number of complex correlators per window $N_{corr} = \frac{W_t}{(\Delta t)_{bin}} \times \frac{W_f}{(\Delta f)_{bin}}$ is equal to the number of bins per window. The $(\Delta t)_{bin}$ and $(\Delta f)_{bin}$ denote the lengths of a time bin and of a frequency bin, respectively, or equivalently, represent the search step resolutions in time and frequency dimensions.

The usage of Fourier transform enables a faster and more effective acquisition, by parallel searching in either (or in both) code-phase and frequency dimensions. Instead of multiplying the input signal with the PRN code with different code-phases, as in serial search, it is more convenient to make a circular cross-correlation between the received signal and the PRN code without shifting the code phase [23]. Thus, the correlation with the reference code over one code epoch can be performed either in time domain [105], [3] or in frequency domain, using the Fast Fourier Transform (FFT) structure [204], [2], [160]. The FFT processing can be used also as a coherent integration method [1]. Different correlation structures, based on time-domain and/or FFT-based processing, are described in [140], where it is stated that the FFT correlation structures are the best choice for full search space in terms of complexity and performance. A new receiver architecture for acquisition of signals with high Doppler shifts is proposed in [183], in which, the partially correlated outputs are subject to FFT processing before being summed in a serial section.

4.3 Classical acquisition model

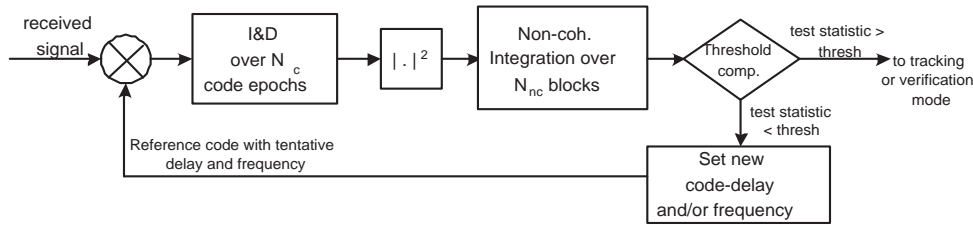


Figure 4.3: Simplified block diagram of an acquisition model.

Fig. 4.3 shows a simplified block diagram of the classical acquisition model. The incoming signal is multiplied by a locally generated PRN sequence, then multiplied by a locally generated carrier signal. The noise level can be further reduced by typically performing coherent and non-coherent integrations. The In-phase (I) and Quadrature-phase (Q) signals are integrated coherently over N_c code epochs (where N_c is the coherent integration period or coherent integration length). Integration is performed by the Integrate and Dump (I&D) block, which acts as a Low Pass Filter (LPF), by removing the higher frequency components from the signal.

For strong signals, a coherent integration period of 1ms (i.e., for C/A code) might be sufficient, but in order to improve the signal sensitivity, it is desirable to maximize the integration period and to get a higher correlation gain [211]. Extending the coherent integration time is ideal for improving the sensitivity, as it fully utilizes the potential of CDMA despreading gain [208]. Coherent integration allows for a narrow pre-detection signal bandwidth, thus enhancing the acquisition of weak signals in the presence of strong in-band interferers [210]. However, large frequency errors due to GPS receiver, satellites motions and oscillators drift degrade the CNR and may render long integration useless. Hence, when performing signal acquisition using long coherent integration, the receiver must use small frequency bins, thus the receiver would have to search a large number of frequency hypotheses. Moreover, due to data bit transition (i.e., in conventional GPS receivers) and large frequency errors, longer coherent integration is not possible. In GPS, coherent integration period is limited, in order to avoid crossing navigation message bit boundaries, data bit being 20 ms long. If the bit transition instant is known but not the polarity, the maximum coherent integration would be limited to 20 ms and consecutive non-coherent summations must be performed.

Normally, non-coherent integration is required after the coherent integration to detect weak signals. The advantage of non-coherently integrating the signal is that it requires neither knowledge of carrier phase nor precise carrier frequency, both of which are not available before the signal has been acquired [99]. However, with this approach the noise is also squared, resulting in what is known as squaring loss. The acquisition time varies directly proportional to the product of the coherent integration interval N_c , and to the number of non-coherent accumulations N_{nc} . The $N_c N_{nc}$ product is sometimes referred to as the dwell time per bin for a single search frequency.

4.4 Signal detection

The aim of the detection stage is to declare if the signal is present or absent, i.e., if there is coarse synchronization between the reference code and the received signal. The detection stage is a statistical process and in each time-frequency bin, the correlation output is a random variable which is characterized by a certain Probability Density Function (PDF). If the signal is absent, the decision variable contains only noise and the random variable, distributed according to this PDF, has zero mean under the assumption of zero-mean additive Gaussian distributed noise; if the signal is present, the random variable has a non-zero mean [101]. The test statistic is based on comparing the global correlation peak against a predefined threshold γ and a decision is taken whether the signal was acquired or not. If the signal energy in a time-frequency cell is greater than γ , then the signal is decided to be present in that cell. The signal is acquired correctly if at least one path delay

is detected within less than one chip error. The probability of a signal being detected correctly is denoted as probability of detection P_d , i.e., the probability that correlation output exceeds the threshold γ , under hypothesis that signal is present. A false alarm P_{fa} happens when the signal is declared present in an incorrect window, i.e., probability that the correlation output still exceeds the threshold γ , under hypothesis that the signal is absent. Assuming the situation of a hybrid acquisition search, the decision is taken over N_{bins} (forming a window), i.e., a single decision variable is formed per N_{bins} . If $N_{bins}=1$ then we have serial acquisition. The correlation outputs in N_{1bins} correct bins are distributed according to a non-central χ^2 -distributed variables with Cumulative Distribution Function (CDF) $F_{nc}(\gamma, \lambda_i)$. Here λ_i is the non-centrality parameter, which depends on CNR, on BOC modulation order and how far the sampling point i is from the maximum correlation value [104]. The ACF outputs in an incorrect bin are distributed according to a central χ^2 -distributed variables with CDF $F_c(\gamma)$ [27]. Assuming that there are no false alarms in a correct window, the global false alarm probability can be computed as the probability that at least one central χ^2 -distributed variable is higher than the detection threshold γ [27]. Therefore the false alarms and detection probabilities are given as [119]:

$$\begin{cases} P_{fa} = 1 - (F_c(\gamma))^{N_{bins}} \\ P_d = \mathbf{E}_\lambda \left(1 - \left(F_c(\lambda) \right)^{N_{bins} - N_{1bins}} \prod_{i=1}^{N_{1bins}} F_{nc}(\gamma, \lambda_i) \right) \end{cases} \quad (4.1)$$

where N_{1bins} is the number of correct bins in correct window, $\mathbf{E}_\lambda(\cdot)$ is the expectation operator with respect to the sequence of non-centrality parameters λ_i , $i = 1, \dots, N_{1bins}$ [119]. The definitions for CDFs χ^2 -distributed variables are expressed as [179]:

$$\begin{cases} F_{nc}(\gamma, \lambda) = 1 - Q_{N_{nc}} \left(\sqrt{\frac{\lambda N_{nc} N_{nc}}{N_0}}, \sqrt{\frac{\gamma N_{nc} N_{nc}}{N_0}} \right) \\ F_c(\gamma) = 1 - \sum_{k=0}^{N_{nc}-1} \exp \left(-\frac{\gamma N_{nc} N_{nc}}{2N_0} \right) \left(\frac{\gamma N_{nc} N_{nc}}{2N_0} \right)^k \frac{1}{k!} \end{cases} \quad (4.2)$$

where $Q_{N_{nc}}(\cdot)$ is the generalized Marcum Q-function of order N_{nc} .

A miss of detection occurs when the decision statistic falls below the threshold for a correct window and this might happen if the threshold is set too high or if the signal is lost into the background noise [101]. It follows that the choice of a suitable threshold value has a significant role in the acquisition process; it can be either a fixed value, selected based on the estimated signal power, or it can be computed adaptively, based on transmission channel conditions [140], [178]. A comparative study of different threshold setting techniques for DS-SS signals can

be found in [87] and the use of multiple thresholds has been also investigated in [111].

Besides the probabilities of detection and false alarm, one performance criterion, which can be employed also at acquisition stages, is the Root Mean Square Error (RMSE). The RMSE is selected for the comparison between the actual and the predicted delay and it is often used as performance measure in the delay estimation literature. If the RMSE of delay estimate is smaller than half of a chip, it can be concluded that code acquisition succeeds, but it does not tell how much time this takes. If there is no interest in how much time it takes to perform the acquisition, but rather in the success of the acquisition process, then the best performance measure for the time delay estimate, when comparing various acquisition algorithms, is the RMSE error. This fact has been recently argued in [159]. Also, RMSE has been traditionally used in many papers related to code synchronization (i.e., acquisition or acquisition plus tracking) in CDMA studies [117], [115], [206]. Sometimes, the RMSE is indeed conditional only to the points where acquisition was successful (e.g., less than half chip), but RMSE can be still a powerful criterion to compare the performance of various acquisition algorithms (either only for the points where they are 'successful', or for all the points, if no condition is imposed on the delay error).

Another representative measure of performance at acquisition stage is the Mean Acquisition Time (MAT), which is the average time to acquire the synchronization between the received signal and the spreading code. For example, the MAT for a serial search can be computed as in eq. (4.3), according to the global detection probability P_d , the false alarm probability P_{fa} , the penalty time K_p and the total number of windows in the search space Q_{win} [154]:

$$MAT = \frac{1 + (2 - P_d)(Q_{win} - 1)(1 + K_p P_{fa})}{2P_d} \tau_d, \quad (4.3)$$

where $\tau_d = N_c N_{nc}$ is the dwell time, if the code epoch is 1 ms as for Galileo and GPS [77] and N_0 is the noise variance after 1 ms integration. In order to compute the MAT, the false alarm probability is associated with some penalty factor K_p , which represents the time lost if a false alarm occur. A generic method to estimate the penalty factor according to the application has not been documented yet in the literature, a typical addressed range being between 1 and 10^6 [153], [147], [156].

If the SNR is high, it is easy to set a threshold that provides a low probability of false alarm (denoted here by P_{fa}) and also a low risk of missed detection. As the SNR is reduced, this is no longer possible due to significant overlap of signal distributions. One possible solution to decrease the acquisition time, is to dismiss the impossible code as soon as possible, by repeated observation on the same region, i.e., a multiple-dwell scheme. By introducing a second integration time (or multiple integration time), the correctness of the previous decision

can be verified, and hence, the false alarm case can be avoided more effectively. This multiple integration time (multiple-dwell) based idea was introduced in [41] and a comprehensive comparison between different multiple-dwell schemes was presented in [42], [53]. It was shown in [42] that the multiple-dwell approach typically yields a shorter mean and standard deviation acquisition time than the single dwell scheme, and this performance is enhanced when the false alarm penalty time is increased. Another approach is to use either a fixed or a variable dwell time detector [99]. A fixed dwell serial search, such as the M of N search detector [99] does not take advantage of any a priori knowledge of noise statistics in the channel and the same time is spent investigating synchronous cells as non-synchronous cells. A variable dwell time detector (known also as sequential detector) makes a Boolean decision that a signal is present based on predefined criteria, thus the integration time is a random variable, being short for non-synchronous cells and longer for synchronous cells. Therefore, using a variable dwell time serial search strategy, the time to dismiss each wrong epoch is usually less than the dwell time of a fixed dwell serial search synchronizer [165], [200], [84].

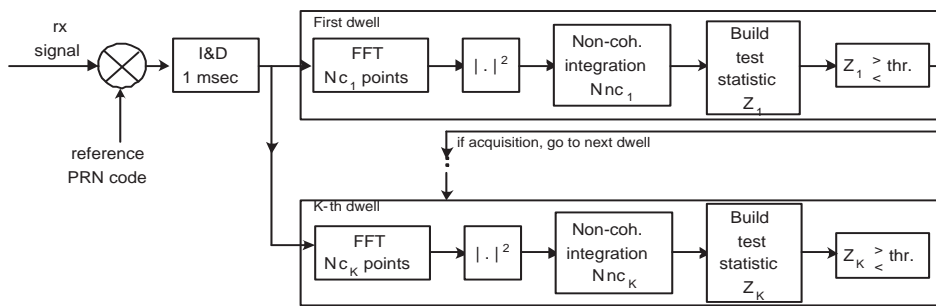


Figure 4.4: Block diagram of the multiple-dwell acquisition structure.

The block diagram of a multiple K -dwell acquisition structure is shown in Fig. 4.4. The coherent integration is performed in frequency domain, via an FFT block, for a faster scanning, in order to cover 1 kHz window length in frequency. The coherent N_{c_k} and non-coherent N_{nc_k} integration intervals may take different values for each dwell stage $k = 1, \dots, K$.

In [104] and [119], the choice of the best number of dwells for a hybrid-search strategy was discussed. In [104], it was shown that single-dwell architectures may still perform better than double-dwell structures, for some values of penalty factors associated with the false alarm rate. The same conclusion has been drawn also in [119], where it was stated that for low to moderate penalty factors, even a single dwell structure can provide sufficient good results, keeping thus the system complexity at minim. Moreover, besides aiming at a low acquisition time, there are constraints for the receiver system in order to attain a target global detection

probability and a target global false alarm, for any number of dwells K , i.e., $P_d = \prod_{k=1}^K P_d^{(k)}$ and $P_{fa} = \prod_{k=1}^K P_{fa}^{(k)}$. In some applications, it is interesting to fix both the detection and the false alarm probabilities from the beginning, and to vary the dwell time until the target performance (i.e., the target P_d and P_{fa} pair) is achieved. Therefore, the optimum detection and false alarm probabilities at each stage should be chosen in such a way to achieve a minimum MAT.

In this context, a comprehensive analysis of the choice of detection and false alarm probabilities at each stage of a double-dwell structure was proposed in [P2], by studying the average and maximum MAT behavior for different possible combinations of detection and false alarm probabilities at each dwell stage. If the $P_d^{(k)}$ and $P_{fa}^{(k)}$ parameters of a double-dwell structure are properly designed, the double-dwell structure is typically better in terms of MAT than a single dwell structure, when high penalty factors and low time-bin steps are used. For hybrid-search and multiple dwells, closed-form expressions of MAT are hard to find in literature. In [119] is one example, where MAT for multiple-dwells hybrid-search is derived. The traditional acquisition has been addressed until now, while the next two sections will present enhanced algorithms and methods that can be used to improve the acquisition performance.

4.5 Differential correlation methods

The Differential Correlation (DC) method has been proposed in the context of CDMA-based wireless communication systems in order to improve the acquisition process. Since the performance of non-coherent processing may be poor due to combining loss when correlation of matched filter is high, the differential method can be seen as a phase compensation method. A phase reference of the current matched filter output is provided by the previous matched filter output in the differential detection [91]. This approach offers an improved suppression of any temporally uncorrelated interferences, such as background noise and multi-access interference. Either coherent [91], [173], [208], [47], [175] or non-coherent differentially combining is used [142], depending on how the test statistic is constructed. For instance, one variant of differential correlation method multiplies each current predetection sample with the complex conjugate of the previous predetection sample, accumulates these products and takes the squared envelope at the very end, leading to the test statistic:

$$z_{DC} = \left| \frac{1}{M-1} \sum_{k=1}^{M-1} y_k^* y_{k+1} \right|^2, \quad (4.4)$$

where y_k are the outputs of coherent integration and M is the differential correlation length. For a fair comparison between conventional non-coherent and

differential correlation method, M needs to be set equal to N_{nc} , where N_{nc} is the non-coherent integration length. If prior differential processing, the coherent integration time is small enough, long time differential correlations can be exploited [142]. The acquisition variable of an enhanced method which takes advantage of the above property is given by eq. (4.5). Over the previous mentioned differential correlation method, this approach offers an improved suppression of any temporally uncorrelated interference [142].

$$z_{DC_2} = \left| \frac{1}{M-2} \sum_{k=1}^{M-2} y_k^* y_{k+1} + y_k^* y_{k+2} \right|^2, \quad (4.5)$$

The acquisition of BOC-modulated signals using differential correlation methods, in conjunction with the Sidelobes Cancellation Methods (SCM), were studied in publication [P9], where it was shown that these methods enhance further the performance when comparing to the traditional non-coherent processing. The performance of the non-coherent differential correlation methods is also presented in Appendix. The SCM method will be described in Chapter 5, Section 5.3.

4.6 Unambiguous acquisition of BOC-modulated signals

As shown in Chapter 2, the acquisition of BOC-modulated signals, based on the ambiguous correlation function, poses some challenges, which can be overcome by decreasing the search step of timing hypotheses. In order to detect the main peak of absolute value of ACF, the search step should be typically a quarter (or at most half) of the width of the main lobe. As this width is dependent on the N_{BOC_1} and N_{BOC_2} modulation orders, the acquisition becomes computationally expensive for higher BOC modulation orders. As an example, for CosBOC(15,2.5) case, proposed for Galileo PRS services, the width of the main lobe of ACF envelope is 0.08 chips, therefore a search step smaller than 0.04 chips should be used for accurate acquisition. Therefore the acquisition time will increase tremendously compared to the BPSK modulation case, where a step of 0.5 chips is typically used. In order to deal with the ambiguities of the ACF envelope and to allow the usage of a higher step in the acquisition process, various unambiguous acquisition techniques have been proposed recently. Among these there are: the 'Sideband correlation' or 'BPSK-like' approaches [10], [20], [63], [129], [81], and the Filter Bank-Based method [128], [123], which are detailed next. A SubCarrier Phase Cancellation Method (SCPC) was also proposed in [81] and extended in [177] to a Full-band Independent Code acquisition (FIC). The SCPC method is based on the idea of removing the sub-carrier from the received signal, after carrier removal. The FIC method was further analyzed in [176]. The SCPC method was implemented on a FPGA/DSP board in [28], which shows that this method offers lower

time to first fix compared with the 'BPSK-like' (or the 'Sideband Correlation') method. Another approach mentioned in [81] is the Very Early + Prompt method, which works on the basis that if the magnitudes of two correlation values of the BOC signal, separated by an appropriate delay, are combined, then it results in a correlation waveform whose shape is similar to the BPSK triangle.

4.6.1 'Sideband correlation' or 'BPSK-like' techniques

One of the families of unambiguous acquisition techniques introduced so far in literature uses single- or dual- sideband correlation and it was proposed by Betz, Fishman&al. (B&F) [10], [20], [63] and analyzed in [62], [122], [177]. The block diagram of the dual sideband correlation method (B&F) is shown in Fig. 4.5, with the spectrum exemplified for SinBOC(1,1) modulation case. The main lobe of one of sidebands of the received signal is selected via filtering and is correlated with the filtered BOC-modulated reference code, which is assumed to be real. In single sideband (SSB) processing approach, only one of the bands (upper or lower) is used. The SSB correlation method needs one complex sideband selection filter for the real reference code and two complex sideband selection filters for the received signal, which is complex. However, since the SSB approach suffers of SNR degradation and non-coherent integration losses [63], in order to compensate these losses, dual sideband processing (DSB) might be used, where both sidebands are kept and combined non-coherently. On the other hand, the DSB approach leads to a higher complexity, since the required number of filters is twice than in SSB processing. Since the effect of sub-carrier modulation is removed by using a pair (or a single) sideband correlators, the correlation function is no longer of a BOC-modulated signal, but it will resemble the ACF of a BPSK-modulated signal. However, due to filtering and correlation losses, there is a power degradation in the signal level compared to the BPSK case.

Another 'BPSK-like' method (M&H) proposed by Martin&al. [129] and by Heiries&al. [81], [82] selects both the main lobes and the lobes between them (if any), as shown in Fig. 4.6, for a SinBOC(1,1)-modulated signal and DSB processing. The reference code is the BPSK-modulated code, held at sub-sample rate and shifted with a quantity equal to the sub-carrier frequency $\pm f_{sc}$, or equivalently with $\pm \frac{N_{BOC1}}{2} f_c$, and not the filtered BOC-modulated reference code, as in the B&F approach. Compared to the sideband correlation method of B&F, this technique has the advantage that uses only one real filter for the complex received signal, for both SSB and DSB processing. This is equivalent with two real filters, one for the in-phase component and one for the quadrature-phase component. On the other hand, simulation results showed that, due to an improper shifting factor, the 'BPSK-like method' (M&H) is unable to cope with odd N_{BOC1} modulation orders [P4], [P5], [P6].

The performance of the unambiguous acquisition techniques depends, on one

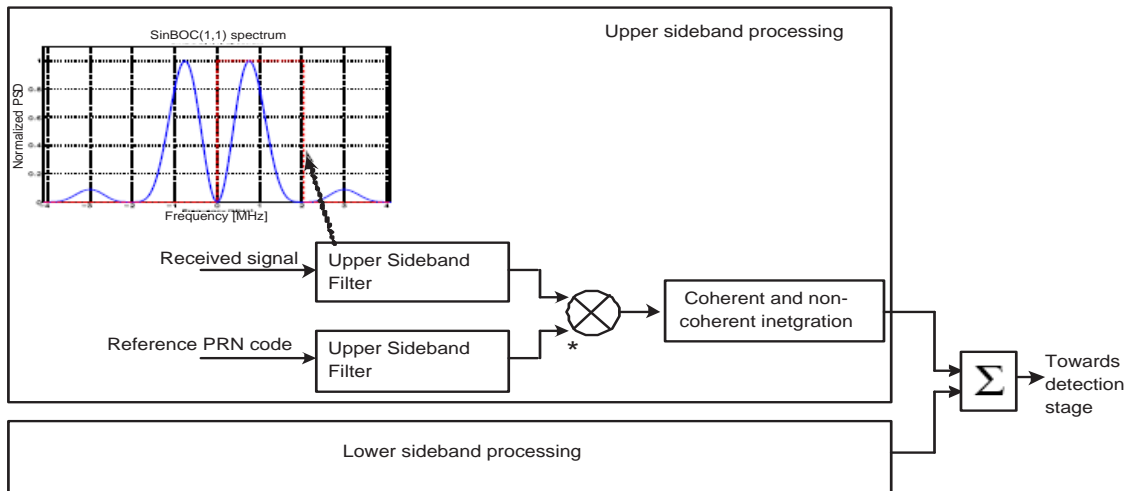


Figure 4.5: Block diagram of 'sideband correlation method' (B&F).

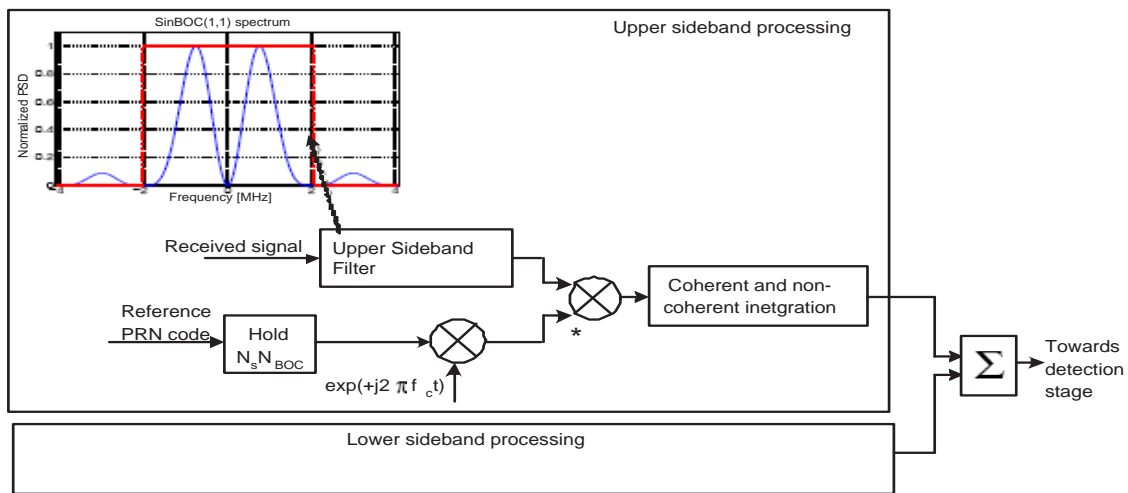


Figure 4.6: Block diagram of 'BPSK-like method' (M&H).

hand, on the correlation part, and on the other part, on the number of filters used for band selection. If the correlation is performed in time-domain and the reference code is a sequence of ± 1 , the complex multiplication between the received signal and the reference code can be performed just by additions and sign inversions, as explained in [105].

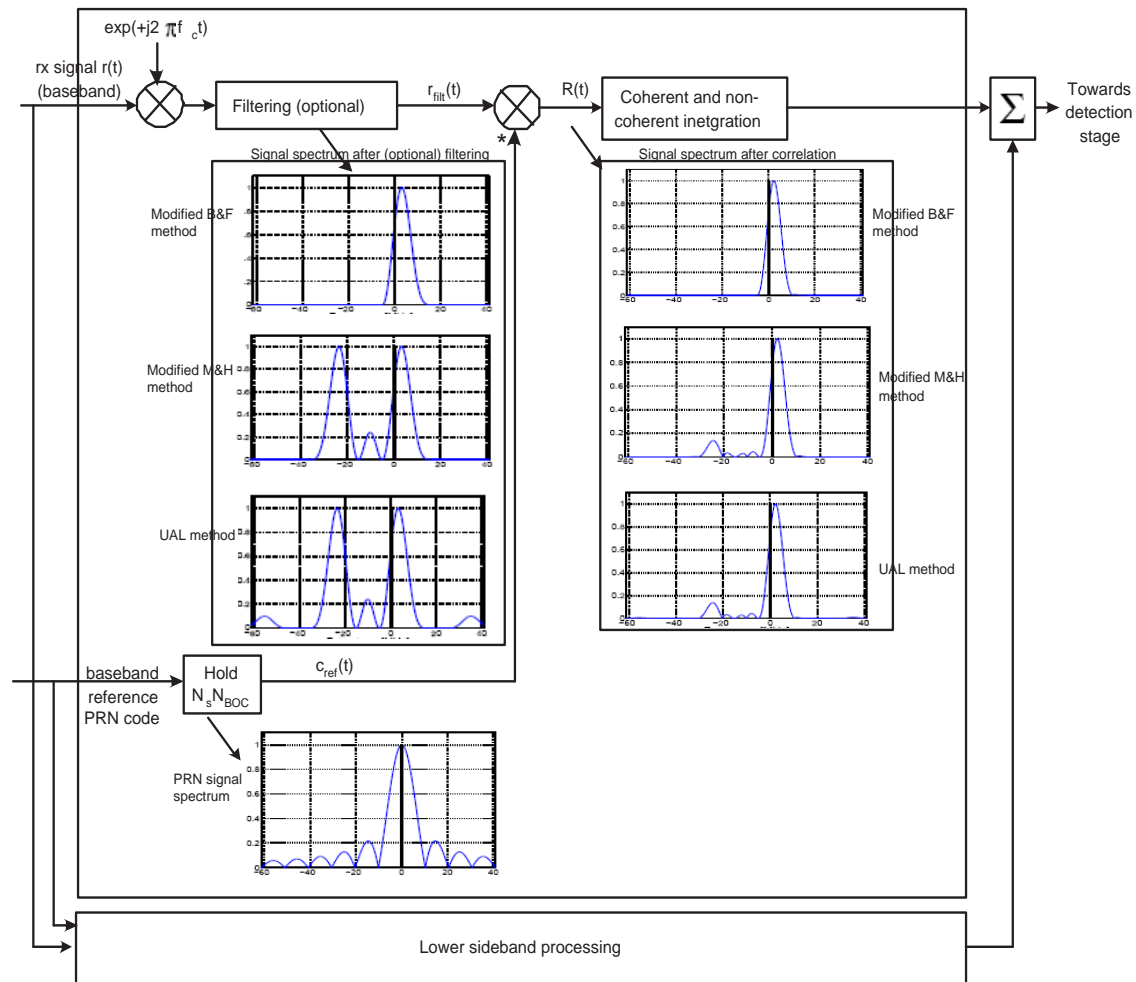


Figure 4.7: Block diagrams of proposed unambiguous acquisition methods.

Taking advantage of this time-domain correlation method, low complex unambiguous acquisition approaches have been proposed, which are modifications of B&F and M&H techniques [P4], [P5], [P6]. Besides reducing the complexity at correlation part, these unambiguous acquisition techniques attempt also to reduce the number of used filters. Their generic architecture is illustrated in Fig. 4.7 and

they are briefly revised in what follows. In order to take advantage of the correlation method from [105], these unambiguous algorithms use the BPSK-modulated PRN reference code of ± 1 . In contrast with B&F method, in the modified variant the main upper or lower lobes of the received signal are first shifted to zero frequency (with a shifting factor dependent on BOC-modulation order), then the upper and/or lower bands are selected via filtering. In the modified M&H method, the same processing is used, with the difference that both the main lobes and everything between them (if any) are selected [P4], [P5]. Using similar processing, but removing completely the filtering part, a third approach, the Unsuppressed Adjacent Lobes (UAL) method, was introduced in [P6]. This technique provides the lowest complexity, since no side-lobe filtering is needed, but on the other hand, the unsuppressed adjacent lobes may affect the performance of the acquisition block. Unlike the M&H method, the proposed unambiguous acquisition algorithms introduced in [P4], [P5] and [P6] can be applied to any sine and cosine, even and odd BOC-modulation order. Moreover, an improved acquisition structure can be obtained by inter-changing the places of the shifting unit with the filtering unit, since the number of filters used for sideband selection is thus reduced [P5].

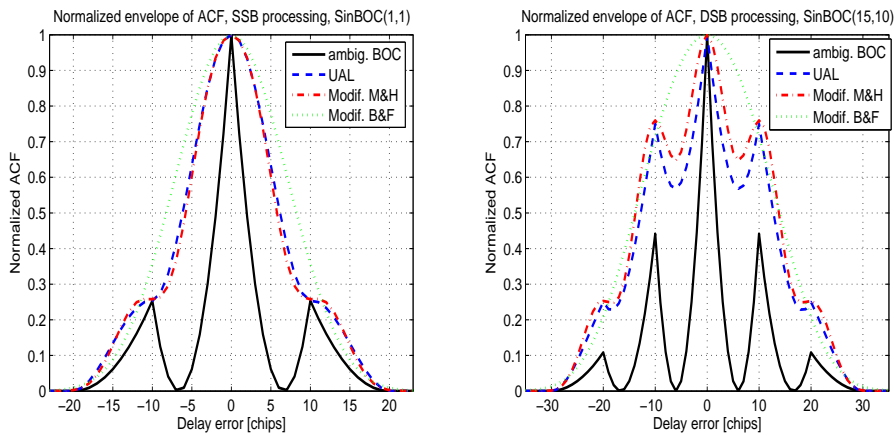


Figure 4.8: Illustration of normalized envelope of correlation functions after processing with the proposed low-complexity unambiguous methods.

The envelopes of normalized correlation functions after processing with the proposed low-complexity unambiguous methods are illustrated in Fig. 4.8, for an even BOC modulation order (SinBOC(1,1), left plot) and for an odd BOC modulation order (SinBOC(15,10), right plot), respectively. Both SSB and DSB processing are represented. As it can be observed, the 're-constructed' BPSK-like shape of correlation function eliminates the ambiguities introduced by BOC modulation and allows the use of a higher step in sweeping the uncertainty time,

which may speed up the acquisition process.

The complexity of the unambiguous acquisition methods depends on both correlation and filtering (sideband selection) parts. A detailed comparison of the estimated complexity of existing and proposed unambiguous acquisition methods was performed in publications [P5] and [P6]. In order to take advantage of the method proposed in [105], the correlation was considered to be performed in time-domain. The reference code was considered to be a sequence of ± 1 and due to this code structure, there were no multiplications involved, only additions and sign inversions were required [105]. As shown in [P5] and [P6], there is a trade-off between the complexity of the acquisition unit and the algorithm performance. For example, the B&F method has the best performance, but also the highest complexity, and the complexity of M&H approach is only slightly smaller than that of B&F algorithm. All three proposed algorithms (i.e., modified B&F, modified M&H and UAL) provide a significant decrease in complexity. The gap between the proposed and the existing methods' complexity increases with the assumed maximum delay search range. If the N_{BOC_1} order is sufficiently high, the best trade-off between the performance (in terms of detection probability and mean acquisition time) and the complexity is given by SSB UAL method [P6]. For lower N_{BOC_1} orders, the modified B&F approach has a similar performance with the original B&F method, while its complexity is significantly lower. Even if the most part in complexity reduction is due to correlation method, a further decrease in complexity can be obtained by choosing suitable filtering structures for sideband selection. The filtering impact in context of unambiguous acquisition method will be considered in Chapter 6.

4.6.2 Filter Bank-Based approaches

A generalized class of frequency-based unambiguous acquisition methods, the Filter-Bank-Based (FBB) approaches have been introduced and analyzed in [128] and [123]. The block diagram of the FBB method is shown in Fig. 4.9. There are $2N_{fb}$ filters used in the filter bank (with adjustable center frequency, and, possibly, adjustable width) to filter both the received signal and the reference BOC-modulated PRN code. After coherent and non-coherent averaging, the correlation outputs are added non-coherently and a test statistic is formed, which is compared with a threshold, in order to determine the presence or absence of signal. Each of the two main frequency lobes (positive and negative) of the BOC-modulated signal and of the reference code can be split into several sub-bands (or pieces), with the help of the bandpass filters. Since most of the signal power is contained in the main spectral lobe, in [123] the filter banks were applied in order to select the main lobe content only. Either one or both bands may be used in the combining, having thus either SSB or DSB FBB methods. If SSB FBB is used, the number of bandpass filters N_{fb} and the number of pieces N_{pieces} are equal. If

DSB processing is employed then $N_{fb} = 2N_{pieces}$.

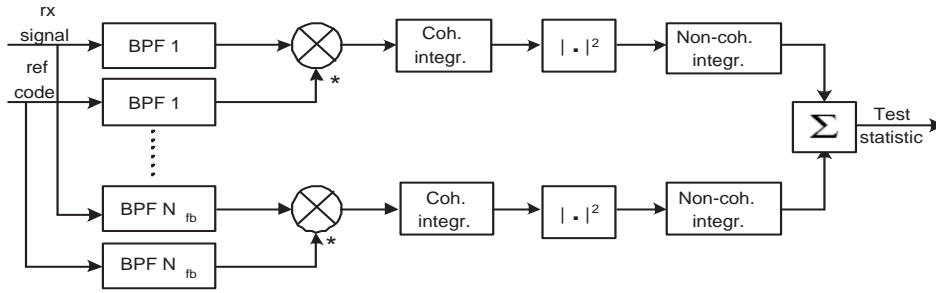


Figure 4.9: Block diagram of the Filter-Bank-Based acquisition method.

The FBB method may be implemented in two ways, which are described next. In the 'equal frequency width' FBB method (denoted by FBB_{efw}), all filters from the filter bank have equal frequency bandwidths. The division into frequency bands for FBB_{efw} method is illustrated in Fig. 4.10 (left plot) for SinBOC(10,5) modulation and DSB processing. The same filters are applied to both received signal and reference code, as illustrated in Fig. 4.9. The correlation was done piece by piece and a single ideal rectangular filter with adjustable center frequency was used to scan the useful frequency range. However, the correlator outputs will have unequal powers since the selected part of frequency spectrum have unequal powers. In both cases $N_{pieces}=4$. In the 'equal power' FBB (FBB_{ep}), the filters have variable width, chosen in such a way to let the same power to be passed through them (Fig. 4.10, right plot). Thus, wider filters are used in the low power frequency regions and narrower filters in the high-power frequency regions. Since most of the signal power is contained in the main spectral lobe, both filter bank methods have been applied in such a way to select the main lobe content only, but optimal frequency band to be passed is a topic of further research [123]. It should be noted that when $N_{pieces}=1$ and BOC modulation is used, both equal-frequency width and equal-power FBB methods are similar with the sideband correlation method of Betz&Fishman.

The effect of FBB on correlation function is illustrated in Fig. 4.11, for DSB processing and $N_{pieces}=4$. Both un-normalized (left plot) and normalized by the maximum signal amplitude (right plot) cases are presented. The ACF here refers to the absolute value of the correlation function. The signal is SinBOC(1,1)-modulated in left plot and SinBOC(15,10)-modulated in right plot. Since the frequency bandwidth before correlation decreases, the width of the main lobe of correlation function will increase. Compared to the ambiguous-BOC processing, after FBB processing the theoretical increase in the width of the main lobe is about N_{pieces} , but due to the noise and multipath effects, this increase may be actually

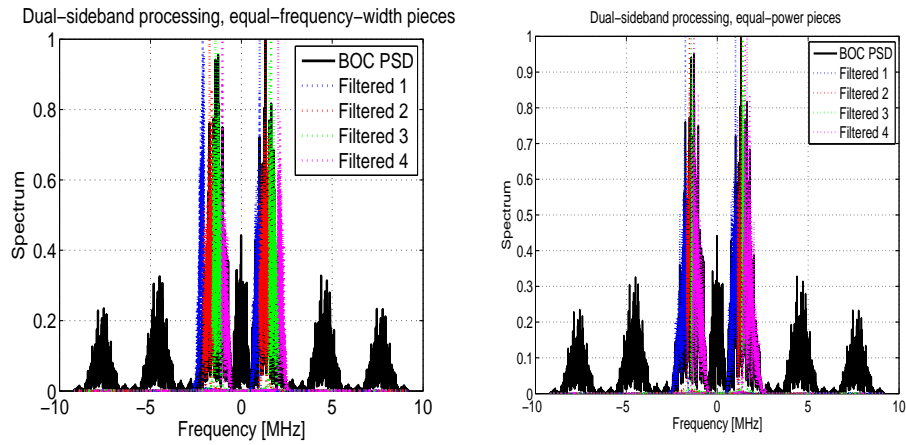


Figure 4.10: Illustration of division into frequency bands for the equal-frequency-width, respectively equal-power FBB acquisition techniques.

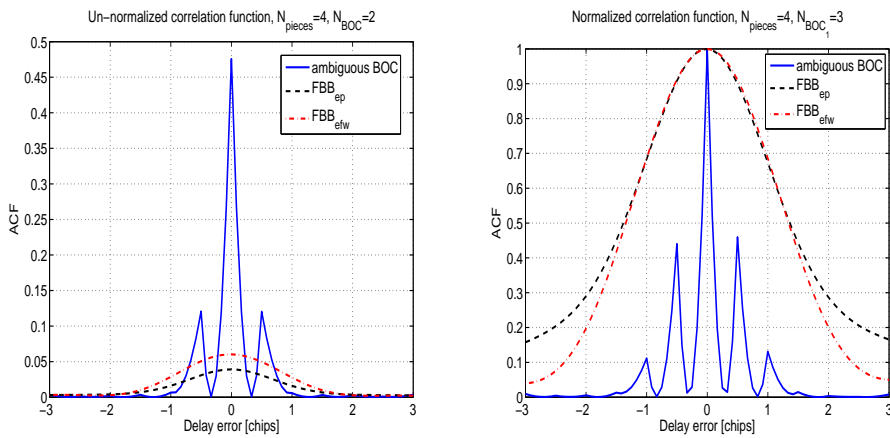


Figure 4.11: Averaged correlation functions after FBB processing. Left plot: un-normalized; Right plot: normalized by the maximum signal amplitude.

lower [123]. On the other hand, it can be observed from the left plot of Fig. 4.11 that there is also a strong degradation in signal power at correlation output.

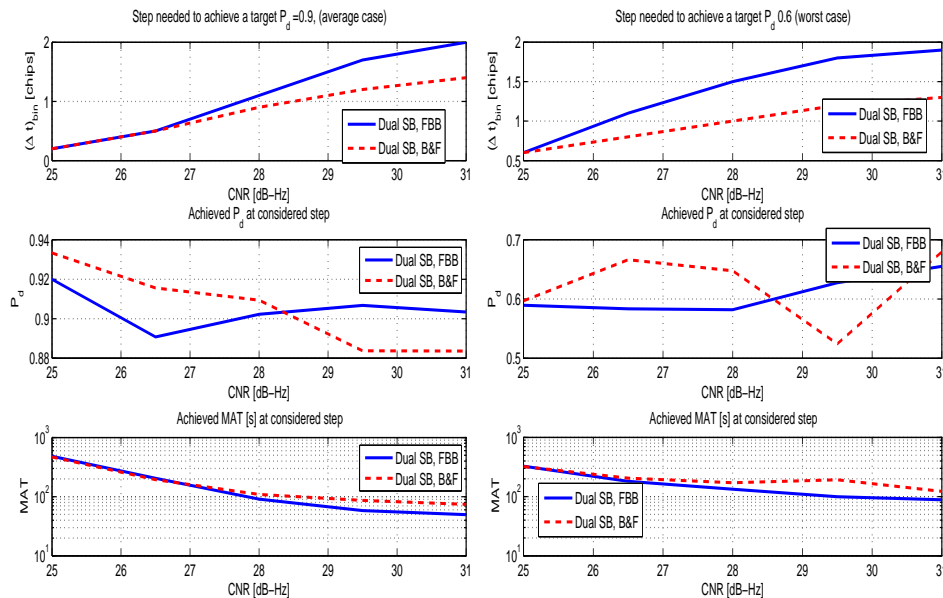


Figure 4.12: Time-step bins needed to achieve a target detection probability, for FBB and B&F unambiguous acquisition methods, average (left plot) and worst (right plot) cases.

In order to have a fair comparison between the FBB and other unambiguous methods (i.e., B&F), it is necessary to determine the time-bin step needed to achieve a target detection probability, at fixed CNR and fixed false alarm. Fig. 4.12 illustrates the time-step bins necessary in order to meet a certain P_d at a false alarm probability of $P_{fa} = 10^{-3}$, for a SinBOC(1,1)-modulated signal. Also, the MAT values are shown for both average and worst detection probabilities cases, considering a penalty factor $K_{penalty}=1$. The DSB B&F method is compared with the DSB FBB, with 2 equal-power filters per sideband (i.e., $N_{pieces}=2$). For example, at CNR=31 dB-Hz, in order to achieve an average $P_d \approx 0.9$, the DSB B&F needs a step of $(\Delta t)_{bin} \approx 1.3$ chips, which corresponds to a MAT of 70.62 s, for a single-frequency serial search and 4092 chip length code. To meet the same target, the DSB FBB method needs a $(\Delta t)_{bin} \approx 2$ chips, which corresponds to a MAT of 48.96 s. Thus, the time-step bin can be about 38 % higher for DSB FBB than for DSB B&F case and about 44 % in the acquisition speed could be gained. However, these values hold for high enough CNR, and below a certain CNR limit the B&F method is better than the FBB method [128].

It should be noted here that the unambiguous approaches presented in this

chapter can be employed also, to a certain extent, at tracking stage. However, they tend to round and widen the main lobe of ACF and, since for accurate delay tracking, preserving a sharp peak of ACF is a pre-requisite, these methods are better suited to be used at acquisition stage. Unambiguous tracking methods of BOC-modulated signals are presented in the next chapter.

Chapter 5

Tracking of Galileo and GPS signals

After initial acquisition of rough estimates of frequency and code phase parameters, perfectly aligned carrier and code replicas are necessary to be tracked long enough in order to be able to demodulate the signal. Two tracking loops, one for the carrier and one for the code are used to track these carrier and code replicas. In closed loop operation, the carrier NCO is controlled by the carrier tracking loop, which can be a frequency and/or a phase locked loop. In Phase Lock Loop (PLL) operation, the carrier tracking loop tries to keep zero phase error between the replica carrier and the incoming carrier signal. Any misalignment produces a non-zero phase angle of the prompt In-phase (I) and Quadrature-phase (Q) vector magnitudes, which drives the carrier tracking loop to correct the amount and direction of phase [92]. A very commonly used PLL is known as Costas loop, which is typically preferred since its performance does not depend on the phase shifts caused by the data bits [103]. The Frequency Lock Loop (FLL) performs the carrier wipe-off by replicating the approximate frequency, which is preferred until the receiver closes its carrier tracking loop. In general, a well-designed receiver starts tracking using a FLL discriminator and a wide band carrier loop filter. It gradually moves to a wideband PLL and finally, when tracking is stable, it is translated to a narrow PLL [99]. Then the I and Q signals are correlated with the replica codes and the code NCO is controlled by the code tracking loop, typically in a closed loop operation. In what follows, an overview of the code tracking process is provided, starting with a discussion regarding the main feedback algorithms and continuing with feedforward tracking algorithms. Next, a comprehensive description of the advanced unambiguous multipath mitigation algorithms is provided.

5.1 DLL-based methods

In the code acquisition process, the delay error between the input signal and the locally generated replica code is reduced to less than one chip. The goal of the code tracking loop is to further reduce this error to zero as close as possible and to track any changes in the code delay. In general, code delay estimators (or code tracking algorithms) can be categorized as either feedback or feedforward estimators [118], [124]. The main characteristic of feedback estimators is that the estimated delay is fed back to the tracking loop so that it can be used to the next estimation stage. Feedforward methods use an open loop structure, without any feedback information and they are based on a threshold computation which should be determined according to the channel condition [118], [124], [120].

The main algorithms usually used for GPS and Galileo code tracking, provided a sufficiently small Doppler shift, are based on a feedback delay estimator and they are implemented based on a feedback loop. The most known feedback delay estimators are the DLLs [10], [16], [17], [9]. The DLL can be designed as either coherent or non-coherent [109], [118], [120]. The coherent DLL requires the PLL to be in lock [23]. Non-coherent DLL uses nonlinear devices, such as squaring or absolute value, in order to remove the effect of data modulations and channel variations [118] and it is typically preferred, since it is able to track the code with the navigation data bit present and it is independent of the phase of the local carrier wave [23].

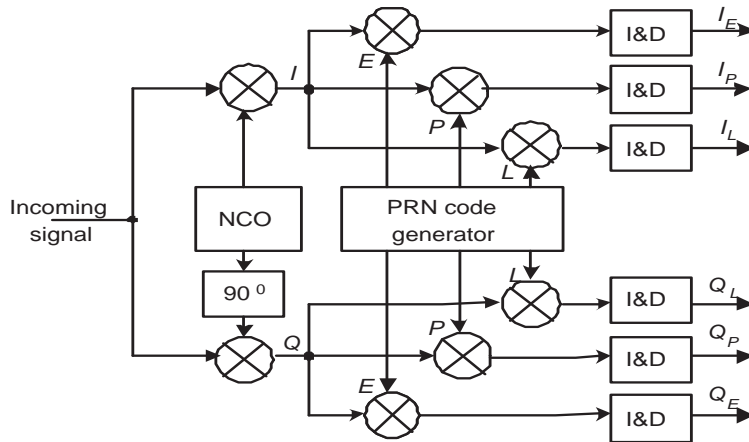


Figure 5.1: DLL block diagram.

A DLL block diagram is presented in Fig. 5.1 [23]. The input signal is multiplied (in three branches) with an early, an in-prompt and a delayed replica of the PRN code, nominally generated with a spacing of $\pm\Delta$ chip. The discriminator

correlator spacing Δ between the in-prompt and early codes determines the noise bandwidth in the DLL. If Δ is larger than half of the chip, the DLL would be able to handle wider dynamics [23]. On the other hand, narrower spacing will provide reduction of tracking errors in the presence of multipath [193]. The outputs of early, prompt and late correlation channels are integrated and dumped and these integrations indicate how much the code replicas correlate with the code in the incoming signal. When there is a phase error on the local carrier, i.e., the local carrier drifts compared to input signal, the signal energy will be in both in-phase and quadrature arms. In this case, the tracking loop has to use both the in-phase and quadrature arms to track the code [23]. The difference between the early and late correlations is referred to as discriminator function and produces an error signal which is driven to zero by the DLL in normal tracking operation. The most common DLL structure is the so-called Early-Minus-Late (EML) discriminator. For example, a non-coherent EML power discriminator function is given as:

$$D_{EML}(\tau) = (I_E^2 + Q_E^2) - (I_L^2 + Q_L^2), \quad (5.1)$$

where I_E, I_L , are the in-phase, and Q_E, Q_L are the quadrature-phase early and late correlation outputs, respectively.

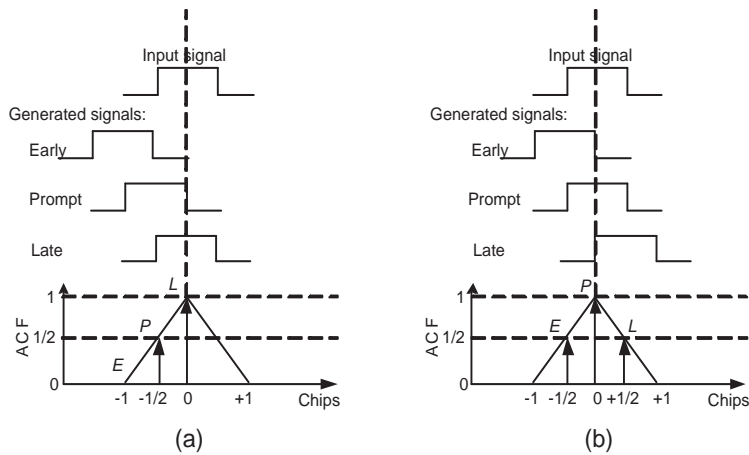


Figure 5.2: Code tracking exemplification for EML discriminator.

Fig. 5.2 [23] exemplifies the code tracking process for an EML DLL discriminator, with a correlator spacing Δ of half of the chip. In Fig. 5.2(a) the late code has the highest correlation, so the code-phase should be delayed. In Fig. 5.2(b) the code phase is properly tracked, since the highest peak is located at the prompt replica and the early and the late replicas have equal correlation output. The classical tracking structure for spread spectrum systems is the wide correlator, where

the two correlators used to form the discriminator function as in eq. (5.1) are spaced at 0.5 chips or 1 chip from each other [193], [194], [189].

5.2 Enhanced feedback tracking algorithms

In order to mitigate the effect of multipath, especially in closely-spaced multipath scenarios (i.e., successive paths are spaced at most one chip apart), several enhanced DLLs techniques have been proposed. One of the first approaches to reduce the influence of multipath is the Narrow Early Minus Late (NEML) technique, introduced for GPS receivers by NovAtel [193], [58], [59], [24]. The NEML method uses the same discriminator function as the wide correlator, but reduces the tracking errors in the presence of both noise and multipath by reducing the spacing between the early and the late codes to less than 1 chip. Multipath effects are reduced since the narrow DLL discriminator is less distorted by the delayed multipath signal [193], but the narrow correlator performance is somehow limited in closely-spaced multipath scenarios [90]. Correlator spacings of 0.1 or 0.05 chips are commercially available for GPS. This approach requires wider precorrelation bandwidth and higher sampling rates [193]. However, if available bandwidth is BW , then there will be no gain in delay tracking performance by decreasing Δ below $1/BW$ [196]. On the other hand, the linear range of the discriminator, which establishes the maximum delay error acceptable from the acquisition stage/the pull-in range (and thus the Mean Time to Lose Lock (MTTL)), has better performance with higher Δ spacing. Also, the noise loop performance is affected by Δ spacing and a good delay-tracker should operate until very low CNR.

Another DLL with a potential of multipath error reduction higher than the classical EML discriminator is the Dot-Product (DP) discriminator [193], [24]. The discriminator function for a non-coherent DP DLL can be expressed as [23]:

$$D_{DP}(\tau) = I_P(I_E - I_L) + Q_P(Q_E - Q_L), \quad (5.2)$$

where I_P and Q_P are the in-phase and quadrature-phase prompt correlation outputs.

In [57], it is shown that, for moderate correlator spacing, a DP DLL discriminator offers a larger potential of multipath error reduction than an EML discriminator due to significantly smaller mean code phase tracking error. However, there is a tendency that the difference between the mean code phase tracking error obtained by an EML and DP discriminator decreases with decreasing correlator spacing Δ [57].

The performance of a DLL is well-characterized by the so-called S-curve, which presents the expected value of the the error signal as a function of the code

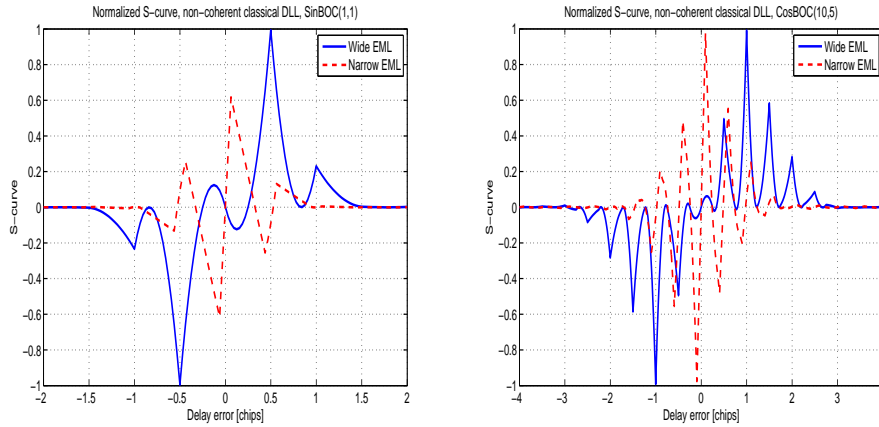


Figure 5.3: S-curves for non-coherent EML, single-path channel.

mismatch [71], [179], [120]. The S-curve illustrates the fact that searching for maxima in the correlation function is equivalent to finding the zeros of the gradient, which can be approximated by first-order differences [118]. Examples of S-curve for a wide ($\Delta = 0.5$ chips) and a narrow ($\Delta = 0.05$ chips) non-coherent EML discriminators are illustrated in Fig. 5.3. The channel is assumed static and the signal is SinBOC(1,1)-modulated in the left plot and CosBOC(10,5)-modulated in the right plot. The correct delay of the LOS path can be estimated by finding the zero-crossing [118]. As it can be observed, due to side-lobes peaks ambiguities brought by BOC modulation, there are some false lock points which may be tracked erroneously. Therefore, for BOC-modulated signals, the search range should be decreased to less than two chips, as it is for BPSK modulation. For example, as seen in Fig. 5.3, for SinBOC(1,1), the search range should be between $-1/(2N_{BOC_1})$ and $+1/(2N_{BOC_1})$ chips, in order to avoid the risk of false lock tracking. This situation becomes even more challenging in the presence of randomly separated multipaths, as the tracking algorithms should deal with both ambiguities and multipath propagation problems.

In the ideal case, for the LOS path, the discriminator function passes through zero when local code-delay is zero. However, when multipath is present, the incoming code, correlation function and consequently discriminator function are distorted. Two examples of S-curve behavior of a non-coherent narrow ($\Delta=0.05$ chip) EML discriminator, in the presence of distant and closely-spaced paths, are shown in Fig. 5.4. In this example, the signal is SinBOC(1,1)-modulated. The presence of a multipath component is signalled here by the zero-crossing from below in the S-curve [118]. Equivalently, the zero-crossings from above are sometimes used [73]. In Fig. 5.4 a two-path Rayleigh fading channel was assumed,

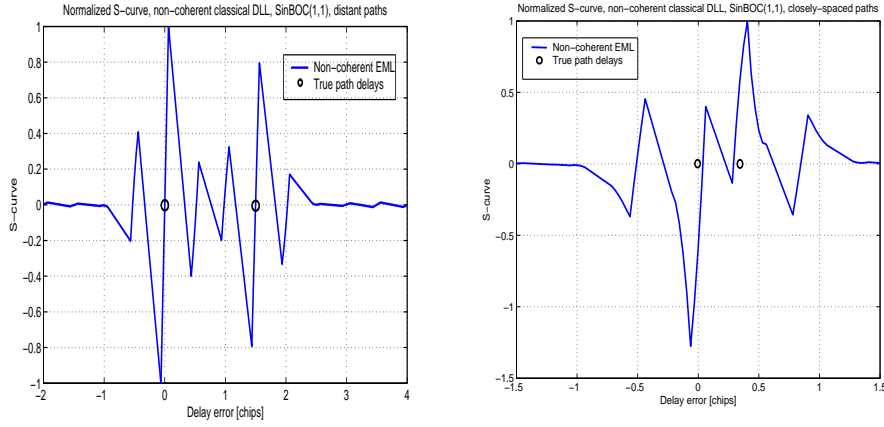


Figure 5.4: S-curves for non-coherent EML with SinBOC(1,1) modulation, in presence of distant paths (left plot) and in presence of closely-spaced paths (right plot).

with average tap power of 0 and -1 dB, with multipath spacings equal to $1.5T_c$ (distant paths) and to $0.5T_c$ (closely spaced paths), respectively. When channel paths are sufficiently apart (as in Fig. 5.4, left plot) the zero crossing show correctly the presence of multipath components, the extra-zero crossings being due to BOC-modulation effect. When the paths are closely-spaced (as in Fig. 5.4, right plot), the correct path delay cannot be distinguished any more from the S-curve output.

In this context, advanced code tracking algorithms, which offer both multipath error reduction and unambiguous tracking, are needed. One family of tracking loops for Galileo and GPS are the so-called Double Delta ($\Delta\Delta$) correlators which use more than three correlators in the tracking loops. Typically, four in-phase/quadrature-phase correlators are formed: two early and two late (with regard to the sampling point of interest), denoted in what follows as VE (very early), E (early), L (late) and VL (very late). The generic name comes from the design of $\Delta\Delta$ technique, where the spacing between the wider correlator pairs (i.e. VE and VL) is usually twice the spacing between the narrow correlators pair (i.e. E and L). The discriminator function for $\Delta\Delta$ method can be expressed as:

$$\begin{aligned}
 D_{\Delta\Delta}(\tau) = & a \left((I_E^2 + Q_E^2) - (I_L^2 + Q_L^2) \right) \\
 & - b \left((I_{VE}^2 + Q_{VE}^2) - (I_{VL}^2 + Q_{VL}^2) \right), \quad (5.3)
 \end{aligned}$$

where a and b are two variables of the model. The $\Delta\Delta$ concept is known under

different designs and several code discriminators may be set up by forming linear combinations out of the four correlators. For example, in [130], the values for a and b are set to 1 and $\frac{1}{2}$, respectively, which is well-known as High Resolution Correlator (HRC). Also, the Strobe Correlator of Ashtec [65], [25], [202] the Pulse Aperture Correlator of NovAtel [93] or the Multipath Mitigation of Leica [185] have the similar performance as HRC and they slightly differ with respect to their actual implementation and parameters [90]. Similar with the $\Delta\Delta$ concept is the Shaping Correlator family, which uses a linear combination of multiple correlators, by shaping the reference sequence in order to narrow down the main lobe and to eliminate the multipath effects [66].

Another correlator structure closely related with $\Delta\Delta$ correlators class is the Early1/Early2 tracker [194], [90] which uses two correlators located on the early slope of correlation function with an arbitrary spacing. The corresponding amplitudes are compared with the amplitudes of an ideal reference correlation function and some delay correction factor is computed by comparing the measured and reference amplitudes. This method brings some improvement over HRC or strobe correlators for very short delays [90]. Compared to the narrow correlator, the $\Delta\Delta$ correlators approach brings an visible gain in positioning accuracy for both Galileo and GPS, [6] and it represents the current state of the art in many current receivers.

In contrast with the discriminator-based multipath mitigation methods, other DLL methods use some form of multipath interference cancelation, by estimating not only the delay of the LOS path, but also the delays, phases, and amplitudes of the NLOS paths. One example is the Rake DLL [64], [110], which uses a separate multipath channel estimation unit to estimate the interfering path parameters [124]. Another algorithm which is conceptually close to Rake DLL is the DLL with Interference Cancelation (IC). The DLL with IC estimates the interfering path effect and subtracts it from the output of the finger, tracking the path of interest [124]. Also, DLL with interference minimization has been proposed, which filters adaptively the outputs of correlators in order to minimize the multipath effect [124].

A typical measure of performance for the ability of a delay tracking loop to deal with multipath errors is the so-called Multipath Error Envelope (MEE) [25], [130], [90], [202], [164]. The MEE is typically computed for two channel paths (one direct path and one reflected path, with a certain variable spacing). For example, in Fig. 5.4, the multipath error is the distance on x-axis between the zero-crossing point which would happen in single-path case and the zero crossing point which really happens due to multipath. In order to find out the MEE, the multipath errors are computed for worst-case multipath scenario, meaning that, in one case when the two paths are added in-phase, the relative multipath phase is 0 (upper MEE), and in the other case, when the two paths are out-of-phase, the relative multipath phase is π radians (lower MEE) [25]. For more than two paths, the

worst cases needed for MEE computation are not so easy to be determined, but, they can be obtained via a maximum likelihood search.

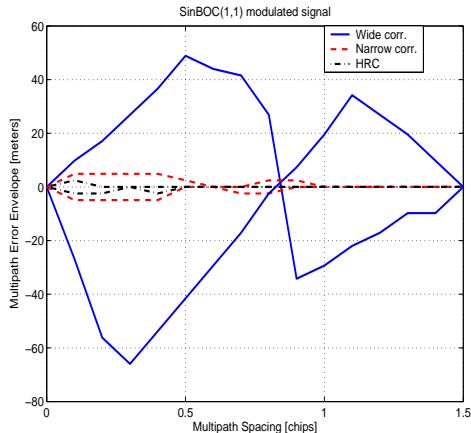


Figure 5.5: Multipath error envelopes for non-coherent wide EML, narrow EML and HRC code tracking algorithms.

The semi-analytical MEEs computed for two paths, with the second path amplitude being 3 dB less than the first path are presented in Fig. 5.5. The delay error in chips is converted in meters, for a SinBOC(1,1)-modulated signal with one chip corresponds to 293.2551 meters [74]. For the wide EML discriminator, the correlator spacing is set to $\Delta=0.5$ chips, while both narrow EML and HRC discriminators use $\Delta=0.05$ chips. The SinBOC modulation order is $N_{BOC_1}=2$ and the oversampling factor is $N_s=60$. Therefore, an error less than $\frac{1}{N_s \times N_{BOC_1}} \times 293.2551 = 2.4438$ meters cannot be detected. As it can be observed from Fig. 5.5, the narrow EML and HRC code tracking algorithms provide smaller multipath errors than the wide correlator.

The feedback DLL-based methods perform well in single-path or multiple distant paths environment. In addition, feedback methods do not require to compute thresholds as is the case for feedforward methods. The feedback DLL is still the tracking structure of choice for many receivers nowadays, since only 3 correlators are typically needed (or at most 5, e.g., for HRC or similar structures). However, the main drawbacks of the DLL-based methods include their reduced performance in closely-spaced multipath scenarios under realistic assumptions (such as the presence of error in the channel estimation process) [124]. They also have relatively slow convergence [71], as well as the possibility to estimate the delays with high estimation error due to feedback error propagation (i.e. the loss-of-lock situation) [179], [118].

5.3 Feedforward-based methods

The purpose of feedback methods is to keep the initial delay estimate as accurate as possible, but once the lock is lost, the signal should be re-acquired. Feedforward delay estimators may be feasible alternatives to feedback tracking loops, in terms of accuracy and reasonable complexity. Feedforward-based methods use an open loop structure, where the estimation is done in a single step, without the need of very accurate initial delay estimates from the acquisition process (delay errors in the order of chips) [124], [120]. A general description of open-loop solution for wideband CDMA application is provided in [118], [120]. The feedforward methods are usually more complex than the feedback methods, since they usually are based on a threshold computation (which should be determined according to the channel condition) and they require a higher number of correlators and additional processing at the receiver [118]. However, it is possible to combine both the feedback and feedforward delay estimation techniques in order to utilize the advantages inherent in both the approaches [74].

The simplest feedforward delay estimator is the correlator or Matched Filter (MF) method, where the LOS is determined based on the threshold computation, computed according to channel conditions [86], [94], [124]. The threshold is computed based on the ideal ACF of BOC-modulated signal by adding the second highest peak with the estimate of the noise variance [124]. The LOS delay is estimated as the first local maximum of the averaged correlation function which is higher than the computed threshold. Another feedforward delay estimator uses the non-linear quadratic TK operator, which was initially introduced for measuring the real physical energy of a system and it has been recently used in CDMA applications due to its good performance in multipath channels [73], [118], [120]. This method is similar with the MF estimator, with the difference that the threshold computation and the delay estimation are performed on correlation function after the TK operator has been applied [120]. The best results are obtained when TK operator is applied after non-coherent integration, on the squared-absolute value of the averaged correlation function [124]. This method is able to distinguish the peak corresponding to zero delay error among spurious sidelobes, which are not completely canceled, but are much diminished after applying TK operator [124]. One recent approach is based on the 2nd-order derivative of the correlation function [112], [74]. This algorithm uses an adaptive threshold based on the correlation function and the estimated noise level, and it could estimate the first path delay even in multipath profiles where the first path power is less than or equal to the consecutive path powers [74].

A technique which attempts to cancel the multipath errors by measuring the distortion of correlation function is the Multipath Elimination Technique [188], referred also as Early-Late Slope technique [202], [90]. This method uses multiple correlators spaced symmetrically, as closely as possible at the top of correlation

peak and since it is not based on S-curve, it can work in both feedforward and feedback configurations. The slopes at both sides of the central peak of the correlation function are used to compute a pseudorange correction that can be applied to the measured pseudorange [90].

A different approach is used by the maximum-likelihood methods, which try to cancel the multipath interference via subtraction from the correlation function of a certain reference pulse. One fine example of this approach is the Multipath Estimation Delay-Lock-Loop (MEDLL) which attempts to reduce both the code and carrier multipath errors by using several correlators (e.g., 6 to 10) per channel in order to determine accurately the shape of multipath-corrupted correlation function [195], [197]. This algorithm also can be used in both feedforward and feedback configurations. The MEDLL method decomposes the received signal into their direct path and multipath components by determining the delays, phases and amplitudes of each of the composite signals. Each estimated multipath correlation function is in turn subtracted from the measured correlation function. A reference correlation is used in order to determine the best combination of LOS and NLOS components (i.e., the number of paths, delays, phases and amplitudes) which would have produced the measured correlation function. Once this process is complete, an estimate of the direct path of correlation function is obtained. Finally, a standard early-late DLL may be applied to the direct path component and an optimal estimate of the code loop tracking error is obtained [189], [190]. One important issue in implementing the MEDLL algorithm is an adequate reference correlation function which could be measured in the absence of any noise or multipath, using a signal simulator and then stored in the memory of the receiver [198].

Since the feedforward estimators do not depend on the previous estimates, possibly erroneous, they have the advantage that they are less affected by the residual initial error coming from the acquisition stage and by the cumulative error propagation, as it is the case in feedback loops. However, compared to feedback methods, they are more complex since they usually require more correlators and are also sensitive to thresholds.

5.4 State-of-art unambiguous tracking algorithms

The BOC modulation gives a narrower center peak of the correlation function, which offers a more accurate code tracking, compared with the case of BPSK-modulated signals. However, as mentioned before, the side-peak ambiguity triggers a new challenge in the delay estimation process which should be taken into account together with the multipath problem. In order to cope with the sidelobe ambiguity at the tracking stage, it is desired to remove the sidelobes while preserving the narrow width of the main lobe. An unambiguous tracking algorithm

is introduced in [61]. This 'bump-jumping' method performs amplitude comparison of the prompt peak with the neighboring peaks, assuming they are very-early and very-late samples separated from the prompt one (i.e. one peak apart). If the prompt peak is not the largest one, the tracker jumps to the largest values between the other two gates and repeats the procedure until the prompt gate has the largest amplitude. This algorithm does not always resolve the ambiguity issue [201] and, in order to make the detection of incorrect tracking at low CNR, a long smoothing time is needed [116]. This 'bump-jumping' method is, to some extent, conceptually similar (from hardware implementation point of view), to HRC algorithm. However, here the additional correlators are used only to check that the main peak is on the prompt, but they are not used directly in the tracking [10]. A unambiguous tracker for GPS M-code signal was introduced in [54], [55], [56], [13]. Very similar with $\Delta\Delta$ correlators, this Multiple Gate Delay (MGD) approach has a larger number of early and late gates and appropriately chosen weighting factors used to combine them in the discriminator. By a judicious choice of number of correlators, gate spacing and weighting coefficients, this method synthesizes a tracker which is monotonic over the entire range of delays where ACF has significant support [54]. It should be noticed that the term MGD was used also in [85], where the unambiguous performance of MGD discriminator was not considered, but different design parameters, such as the weighting factors or gates spacing were optimized. Another type of unambiguous tracking method is the Partial Sideband discriminator which uses a linear weighted combination of the upper and lower sidebands of the received signal [13]. However, these Partial Sideband and MGD classes are very sensitive to the weighting factors and the number of correlators, especially in the case of multipath distortion and may have poorer performance than the narrow EML [74].

In order to be able to get rid of the false lock points due to BOC sidelobes, a combination of narrow correlator and unambiguous wideband correlator was proposed in [116], for SinBOC(10,5)-modulated signals. The unambiguous correlation is obtained via sideband processing, by selecting the upper and lower sidebands via filtering, and combining them non-coherently. This discriminator has the advantages of less zero-crossings, while preserving a narrow linear region, but it also suffers of noise penalty which increases as CNR decreases [116]. Another unambiguous tracking and acquisition approach, described in [201], introduced a novel replica code, which is used in various discriminator combinations in order to eliminate the sidelobe ambiguities.

The above mentioned unambiguous tracking methods tend to destroy the narrow shape of the main lobe of correlation function, which may impair the tracking process. An innovative unambiguous tracking method was introduced and studied in [96], [97], [98], [43]. This method emerged while observing that by cross-correlating a SinBOC(1,1) signal with its spreading pseudorandom sequence, the shape of the sidelobe can be reconstructed. By subtracting this BOC/PRN corre-

lation function from the ambiguous ACF, the sidelobe ambiguities can be completely removed while preserving the narrow width of the main lobe. Since the correlation values spaced at more than 0.5 chips are very close to zero, this approach offers an improved resistance to long-delay multipath [96]. This unambiguous scheme has the disadvantage that it can only be applied to SinBOC(n,n) signals. Also, in the method of [96], the BOC/PRN correlation should be computed for each code epoch, which in turn increases the computation time at the receiver. The solution proposed in [P7] and [P8], described briefly in the next section, overcomes this disadvantage. The PRN-BOC correlation method of Julien&al. has been extended to MBOC modulation in [37]. In there, an unambiguous discriminator for the SinBOC(6,1)-modulated signal was produced, by combining two BOC-PRN discriminators.

5.5 Sidelobes Cancellation Method

A new unambiguous tracking class has been introduced and analyzed in publications [P7], [P8]. This method, named in a generic way as Sidelobes Cancellation Method (SCM), removes or diminishes the side-peak threats while keeping the sharp shape of the main lobe. The SCM algorithm is explained in detail in [P7] and [P8] and is summarized in what follows. For subtraction, an ideal reference correlation function is computed as in eq. (5.4) which reconstructs the shape of the sidelobes. This ideal reference function may be generated only once and stored at the receiver.

$$\mathcal{R}_{sub}^{ideal}(\tau) = \sum_{i=0}^{N_{BOC_1}-1} \sum_{j=0}^{N_{BOC_1}-1} \sum_{k=0}^{N_{BOC_2}-1} \sum_{l=0}^{N_{BOC_2}-1} (-1)^{i \times j + k + l} \Lambda_{T_B} \left(\tau + (i - j)T_B + (k - l) \frac{T_B}{N_{BOC_2}} \right), \quad (5.4)$$

where $T_B = T_c / N_{BOC_1} N_{BOC_2}$ is the BOC interval, T_c is the chips period, N_{BOC_1} is the sine BOC modulation order, N_{BOC_2} is the cosine BOC modulation order and $\Lambda_{T_B}(\cdot)$ is the triangular function with a width of $2T_B$ chips and unit maximum value, T_B is the pulse duration and \times is the product sign. In order to remove the sidelobe ambiguities, the squared function $\mathcal{R}_{sub}^{ideal}(\tau)$ multiplied by a weight factor w is subtracted from the ambiguous correlation between the received signal and the reference BOC-modulated PRN code $\mathcal{R}_{amb}(\tau)$:

$$\mathcal{R}_{unamb}^{ideal}(\tau) = \left(\mathcal{R}_{amb}(\tau) \right)^2 - w \left(\mathcal{R}_{sub}^{ideal}(\tau) \right)^2, \quad (5.5)$$

The multiplication with the weighting factor w normalizes the ideal subtraction function in order to compensate for various channel effects, such as multipath or noise, which can modify the amplitude power of $\mathcal{R}_{amb}(\tau)$ function. After the peak-magnitudes of $\mathcal{R}_{amb}(\tau)$ function are sorted in ascending order, the weighting factor w is computed as the ratio between the second local maximum and the highest peak.

Fig. 5.6 illustrates the basic concept of SCM technique. Two BOC modulation cases are exemplified: SinBOC(1,1) in the left plot, and CosBOC(10,5) in the right plot. In both the cases, the sidelobes closest to the central peak, which are the main threats in the tracking process, are removed after the subtraction process. By comparison with the Julien&al. method, the SCM algorithm has the advantage that it can be applied to any sine or cosine BOC-modulated signal. It also has less computational complexity since the number of correlations at the receiver is reduced by half, in contrast with Julien&al. approach, which uses two correlation channels. Details are given in publications [P7] and [P8].

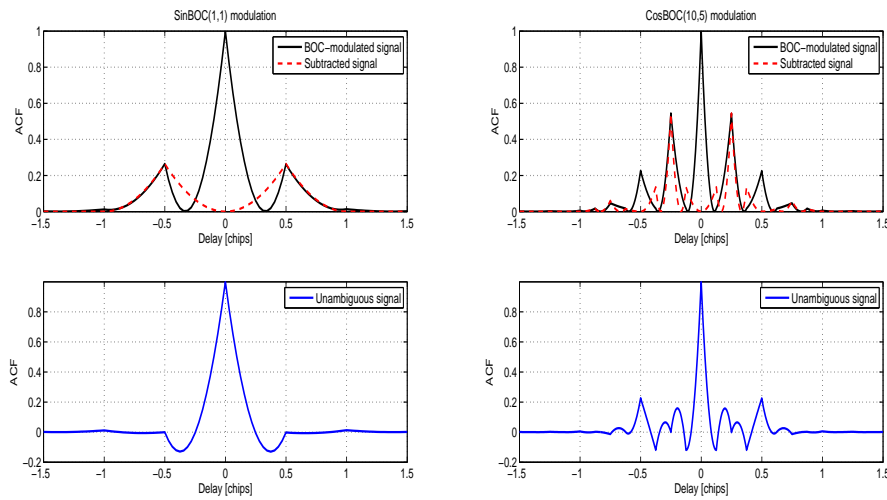


Figure 5.6: Exemplification of SCM technique, single-path static channel. Left: SinBOC(1,1) case. Right: CosBOC(10,5) case. Upper plots: BOC-modulated signal and reference subtraction pulse. Lower plots: the correlation function after SCM.

In order to cancel the correct sidelobes, one important step of this technique is to align the subtraction pulse to the LOS path. This can be achieved by obtaining an initial estimate of the LOS delay, using the multipath eliminating DLL concept, as explained in [P7], [P8]. After obtaining an estimate of the channel impulse response and removing the sidelobe ambiguities, the unambiguous correlation can

be used in various feedback or feedforward tracking configurations, in order to enhance the performance in multipath channels. For example, in [P8], several SCM enhanced algorithms were proposed and studied: SCM with NEML correlator, SCM with HRC correlator, SCM with differential correlation, SCM with IC and SCM with threshold comparison. Besides removing the side-peak ambiguities, these methods could also bring an improvement in the presence of fading multipath channels in problematic scenarios (for example, in closely-spaced multipath case). As shown in [P8], when using the SCM approach in feedback configuration, the highest performance improvement was observed with the combination of SCM and the narrow correlator. The combination of SCM and HRC did not bring much improvement, since HRC already provides improved performance in multipath channels. When comparing the SCM enhanced by various feedforward delay estimation algorithms, the best performance was obtained by the SCM combined with IC and by the SCM with threshold comparison. As illustrated in [P7] and [P8], the higher the used BOC modulation order was, the more advantageous was to apply SCM technique in order to cope better with the false lock points.

The SCM concept was mainly targeted to be used at the tracking stage, since it maintains the narrow width of the main lobe. However, this approach was found to bring an improvement also at acquisition stage, when the search step of time uncertainty was kept sufficiently small. The performance of SCM method, used in conjunction with two differential non-coherent correlation methods [142] was presented in publication [P9]. Also, more simulation results of the SCM method used in signal acquisition, are presented in Appendix A.

Chapter 6

Filter design consideration in context of BOC-modulated signals

For the GNSS systems, the frequency spectrum represents the most important resource, therefore it is important to achieve good spectral properties and suitable spectral shaping. Even if theoretically GPS or Galileo signals are rectangular (infinite bandwidth) pulses, some form of band-limitation is introduced in practical implementations, and this constraint is practically significant. Both acquisition and tracking performances can be optimized by including a pre-filter, as a part of the receiver matched filter, with the task of discarding the spectral regions containing interference. In order to get a realistic assessment of the performance of Galileo and modernized GPS systems, important receiver parameters, such as the filter characteristics and the front-end (or pre-correlation) bandwidth need to be considered. This chapter summarizes the bandlimiting constraints for Galileo and modernized GPS systems. Several digital filtering structures which can be employed at receiver at various signal processing stages are then presented briefly and the effect of the transition band is considered. The complexity coming also from sideband selection part, for different unambiguous acquisition methods, is finally considered.

6.1 Bandlimiting constraints in GNSS

Theoretically, the receiver bandwidth should be infinite in order to recover all the spread-spectrum energy by the correlation process [99]. However, in order to reduce the power consumption, mass-market receivers use limited bandwidth through spectrum shaping of received signal. The front-end bandwidth determines the amount of code information passed to the acquisition and it affects directly the

code tracking errors. It also determines the amount of thermal noise introduced into the correlator. Considering the GPS C/A signal as an example, a bandwidth below the minimum null-to-null value (i.e. 2.046 MHz) filters out considerable signal information, which causes some losses in the signal processing gain. A larger bandwidth, on the other hand, allows more signal information along with more noise. Since, about 90 % of the signal power is contained in the main lobe, a bandwidth above 2 MHz does not provide much increase in the signal gain compared to the increase in noise power [40], [99]. Selectivity insured by the baseband digital filtering is more flexible and can be easily adapted to different systems. Here, by pre-correlation bandwidth, BW , we understand the last bandwidth before despreading operation (or code matched filtering). The optimum bandlimiting pulse should distribute the pulse energy as close as possible to the band edge in order to preserve optimally the received information. An additional effect of filtering stage is the rounding and skewing of the signal autocorrelation peak. Consequently, the correlation function at the receiver is distorted and it becomes different from the autocorrelation in the ideal case (without bandwidth limitation). It can be concluded that the pre-correlation bandwidth and the signal modulation type of the incoming signal determine the actual shape of the correlation function.

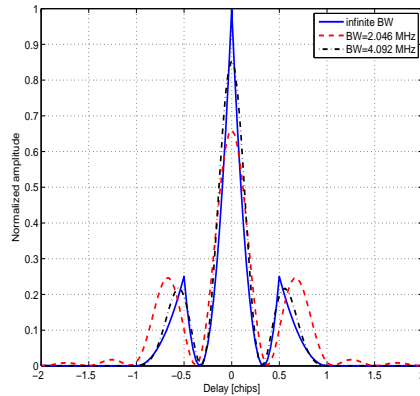


Figure 6.1: ACF for bandlimited SinBOC(1,1) signal.

Fig. 6.1 illustrates the effect of the bandwidth limitation on the ACF shape, for the SinBOC(1,1) signal, which assumes an ideal rectangular filter. For limited bandwidth (i.e., $BW = 4.092$ MHz and $BW = 2.046$ MHz), the peak value is less than one. This reflects the fact that the signal power is diminished by the bandlimiting process. For $BW = 2.046$ MHz, the bandlimiting results in oscillations outside the chip length region, which could lead to undesirable side-lobe effects

Table 6.1: GPS and Galileo receiver bandwidths

	Signal band	Carrier frequency	Receiver bandwidth
GPS	L1(C/A)	1575.42 MHz	2.0460 MHz
	L1(P(Y))	1575.42 MHz	20.460 MHz
	L2C	1227.60 MHz	2.0460 MHz
	L5	1176.45 MHz	24.552 MHz
Galileo	L1	1575.42 MHz	4.0920 MHz
	E5 (E5a+E5b)	1191.795 MHz	51.150 MHz
	E6	1278.75 MHz	40.920 MHz

in the case of multipath channels [23].

The double-sided bandwidths at the receiver front end and the carrier frequency centers for both GPS and Galileo signals are summarized in Table 6.1, according to [99], [78], [144], [26]. These bandwidths represent the null-to-null bandwidths, used in order to include the main lobes of transmitted signals and therefore they will apply to narrowband receivers. There is no common definition regarding the values which distinguish between narrowband and wideband receivers, this rather depends on particular application and simulations settings [24], [78], [152], [79], [186]. In this thesis, we consider a narrowband receiver case, i.e. the receiver front-end double-sided bandwidth is selected in such a way to include only the main lobes of incoming BOC-modulated signal.

Due to the desired low cost and robustness to jamming, commercial receivers are usually narrowband receivers. As they operate in harsh RF environments, they are less vulnerable to the out-of-band noise and interference, and they are more robust against signal faults. However, narrowband receivers tend to have relatively poor multipath performance, since the rounding of the correlation peak becomes significant. On the other hand, wideband receivers provide better signal resolution, more accuracy in the delay estimation process and, thus, improved performance can be obtained if the receiver processes more than the main lobes [24], [30]. Larger signal bandwidths allow the use of a very narrow correlator spacing and thus better multipath mitigation performance [193]. The finite bandwidth effects are most apparent at medium and long delays with errors increasing by 20 % to 40 % over the infinite bandwidth case [24]. The BOC signals have the advantage of an increasing bandwidth, as the minimum receiver bandwidth is generally twice the chipping rate for simple codes, while for BOC codes, this minimum receiver bandwidth is twice the sum of chipping rate and offset code rate [23]. For example, in order to take advantage of the narrow correlator spacing, it is necessary to sharpen up the ACF peak by using a higher pre-correlation bandwidth, so that the correlators are operating in the linear range of discriminator. The sharper the peak, the closer the successive correlators can be positioned with respect to each other and thus the range estimate becomes more accurate [193]. However,

by enlarging the pre-correlation bandwidth, the noise is enlarged too and, in this case, it is more likely to get unacceptably large pseudorange errors in the presence of satellite signal anomalies [152]. Another penalty when using the wideband receivers is that higher sampling frequency is required for wider bandwidths in order to acquire the signal.

Since the GPS L1 and Galileo E1 OS will use the same frequency band (with a center frequency of 1575.42 MHz), a dual-radio that operates with both systems may be employed. The receiver bandwidths and sample rates should be chosen in order to match the received signal power. Considering the full system bandwidths, the minimum received power specified for the Galileo L1 data modulated signal is essentially the same as that one specified for the GPS C/A code. Hence the GPS and Galileo signal bandwidths can be selected in such a way that the same power is received for both. In this case, the receiver bandwidth should therefore be large enough in order to allow the use of narrow correlation, but it also should be small enough in order to avoid the use of too high sampling rates [138]. For example, for OS signal candidates on E1/L1 band, mass-market narrowband receivers with a bandwidth of 4 MHz are specified [78]. Also wideband receivers with a bandwidth of 24 MHz are specified in [78].

In this context, it is important to set a sufficiently high bandwidth in order to insure the transmission of information at the rate and with the required quality under specific conditions [161], [162]. For navigation systems, a relevant performance measure is given by the power containment bandwidth, which represents the percentage of the signal power contained within a certain bandwidth and which is directly related to the demodulation and the tracking properties of the signal. The smaller the power containment bandwidth needed for a certain power containment, the better the bandwidth efficiency that can be achieved [162]. Fig. 6.2 shows the power containment factor ε versus the bandwidth for several BOC and BPSK modulated signals [125]. It can be seen from Fig. 6.2 that a double-sided receiver bandwidth of about 1.7 MHz is needed for BPSK-modulated signals in order to capture at least 90% of the signal power, while the bandwidth requirements for SinBOC(1,1) and MBOC signals with the same 90% power containment are 6.2 MHz and 12.1 MHz, respectively. For SinBOC(1,1)-modulated signal, 85.57 % of the signal power is contained within 4.092 MHz (double-sided) null-to-null bandwidth. For the PRS CosBOC(15,2.5)-modulated signals, 77.45 % of the signal power is contained in 40 MHz bandwidth, and increasing the band above 40 MHz gives very slow improvement. The PRS candidate cannot achieve more than 80 % containment with realistic bandwidth, i.e., up to 60 MHz [15], [125].

6.1.1 IIR versus FIR filters

Even if, theoretically, the GPS and Galileo signals are born with rectangular (infinite bandwidth) pulses, the bandlimitation, using real filtering, affects on the

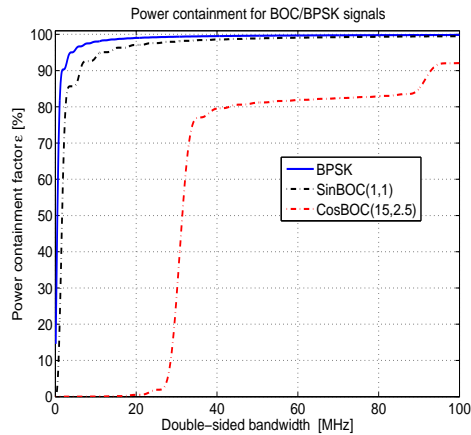


Figure 6.2: Power containment for BPSK, SinBOC(1,1) and CosBOC(15,2.5)-modulated signals.

pulse shaping. The filtering has the role to allow only certain frequencies to pass and to attenuate the others. Typically, the filtering adds a delay to the incoming code relative to the local code. Therefore the ACF peak does not correspond to zero-time delay error and this delay bias should be compensated. Among other receiver front-end components, the various filters employed at different receiver stages are meant to condition and preserve optimally the received signal power. Since the practical filters always introduce some level of attenuation, some filter structure could be more suited than other, depending on filter's specific role and on its properties.

The choice between various digital filters, in the context of filtering requirements, affects both the filter design process and the implementation of the filter. Some characteristics of the digital filtering structures, which can be used as possible bandlimiting filters, are briefly underlined next. The FIR filters have a number of useful properties, which make them sometimes preferable over Infinite Impulse Response (IIR) structures. FIR filters are inherently stable, they can be designed to be linear phase and to make better use of the available precision. For an FIR structure, due to the symmetry of coefficients, some practical implementations allow for a linear-phase response using only half of the number of coefficients [135]. However, if a large number of coefficients is needed, an FIR filter might become too difficult and expensive to implement. The IIR filters are also called recursive filters due to the feedback necessary in their implementation [207]. In contrast to FIR filters, an IIR filter has fewer stored coefficients, requires less computing and it can give a sharper cutoff than an FIR filter, which meets the same frequency-domain specifications [148]. However, due to the feedback, the IIR fil-

ter may have problems with instability, arithmetic overflow and limit cycles. An exact linear phase is not possible with IIR filters and the phase and group delay characteristics of IIR filters are, generally, poorer than those of FIR filters [148]. In order to design the filter with the given constraints, different approaches can be used, as for example, the Chebyshev or Butterworth IIR filtering methods or Parks-McClellan optimal equiripple FIR filter algorithm [148], [207].

An extensive research is on-going all over the world in order to find improved filtering structures, which are computationally efficient. One class of digital filters which can implement lowpass FIR filters with significantly reduced computational workload, is represented by the Interpolated FIR (IFIR) filters [172]. These filtering structures yield linear-phase response and they can meet the given specification, with a reduced number of multipliers. Due to a relaxed sub-filter requirements and reduced time-domain redundancies, the IFIR filters possess significantly lower multiplication rates than the corresponding direct-form single rate filters. Also, other IIR structures could be considered, such as lattice-ladder [207] or lossless discrete integrators, which provide low sensitivity to coefficient quantization [131], [8].

Digital filters can be characterized by their attenuation of the desired frequency components and by the 3 dB bandwidth (cutoff frequency), which indicates that at which frequency the attenuation will be 50 % of the signal power. As input specifications, a low-pass digital filtering structures can be characterized by the passband f_{pass} and stopband f_{stop} edge frequencies, the passband ripple and the stopband attenuation. The passband ripple defines the maximum allowable deviation r_p from the desired passband gain. Minimum stopband attenuation indicates the maximum allowable deviation r_s from zero stopband gain. For a fair comparison between various filter types, the bandwidth considered here was normalized to the BOC sub-carrier frequency, i.e. the normalized sampling rate corresponds to $f_s = N_s N_{BOC_1} N_{BOC_2} f_c$ (in MHz). The un-normalized passband frequency f_{pass} was taken to be equal to the positive bandwidth, i.e. $BW/2$. The passband and stopband edge frequencies, with respect to the normalized bandwidth, can be expressed as $f_{pass} = \frac{1-\alpha_1}{2}$, and $f_{stop} = \frac{1+\alpha_2}{2}$, respectively. Here, α_1 and α_2 are the so-called roll-off parameters.

6.1.2 Effect of the transition band

In an ideal design, a digital filter has a certain target gain in the passband and zero gain in the stopband. In a real implementation, a finite transition between the passband and stopband (which is known as the transition band) always exists. The width of this transition bandwidth determines the required order of the filter for the given specifications [148] and by taking into account this region, the resulting approximation ripple can be significantly reduced [134]. The width of the transition bandwidth is defined by the roll-off parameters α_1 and α_2 , and this

transition region could be either symmetric, i.e. $\alpha_1 = \alpha_2 \in (0, 1)$ or asymmetric, i.e. $\alpha_1 \leq \alpha_2$, where $\alpha_1, \alpha_2 \in (0, 1)$.

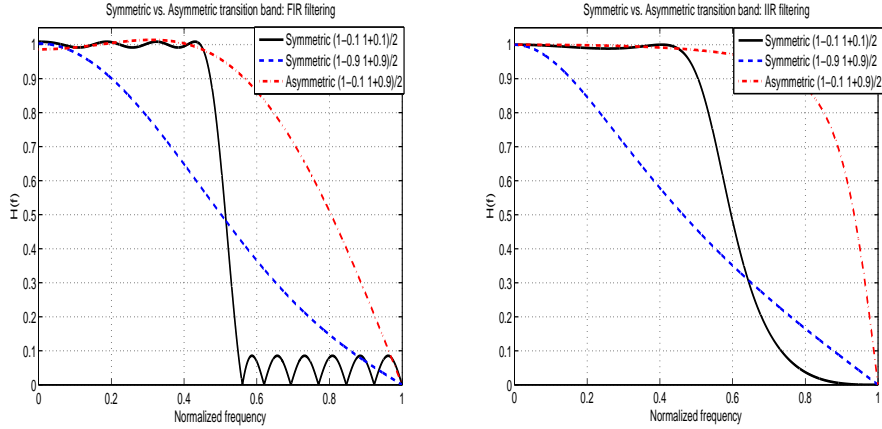


Figure 6.3: Frequency responses for FIR and IIR filtering, with different transition bands.

Fig. 6.3 illustrates the frequency responses for different choices of symmetric and asymmetric transition bands, for FIR and IIR filters. The desired amplitude in passband is set to one and the minimum order filters for which the design specifications are met, are used. The IIR filter is a digital Chebyshev Type I filter. It can be observed that the use of an asymmetric transition band (i.e. $\alpha_1 = 0.1$, $\alpha_2 = 0.9$) allows for a larger area under the frequency response curve. Since for BOC-modulated signals the signal power is concentrated near the band edges (and this power near the band edges increases when BOC modulation order increases) this design could allow for more signal energy to be captured through filtering process. As shown in publication [P3], the best performance is achieved when the transition band is asymmetric, with high values of stopband edges frequency α_2 and with small values of passband frequency α_1 . Since for any FIR design algorithm, the filter order tends to grow inversely proportional to the transition bandwidth, the use of asymmetric transition region with small α_1 and higher α_2 requires fewer computations and thus, it could lower the filter implementation complexity.

6.2 Filtering in the context of unambiguous acquisition approaches

Previously, ideal rectangular filters have been assumed for sideband separation in the context of unambiguous acquisition approaches (described in Chapter 4,

Table 6.2: Number of filters needed for the ambiguous and unambiguous acquisition methods)

Method	Number of real filters	
	Dual Sideband Processing	Single Sideband Processing
B&F	12	6
M&H	2	2
modified M&H	8	4
modified B&F	8	4
UAL	0	0
ambiguous BOC	0	0

Table 6.3: Number of operations for 1 ms receiver processing, per real filter

Filter type	Additions	Multiplications
FIR single stage	$(N_{FIR} - 1) \cdot N_{sh}$	$\lceil \frac{N_{FIR}}{2} \rceil \cdot N_{sh}$
IFIR S stages	$\left(\sum_{s=1}^S N_{IFIR}(s) - 1 \right) \cdot N_{sh}$	$\sum_{s=1}^S \lceil \frac{N_{IFIR}}{2} \rceil \cdot N_{sh}$
IIR direct form	$2N_{IIR} \cdot N_{sh}$	$(2N_{IIR} + 1) \cdot N_{sh}$
IIR lattice	$3N_{IIR} \cdot N_{sh}$	$N_{IIR} \cdot N_{sh}$
IIR lossless discrete integrators	$2N_{IIR} \cdot N_{sh}$	$N_{IIR} \cdot N_{sh}$

in Section 4.4). Even if the advantage of the proposed unambiguous algorithms comes from the method used at the correlation part, a further decrease in the implementation complexity could be obtained by choosing suitable filtering structures for sideband selection, as it was shown in [P5] and [P6]. The number of required filters for the ambiguous and unambiguous acquisition methods are summarized in Table 6.2. The front-end filtering is assumed to be the same for all the considered methods and it is not included in this filter count. In computing the values from Table 6.2, the following rules have been considered: one complex filter applied to a complex signal is equivalent to 4 real filters; one real filter applied to a complex signal (or one complex filter applied to a real signal) is equivalent to 2 real filters. The filter is real if it has an even symmetry in amplitude response and an odd symmetry in phase response with respect to 0 frequency.

In order to give some estimates of the complexity of the sideband filtering part, several typical IIR and FIR filtering structures were selected for comparison in [P5], [P6]. The number of operations required by these filters are summarized in Table 6.3. The filter orders are denoted by N_{FIR} , N_{IFIR} and N_{IIR} for FIR, IFIR and IIR filters, respectively. The term N_{sh} represents the shifting factor applied at a sample level. The interpolated FIR gives a lower computational complexity than a single-stage FIR and comparable complexity with the direct-form and lattice IIR structures.

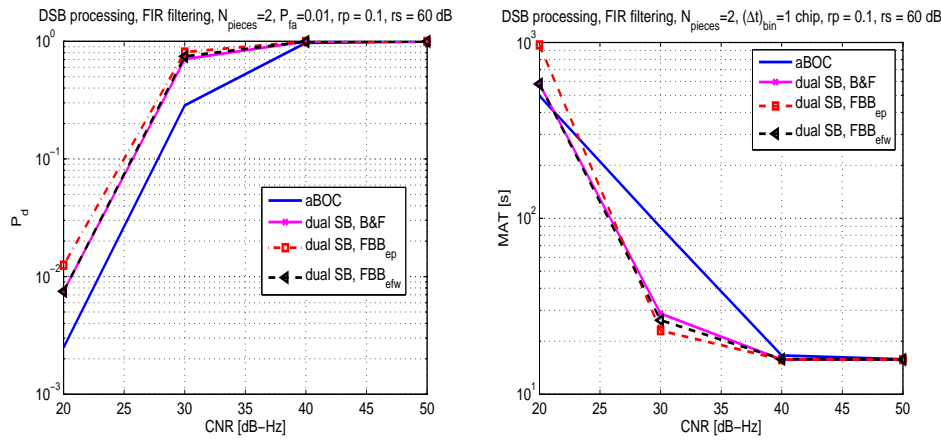


Figure 6.4: Performance of dual-sideband FBB methods using FIR filtering. Left plot: Detection probability. Right plot: Mean acquisition time.

Another example of filtering effects in the context of unambiguous acquisition of BOC-modulated signals, besides those given in [P5] and [P6] is related to the performance of FBB acquisition methods employing bandwidth-limiting filters. In order to analyze the performance of FBB acquisition methods, the ideal rectangular filtering was previously considered [128], [123]. The problem of filtering effects in the context of FBB unambiguous processing is addressed next. Figs. 6.4 illustrate the performance (in terms of detection probability and mean acquisition time) for DSB FBB methods, in comparison with the DSB B&F and ambiguous BOC processing. The signal is SinBOC(1,1)-modulated and it is sent through a single-path static channel. The time-bin step is $(\Delta t)_{bin} = 1$ chip and the target false alarm is $P_{fa}=0.01$. The number of filters per sideband is $N_{pieces}=2$ and they are designed as FIR structures with $r_p=0.1$ dB and $r_s=60$ dB. The filters have either the same frequency bandwidths or use variable bandwidths, chosen in such a way to allow for the same signal power to be captured by each filter. As it can be observed, both FBB approaches give some improvement in the results over both the B&F and the ambiguous BOC processing. By comparing Fig. 6.4 with Fig. 4.12 (from Chapter 4), where the ideal rectangular filtering was assumed, there is some performance degradation due to overlapping transition bands.

Fig. 6.5 shows two illustrative plots which compare the number of operations (additions and multiplications) required by the DSB B&F and FBB methods, for both correlation and filtering parts. The signal is SinBOC(1,1)-modulated and the time-steps bins are chosen as $(\Delta t)_{bin}=1.3$ chips and $(\Delta t)_{bin}=2$ chips for B&F and FBB approaches, respectively. The number of equal-power filters per sideband for FBB technique is $N_{pieces}=2$ and $N_{pieces}=4$, in the left and right plots, respectively.

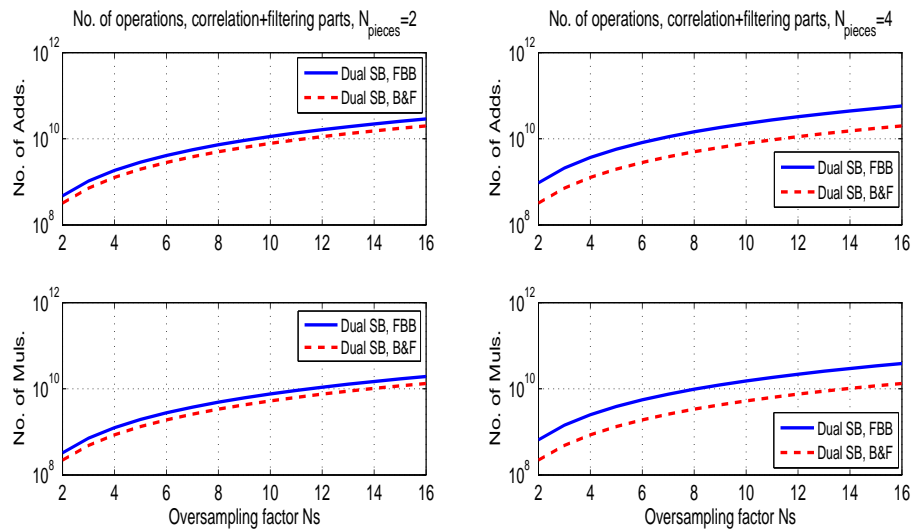


Figure 6.5: Complexity comparison of DSB FBB and DSB B&F methods. Left plot: $N_{pieces}=2$. Right plot: $N_{pieces}=4$.

Both the correlation and the filtering parts are included in these complexity figures. An IIR direct-form filter with 5 taps is assumed for the filtering part. As it can be observed, for $N_{pieces}=2$, the FBB method requires about 1.5 times more additions and multiplications than the B&F approach. If the number of filters per sideband is increased, more operations would be necessary for the FBB method, as it can be observed from Fig. 6.5, the right plot. Therefore, the performance of FBB methods is given by the trade-off between a faster acquisition time and an increase in the complexity at the receiver part (obtained with an increased number of N_{pieces}). The optimal number of pieces or filters to be used in the filter bank depends on the CNR, on the method (single or dual SB), and on the BOC modulation orders. A too high N_{pieces} parameter would deteriorate the signal power too much. The best values for N_{pieces} , observed in [128] was between 2 and 6. Due to the performance degradation when comparing with rectangular filtering, there is room for further optimization of real filter structures used for piece-band selection.

Chapter 7

Summary of publications

The second part of this thesis is based on nine publications [P1]-[P9]: seven conference articles and two articles published in peer-reviewed scientific journals. None of these publications have been used (or planned to be used) as a part of any other dissertation.

The main topic considered in these publications is the development of code acquisition and tracking algorithms for BOC-modulated CDMA signals, transmitted over multipath channels. The simulations and theoretical models focus on Galileo receivers. However, some of the algorithms described here can be implemented in the context of any direct sequence-CDMA signal with BPSK or split-spectrum modulation.

7.1 Overview of the publication results

In publication [P1], we studied the impact of oversampling factor on the BOC-modulated PRN codes during the code acquisition process. We showed that the performance, in terms of both mean acquisition time and detection probability, is typically deteriorated in the presence of non-integer oversampling factors. We also focused on the design of the time-bin step size according to the BOC modulation order in order to improve the performance. The effect of non-integer oversampling, as well as the design of the step time-bin according to BOC modulation, even if rather intuitive, were hard to be found in the literature at the time [P1] was written.

In [P2], the double-dwell hybrid-search acquisition method was studied for SinBOC(1,1)-modulated signal and an optimization of the dwell parameters and number of dwells was undertaken. It was shown that, if the parameters of a double-dwell structure (i.e., detection and false alarm probabilities at each stage) are properly designed, the double-dwell structures have indeed an advantage (in terms of mean acquisition times) over single-dwell structures. However, at low

penalty factors or higher time-bin steps, a single-dwell structure gives the best trade-off between the complexity and performance. Also, the choice of the penalty factor has been discussed. The results of this paper show that the double-dwell approaches are not always better than the single-dwell approaches, as it is the general understanding.

Publication [P3] analyzed the effect of receiver bandwidth-limiting filter, taking into account different digital filtering structures during the code acquisition of a BOC-modulated and oversampled signal. Both OS and PRS Galileo signals were considered (i.e., SinBOC(1,1) and CosBOC(15,2.5) modulations, respectively), and as the optimum bound, the ideal rectangular pulse was employed. In comparison with the rectangular shaping (i.e., infinite bandwidth), the investigated filtering methods suffered some performance degradation. It was shown that by using an asymmetric transition bandwidth design with respect to one-fourth of the sampling rate, the performance (in terms of root mean square error) could be enhanced, when compared to the situation when a symmetric transition band is used. Here, the nominal value for passband edge was not modified, but instead transition band was designed to be asymmetrical.

Publication [P4] dealt with unambiguous acquisition of BOC-modulated signals, unambiguous acquisition which attempts to reconstruct the BPSK-like shape of the correlation function envelope and thus enable the use of a higher time-bin searching step. A BPSK-like technique, namely the modified Martin&Heiries (M&H) technique was introduced here and its performance and, partly, its complexity as well, were compared with the classical Betz&Fishman (B&F) or side-band correlation method and with the ambiguous acquisition case. In contrast with M&H method [81], [129], our method worked for both even and odd BOC-modulation order. It provided lower complexity compared with B&F method, while its performance was much better than the ambiguous acquisition performance and only slightly worse compared with the B&F performance. Both single-side band processing and dual-side band processing were analyzed.

Publication [P5] continued the work presented in [P4] and improved further the architecture of the proposed modified M&H approach, by inter-changing the places of the shifting unit with the filtering unit and thus reducing the number of filters used for band selection. A detailed complexity analysis of the proposed unambiguous method was performed and this method was compared with ambiguous and other unambiguous approaches in terms of required operations and number of filters. Also, the filter design for unambiguous approaches is addressed here for the first time, and an interpolated FIR structure is proposed.

Publication [P6] introduced a new low-complexity unambiguous method, namely the Unsuppressed Adjacent Lobes (UAL) technique. The work about unambiguous acquisition methods was extended, by studying various implementations of the algorithms proposed previously by the author in [P4], [P5] and by B&F. A thorough underlying theoretical model was employed to prove the choice of the

shifting factors used in UAL and modified unambiguous techniques. The performance analysis was based on single-dwell serial-search acquisition and static channels, in order to find out the maximum achievable performance of these algorithms (i.e., in the absence of multipaths and fading distortions).

A new unambiguous method, which can be applied in both acquisition and tracking stage, the Sidelobes Cancellation Method (SCM) was introduced in publication [P7]. In there, its performance was analyzed at the code tracking stage. In order to compensate for multipath effects after the ambiguities are eliminated, an improved SCM method with interference cancellation was proposed. The SCM technique had as a starting point the unambiguous tracking method proposed in [96], [97]. Our approach was extended to cover more Galileo signals, that is, it can be used with arbitrary sine and cosine BOC-modulated signals. We also showed in [P7] that this method has a reduced complexity.

In publication [P8], we analyzed and developed further the SCM method introduced in [P7], by considering its usage in conjunction with various feedback and feedforward tracking algorithms. The performances of the proposed SCM algorithms were analyzed in the context of both ideal single-path AWGN and fading multipath channels. It was shown, through extensive simulations, that these methods improve the delay tracking accuracy, also in the case of closely-spaced paths, which are the most problematic from the accurate positioning point of view. Also, the higher the BOC-modulation order, the more advantageous is to apply the SCM techniques in order to cope better with the false lock points.

The SCM method, proposed previously to be used at code-tracking stage [P7], [P8] was analyzed also in the context of acquisition in publication [P9]. The SCM approach here was combined with two types of differential correlation methods and was studied for both sine and cosine BOC-modulated signals. The SCM method was proved to be beneficial also at acquisition stage, if the search step of the time uncertainty was sufficiently small. Also, it was shown in [P9] that, by combining the SCM with differential correlation techniques, the acquisition performance when compared to the traditional non-coherent processing could be enhanced even further.

7.2 Author's contribution to the publications

The research work for this thesis was carried out at the Department of Communications Engineering (formerly, the Institute of Communications Engineering) of Tampere University of Technology, as part of the Tekes-funded research projects "Advanced Techniques on Mobile Positioning", "Advanced Techniques for Personal Navigation", "Future GNSS Applications and Techniques", and of the Academy-funded research project "Digital Signal Processing Algorithms for Indoor Positioning Systems".

During the research work, the author has been a member of an active research group, involved in studying and developing signal processing algorithms for wireless positioning, and especially, for GNSS-based positioning. Several of the ideas have originated in discussions within the group, and some of the simulation models (built in Matlab) have been designed in cooperation with the co-authors. Therefore, the author's contribution cannot be separated completely from the co-authors' contributions. However, the author's contribution to all of the publications included in the thesis has been essential in that she carried out the theoretical derivations, developed new algorithms, performed the simulations and wrote the most part of the manuscripts where she is the main author, and a significant part of the manuscripts where she is the second author. The main contributions of the author to the publications can be summarized as follows:

In [P1] the author came out with the idea of analyzing the oversampling limits in the context of acquisition of Galileo signal, built the simulation model, carried out the simulations, and wrote most of the manuscript. The co-authors helped in developing the theoretical model.

The theoretical model for double-dwell characterization in publication [P2] was derived together with the co-authors of the paper. The author carried out the main simulations and analyzed the performance of single-dwell and double-dwell structures under various parameter assumptions.

In [P3] the author introduced the idea of asymmetrical transition bands, derived the main parts of the theoretical model, carried out all the simulations and wrote the manuscript. The idea of analyzing the impact of filter design on the acquisition performance was proposed by the co-authors and the choice of some of the FIR and IIR filter parameters was done with the help of co-authors.

The author proposed the unambiguous method from publication [P4], built the simulation algorithm and carried out the simulations. The manuscript was prepared by the author.

In publication [P5], the unambiguous acquisition method (i.e., the modified M&H algorithm) proposed by the author is further investigated in terms of complexity. The author built the simulation model, derived the theoretical model starting from the ideas presented in [P4], and carried out the simulations. The calculus of the complexity and the design of the interpolated FIR filter was done with the help of co-authors.

The author is the co-developer of Unsuppressed Adjacent Lobes (UAL) technique and of the modified B&F technique, and the main developer of the modified M&H technique in [P6]. She also carried out the main simulation parts, and a significant part of the theoretical derivations and of the complexity calculus.

In publication [P7], the author proposed the Sidelobes Cancellation Method in the context of unambiguous code tracking. She built the simulation model, wrote most of the theoretical derivations, performed the simulations and wrote the manuscript. The derivations with respect to the Multipath Estimating De-

lay Locked Loop (used for comparison purposes) were done with the help of co-authors.

In [P8], the unambiguous tracking method proposed by the author is more thoroughly investigated. The author developed the simulation model, analyzed the results in the context of fading channels and wrote most parts of the manuscript.

In [P9], the author came with the idea of using the Sidelobe Cancellation Method in the context of acquisition. She also built the simulation model, performed all the simulations and wrote the manuscript. The ideas of differential correlation were suggested by the co-authors.

Chapter 8

Conclusions

This thesis addresses the problems of acquisition and tracking of BOC modulated signals, transmitted over static or multipath fading channels. In Chapter 1, the challenges, the motivations and the prior work were introduced. Chapter 2 presented briefly the principles of satellites-based positioning and gave an overview of the GPS and European Galileo signal structures. The channel and baseband signal models were described in Chapter 3. The BOC modulation concept as well as the effect of other receiver constraints such as the sampling rate or the pre-correlation bandwidth were also addressed here. In the presence of BOC modulation there are always periodical side-peaks at certain delay lags of the envelope of the correlation function, which should be avoided.

One solution that provides an enhanced timing accuracy for BOC-modulated signal is to oversample the signal at the sub-chip interval. We showed in [P1] that the performance is typically degraded in the presence of non-integer oversampling factors, but sufficient performance can be achieved if the time-bin step is designed properly, according to the BOC modulation order.

In Chapter 4, an overview of the acquisition process in the context of BOC modulated signal is provided. Different search methods and detector structures, such as single-dwell or multiple-dwell structures were presented. The aim of such design is to minimize the acquisition time, while attaining the required global detection probability and false alarm. In this context, it is interesting to see under which conditions the double-dwell structure is indeed better than the single-dwell one and what are the optimum detection and false alarm probabilities to be met at each stage required for the minimum acquisition time. As shown in [P2], if the detection and false alarm probabilities at each stage of a double-dwell structure are properly chosen, the double-dwell structures have indeed an advantage over single dwell structures. However, such a design is tedious and sensitive to various parameters such as CNR, time-bin step, global probabilities, etc. Also, a double-dwell structure typically provides better acquisition time than a single-dwell structure only for high penalty factors and for low enough steps of the time

bin. Extensions of the work presented in [P2] to more than two dwell stages is also of interest and might consist a topic for further investigation. Also, the author believes that the work related to single and double-dwell approaches is not limited to Galileo applications, but could find its applicability in any system involving signal detection in noise (e.g., radar, UWB communications, etc.).

In order to allow for a more efficient acquisition of BOC-modulated signals, various unambiguous acquisition methods were presented in Section 4.4. These methods eliminate the ambiguities introduced by BOC modulation by reconstructing the BPSK-like shape of the correlation function and thus allow the use of a higher search step compared with the ambiguous acquisition situation. The unambiguous BOC acquisition techniques which are introduced earlier in the literature, suffer from high implementation complexity, and some of them are also unable to cope with odd BOC-modulation orders [129], [81]. In this context, we proposed three reduced-complexity methods which remove the ambiguities from the correlation function of the split-spectrum signals and work for both even and odd BOC-modulation orders. Two of the proposed methods, namely the modified Martin&Heiries [P4], [P6] and the modified Betz&Fishman [P6] are extensions of the previously mentioned techniques, and the third one, the Unsuppressed Adjacent Lobes (UAL) method was first introduced by the authors in [P6]. The choice of the optimal parameters of the proposed unambiguous acquisition methods was done via theoretical analysis [P6]. Currently, the hardware complexity of the unambiguous acquisition methods, e.g., when implemented via FPGA, is investigated at TUT. A further research direction may consist in hardware designs based on the proposed unambiguous acquisition methods. Also as further research work, the performance of the unambiguous acquisition algorithms introduced in [P6] could be tested also for a multiple dwell hybrid-search acquisition model in multipath fading channels.

Chapter 5 provided a description of the code tracking process, by considering both feedback and feedforward tracking structures. A novel unambiguous processing technique, the Sidelobes Cancellation Method (SCM) was first proposed to be employed at the tracking stage [P7], [P8]. In comparison with other methods introduced in the literature for eliminating the sidelobes ambiguities at tracking stage, e.g., [96], [97], the SCM approach has the advantage that it can be used with any sine and cosine BOC-modulated signal and provides a lower complexity solution. However, this technique relies on subtracting the ideal reference correlation function from the ambiguous one, and thus it requires a correct estimation delay for correct subtraction. The performance of the SCM approach in multipath channels can be enhanced by employing other tracking structures after removing the side-peak threats [P8]. Since the SCM technique preserves the narrow width of the main lobe, it is mainly suited to be used at the tracking stage. However, since the receiver's hardware may constrain the use of the same search step at both acquisition and tracking stages, the SCM method was also tested during the signal

acquisition process [P9]. It was shown that the SCM method used in conjunction with two differential correlation methods could also enhance the performance at the acquisition stage, when keeping the search step of time uncertainty sufficiently small.

The research work presented in this thesis has mainly focused on SinBOC(1,1) signal, proposed previously for L1F (OS/ CS/SoL) band and CosBOC(15.2.5) signal, proposed for L1P (PRS) band. Few of the simulation models were also verified for BPSK modulation, as well as for other sine/cosine BOC modulations. However, more recently, MBOC modulation (with various implementations such as CBOC and TMBOC) has been recommended in Galileo draft specifications [52], with the scope of increasing the tracking abilities of Galileo Open Service signals and of GPS L1 civil signal. Therefore, a further research direction of high interest for Galileo community is to extend the proposed methods to MBOC cases. Indeed, part of the author's work has been continued by colleagues at TUT and a recent paper [171] shows the benefit of unambiguous methods in the context of MBOC modulation as well. The author also believes that many of the algorithms presented in this thesis are valid for any split-spectrum DS-SS-modulated signal, and therefore they might find applicability in other consumer electronics areas as well (e.g., systems using Manchester coding and spread spectrum, etc.)

The bandlimiting constraints and effects in the context of Galileo and modernized GPS receivers were emphasized in Chapter 6. Several digital filter structures which can be employed at various stages of signal processing were briefly described and the effect of the transition band (i.e., the band between the pass-band and stopband frequencies) was considered. The front-end filtering is prone to decrease the performance, since the autocorrelation function becomes flattened around the peaks and also its symmetry may become skewed and delayed, depending on the filter design. As shown in [P3], the performance, in terms of root mean square errors could be improved if asymmetric transition bands are used (i.e., symmetry point was taken with respect to one fourth of the sampling rate). Chapter 6 considered also the effect of real filtering in the context of sideband selection for various unambiguous acquisition methods. The implementation complexities of the existing and the proposed unambiguous acquisition methods were compared by taking into account both the correlation and the sideband selection [P5], [P6]. Different FIR and IIR filter structures for sideband selection were considered, and an interpolated FIR filter which can decrease the overall implementation complexity even further, was proposed [P5]. However, research towards better/novel filter structures to be used with GNSS signals is still an open issue, especially when severe bandwidth limitation is imposed (e.g., when aiming to use Galileo signals with minimum modifications of GPS receivers in terms of receiver bandwidths).

A summary of the presented publications was given in Chapter 7, where the author's contributions to the presented work are emphasized.

As the GNSS field is a fast evolving field, with many potential applications,

it remains a challenging topic for future research to investigate the feasibility of the algorithms proposed here with the multitude of signal modulations, spreading codes and spectrum placements that are (or are to be) proposed. Also, high-sensitivity receivers are becoming more popular in order to offer better solutions in low CNR areas, such as densely populated urban canyons. The inclusion of the unambiguous acquisition and tracking algorithms in the high-sensitivity receiver and its performance analysis is also a possible topic of future investigation. A comprehensive analysis and comparison of unambiguous acquisition and tracking algorithms have not yet been found in the literature, and therefore, it offers an interesting area of further development.

APPENDIX

In publication [P9] the performance of the SCM method enhanced by differential correlation was compared with that of the traditional non-coherent processing, at acquisition stage. The non-coherent processing was kept as benchmark in [P9], since the comparison between the non-coherent acquisition and the differential acquisition methods had been already presented in [142]. In this Appendix more simulation results are shown, by comparing the performance of the SCM methods also with the differential correlation methods.

The settings for simulations are as described in [P9]. For all presented simulations a fixed probability of false alarm of $P_{fa} = 10^{-2}$ was assumed. In order to take advantage of the SCM methods used at acquisition stage, the step time bin was selected to be sufficiently small, i.e., $\Delta_t = 1/N_s N_{BOC_1} N_{BOC_2}$. The N_s is the oversampling factor and the N_{BOC_1} , respectively N_{BOC_2} , are the BOC-modulation orders, as described in Chapter 2. To recall from [P9], the NC stands for conventional non-coherent processing, DN1 is the first non-coherent differential correlation method and DN2 is the second enhanced differential method. By SCM we denoted the Sidelobes Cancellation Method. The SCM DN1 and SCM DN2, denote the SCM enhanced by DN1 and DN2 methods, respectively.

Figures 8.1 present the simulations results for a SinBOC(1,1)-modulated signal, in terms of probability of detection (left plot) and mean acquisition time (right plot), respectively. The simulated channel has fixed Rayleigh distribution, with 2-paths with average PDP of 0 and -2 dB. The mobile speed is 1 km/h, the signal is integrated coherently over 20 ms, the non-coherent integration length is 10. The successive channel paths have uniformly random distribution spacing between $1/N_s N_{BOC_1} N_{BOC_2}$ and $x_{max} = 0.5$ chips. From both figures, it can be observed that the SCM DN1 and SCM DN2 approaches still outperform the DN1 and DN2 methods. On the other hand, the SCM approach, used solely, may be outperformed by both DN1 and DN2 techniques.

The same conclusion can be drawn from Figures 8.2, which present the simulations results for a CosBOC(10,5)-modulated signal, transmitted over a Rayleigh channel with average PDP of -1, 0 and -2 dB. Also here, all the SCM enhanced techniques still outperform the DN1 and DN2 methods, while SCM used solely may performs worse than both differential methods. As a final conclusion, all the SCM and DN methods still give better results than the traditional non-coherent processing.

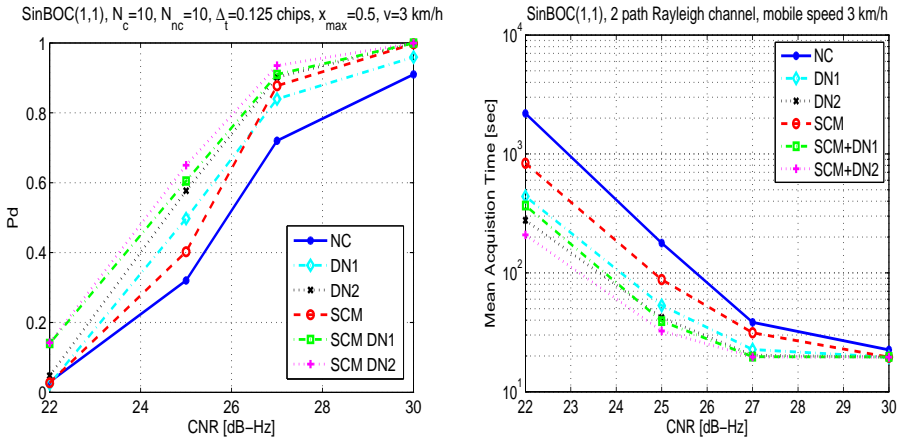


Figure 8.1: Performance in terms of detection probability (left plot) and mean acquisition time (right plot), for a SinBOC(1,1) modulated signal, transmitted over a Rayleigh channel with 2 paths.

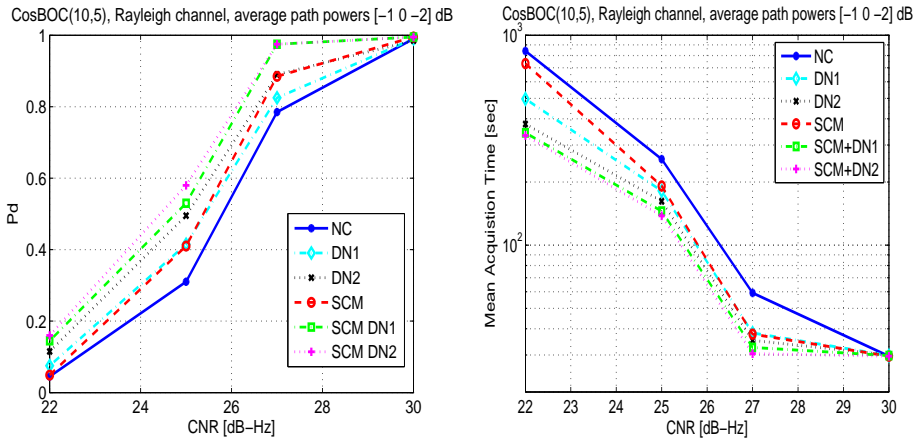


Figure 8.2: Performance in terms of detection probability (left plot) and mean acquisition time (right plot), for a CosBOC(10,5) modulated signal, transmitted over a Rayleigh channel with 3 paths.

Bibliography

- [1] D. Akopian. A fast satellite acquisition method. In *Proceedings of ION-GPS 2001 Conference*, Salt Lake City, US, Sept. 11-14, 2001.
- [2] D. Akopian. Fast FFT based GPS satellite acquisition methods. In *Proceedings of IEE Proceedings on Radar, Sonar and Navigation*, vol. 152, no. 4, pp. 277–286, Aug. 2005.
- [3] D. Akopian and S. Agaian. Fast matched filters in time domain. In *IEE Proceedings on Radar, Sonar and Navigation*, vol. 153, no. 6, pp. 525–531, Aug. 2006.
- [4] D. Akos, M. Stockmaster, J. B. Tsui and J. Cashera. Direct bandpass sampling of multiple distinct RF signals. In *IEEE Transactions on Communications*, vol. 42, no. 7, pp. 983–988, July 1999.
- [5] J. A. Avila-Rodriguez, S. Wallner, G. W. Hein, J. L. Issler and A. R. Pratt. MBOC: The new optimized spreading modulation recommended for Galileo E1 OS and GPS L1C. In *Proceedings of ESA Navitec*, Dec. 11-13 2006, Noordwijk, The Netherlands.
- [6] J. A. Avila-Rodriguez, M. Irsigler, G. W. Hein and T. Pany. Combined Galileo/GPS frequency and signal performance analysis. In *Proceedings of the International Technical Meeting of the Satellite Division of the Institute of Navigation, ION GNSS 2004*, . Long Beach, CA, US, Sep. 2004.
- [7] J. A. Avila-Rodriguez, S. Wallner, G. W. Hein, E. Rebeyrol and O. Julien. CBOC - An implementation of MBOC. In *Proceedings of First CNES Workshop on Galileo Signals and Signal Processing*, Toulouse, France, Oct. 2006.
- [8] F. Balestro, A. Chianale, G. Privat, M. Tawfik and T. Vandeweerd. Design of digital filters for advanced telecommunications ASIC's using a special purpose silicon compiler. In *IEEE Journal of Solid-State Circuits*, vol. 26, pp. 1047–1055, Jul. 1991.

- [9] J. Baltersee, G. Fock, and P. Schulz-Rittich. Adaptive code tracking receiver for direct-sequence code division multiple access communications over multipath fading channels and method for signal processing in a RAKE receiver. *U.S. Patent Application Publication, US 2001/0014114 A1 (Lucent Technologies)*, Aug. 2001.
- [10] B. C. Barker, J. W. Betz, J. E. Clark, J. T. Correia and J. T. Gillis. Overview of the GPS M code signal. In *Proceedings of Institute of Navigation National Technical Meeting (ION NTM): Navigating into the New Millennium*, pp. 542–549, Jan. 2000.
- [11] F. Bastide, O. Julien, C. Macabiau and B. Roturier. Analysis of L5/E5 acquisition, tracking and data demodulation thresholds. In *Proceedings of Institute of Navigation GPS Meeting*, pp. 2196–2207, 2002.
- [12] C. Baum and V. Veeravalli. Hybrid acquisition schemes for Direct Sequence CDMA systems. In *IEEE International Conference on Communications*, vol. 3, pp. 1433–1437, 1994.
- [13] P. Bello and R. Fante. Code Tracking Performance for Novel Unambiguous M-Code Time Discriminators. In *Proceedings of Institute of Navigation National Technical Meeting ION NTM*, vol. 3, pp. 293–298, San Diego, CA, US, Jan. 2005.
- [14] H. Bertoni. *Radio Propagation for Modern Wireless Systems*. Prentice Hall, 2000.
- [15] J. W. Betz. The offset carrier modulation for gps modernization. In *Proceedings of Institute of Navigation National Technical Meeting (ION-NTM)*, pp. 639–648, Cambridge, Massachusetts, US, 1999.
- [16] J. W. Betz. Design and performance of code tracking for the GPS M code signal. In MITRE Technical Papers, available via http://www.mitre.org/work/tech_papers/tech_papers_00, Sep. 2000.
- [17] J. W. Betz. Extended theory of early-late code tracking for a bandlimited GPS receiver. In *Journal of the Institute of Navigation*, vol. 47, no. 3, Fall 2000.
- [18] J. W. Betz. Binary offset carrier modulations for radio navigation. In *Journal of the Institute of Navigation*, vol. 48, no. 4, pp. 227–246, 2002.
- [19] J. W. Betz and D. B. Goldstein. Candidate design for an additional civil signal in GPS spectral bands. In *Proceedings of the US Institute of Navigation NTM Conference*, pp. 622–631, San Diego, CA, US, Jan. 2002.

- [20] J. W. Betz and P. Capozza. System for direct acquisition of received signals. *US Patent Application Publication, US 2004/0071200 A1*, Apr. 2004.
- [21] J. W. Betz, C. R. Cahn, P. A. Dafesh, C. J. Hegarty and K. W. Hudnut. L1C signal design options. In *MITRE Technical Papers*, available via http://www.mitre.org/work/tech_papers/tech_papers_06, Jan. 2006.
- [22] R. Bischoff, R. Hab-Umbach, W. Schulz and G. Heinrichs. Employment of a multipath receiver structure in a combined Galileo/UMTS receiver. In *Proceedings of 55th Vehicular Technology Conference (VTC Š02)*, vol. 4, pp. 1844–1848, Birmingham, AL, US, May 2002.
- [23] K. Borre, D. M. Akos, N. Bertelsen, P. Rinder and S. H. Jensen. *A software-defined GPS and Galileo receiver - A single-frequency approach*. Birkhäuser, Boston, 2007.
- [24] M. Braasch and A. J. Van Dierendonck. GPS receiver architectures and measurements. In *Proceedings of the IEEE*, vol. 87, no. 1, pp. 48–64, Jan. 1999.
- [25] M. Braasch. Performance Comparison of Multipath Mitigating Receiver Architectures. In *the IEEE Proceedings of Aerospace Conference*, vol. 3, no. 3, pp. 1309–3/1315, 2001.
- [26] G. Brodin, J. A. Cooper, D. M.A. Walsh and A. Cartmell. A Galileo Receiver: Design, Development and Results. In *Proceedings of GNSS 2003 The European Navigation Conference*, Graz, Austria, Apr. 2003.
- [27] C. Caini, G. E. Corazza and A. Vanelli-Coralli. Multi dwell architectures for DS-CDMA code acquisition in fading channels. In *Proceedings of ISSSTA*, 2002.
- [28] Y. H. Chen, J. C. Juang and T. L. Kao. Implementation of BOC Signal Acquisition Using a DSP/FPGA Board. In *Proceedings of IAIN/GNSS*. Jeju, Korea, Oct. 2006.
- [29] A. J.R.M. Coenen. Combating digitizing errors in GNSS-receivers. In *Proceedings of Institute of Navigation ION GPS Meeting*, 2001.
- [30] A. J.R.M. Coenen. Combating short-delay multipath requires enhanced peak-detection. In *Proceedings of 2nd ESA Workshop on Satellite Navigation User Equipment Technology Navitec*, 2004.
- [31] A. J.R.M. Coenen. On elementary filters (IIR and FIR) for acquisition and tracking of GPS receiver. In *Proceedings of 2nd ESA Workshop on Satellite Navigation User Equipment Technology Navitec*, 2004.

- [32] Communication from the Commission of 10 February 1999. *Galileo - Involving Europe in a new generation of satellite navigation services*. COM(1999)54 final.
- [33] COSPAS-SARSAT web site. International satellite system for Search and Rescue <http://www.cospas-sarsat.org>. Referred May 12, 2006.
- [34] A. G. Dempster. New GNSS Signals: Receiver Design Challenges. In *Proceedings of 2004 International Symposium on GNSS*, Sydney, Australia, Dec. 2004.
- [35] A. G. Dempster and S. Hewitson. The 'System of Systems' Receiver: an Australian Opportunity? In *Proceedings of International Global Navigation Satellite Systems Society IGNSS Symposium*, Dec. 2007.
- [36] A. G. Dempster. Satellite Navigation: New Signals, New Challenges. In *Proceedings of IEEE International Symposium on Circuits and Systems (IS-CAS)*, pp. 1725–1728, May 2007.
- [37] A. G. Dempster and J. Wu. Code Discriminator for Multiplexed Binary Offset Carrier Modulated Signals. In *Electronics Letters*, vol. 44, no. 5, pp.384–385, Feb. 2008.
- [38] P. A. Dafesh and J. K. Holmes Practical and theoretical trade-offs of active parallel correlator and passive matched filter acquisition implementation. In *Proceedings of IAIN World Congress in association with ION Annual Meeting*, pp. 352–366, 2000.
- [39] P. Daly Navstar GPS and GLONASS: Global Satellite Navigation Systems. In *IEEE Electronics and Communication Engineering Journal*, vol. 5, pp. 349–357, May 1993.
- [40] S. Deshpande and M. E. Cannon Analysis of the Effects of GPS Receiver Acquisition Parameters. In *Proceedings of ION GNSS*, Long Beach, CA, US, Sep. 2004.
- [41] D. DiCarlo and C. Weber. Multiple dwell serial search: Performance and application to direct sequence code acquisition. *IEEE Transactions on Communications*, vol. 31, no. 5, pp. 650–659, May 1983.
- [42] D. DiCarlo and C. Weber. Comparison of multiple-dwell code acquisition detector rules in DS-SS serial search by envelope correlator. In *IEEE International Symposium on Spread Spectrum Techniques and Applications*, vol. 2, pp. 614–618, 1994.

- [43] F. Dovis, P. Mulassano, L. Lo Presti. A Novel Algorithm for the Code Tracking of BOC(n,n) Modulated Signals. In *Proceedings of ION GNSS 2005*, Long Beach, CA, pp. 152–155.
- [44] F. Dovis, L. Lo Presti, M. Fantino, P. Mulassano and J. Godet. Comparison between Galileo CBOC Candidates and BOC(1,1) in Terms of Detection Performance. In *Eurasip International Journal of Navigation and Observation*, vol. 2008, Article ID 793868, 9 pages, doi:10.1155/2008/793868.
- [45] European Commission: Directorate General for Energy and Transport. GALILEO: An imperative for Europe. Available via <http://europa.eu.int>.
- [46] V. Erola. Rapid parallel GPS signal acquisition. In *Proceedings of ION GPS*, Salt Lake City, UT, US, Sep. 2000.
- [47] H. Elders-Boll and U. Dettmar. Efficient Differentially Coherent Code/Doppler Acquisition of Weak GPS Signals. In *Proceedings of IEEE International Symposium on Spread Spectrum Techniques (ISSSTA '04)*, Australia, 30 Aug.-2 Sep. 2004.
- [48] P. Enge. GPS modernization capabilities of the new civil signals. In *Proceedings of the Australian International Aerospace Congress*, Brisbane, Australia, Aug. 2003.
- [49] European Commission: Directorate General for Energy and Transport. The Galilei project-GALILEO design consolidation. Available via http://ec.europa.eu/dgs/energy_transport/galileo/doc/galilei_brochure.pdf.
- [50] European Space Agency. Navigation applications. Available via <http://www.esa.int/esaNA/>.
- [51] European Space Agency. Galileo Full Operational Capability (FOC) Procurement. Tender Information Package. Clarification set no. 4. 28/07/2008. Available via <http://estext231.estec.esa.int/Galileo-FOC/Clarifications/FOC-TIP-QandA-part4.pdf>,
- [52] European GNSS Supervisory Authority. Galileo Open Service Signal-In-Space Interface Control Document (Galileo OS SIS ICD), 2008. Available via <http://www.gsa.europa.eu/go/galileo/os-sis-icd>.
- [53] A. J. Eynon and T. C. Tozer. A comparison of multiple-dwell cell testing strategies in serial search direct sequence spread spectrum code acquisition. In *Proceedings of the IEEE Military Communications Conference*, vol. 1, pp.357–361, 1995.

- [54] R. Fante. Unambiguous tracker for GPS binary-offset carrier signals. In *Proceedings of the ION National Technical Meeting*, Albuquerque, NM, US, Aug. 2003.
- [55] R. Fante. Unambiguous first-order tracking loop M-code. *MITRE Technical Report*, MTR 94B0000040, Jul. 2004.
- [56] R. Fante. Code tracking performance for novel unambiguous M-code time discriminators. In *Proceedings of the ION National Technical Meeting*, San Diego, CA, US, Jan. 2005.
- [57] T. Felhauer. Comparison of EML and DOT discriminator DLL multipath performance in GPS/GLONASS navigation receivers. In *Electronics Letters*, vol. 33, no. 3, pp.179–181, 30 Jan. 1997.
- [58] P. Fenton. Pseudorandom noise ranging receiver which compensates for multipath distortion by making use of multiple correlator time delay spacing. *NovAtel Patent, US 5 414 729*, May 1995.
- [59] P. Fenton and A. J.V. Dierendonck. Pseudorandom noise ranging receiver which compensates for multipath distortion by dynamically adjusting the time delay spacing between early and late correlators. *NovAtel Patent, US 5 495 499*, Feb. 1996.
- [60] P. Fenton, B. Smith and J. Jones. Theory and Performance of Pulse Aperture Correlator. NovAtel Technical Paper. Available via <http://www.novatel.com>.
- [61] P. Fine and W. Wilson. Tracking algorithm for GPS offset carrier signals. In *Proceedings of the Institute of Navigation National Technical Meeting ION NTM*, pp. 25–27, San Diego, CA, US, Jan. 1999.
- [62] S. Fisher, A. Guerin and S. Berberich. Acquisition concepts for Galileo BOC(2,2) signals in consideration of hardware limitation. In *Proceedings of IEEE Vehicular Technology Conference*, vol. 5, pp. 2852–2856, May 2004.
- [63] P. Fishman and J. W. Betz. Predicting performance of direct acquisition for the M-code signal. In *Proceedings of the Institute of Navigation National Technical Meeting ION NTM*, pp. 574–582, 2000.
- [64] G. Fock, J. Baltersee, P. Schulz-Rittich and H. Meyr. Channel tracking for RAKE receivers in closely spaced multipath environments. In *IEEE Journal on Selected Areas in Communications*, vol. 19, no. 12, pp. 2420–2431, 2001.

- [65] L. Garin and J. M. Rousseau, Enhanced strobe correlator multipath rejection for code and carrier. In *Proceedings of 10th International Technical Meeting of the Institute of Navigation ION-GPS*. vol. 1, pp. 559–568, Kansas City, US, Sep. 1997.
- [66] L. Garin, The Shaping Correlator, novel multipath mitigation techniques applicable to Galileo BOC(1,1) modulation waveforms in high volume markets. In *Proceedings of the European Navigation Conference GNSS 2005*. München, Germany, Jul. 2005.
- [67] Galileo Joint Undertaking (GJU) - The European programme for global navigation services. Galileo standardization document for 3GPSS. Available via <http://www.galileoju.com>.
- [68] Galileo Joint Undertaking (2005). L1 band part of Galileo signal in space ICD. Available via <http://www.galileoju.com>.
- [69] Galileo Joint Undertaking - GPS-Galileo Working Group. A (WGA) recommendations on L1 OS/L1C optimization. Available via <http://www.galileoju.com/page3.cfm>, Mar. 2006.
- [70] European Space Agency. European GNSS Supervisory Authority. Signal In Space Interface Control Document. OS SIS ICD, Draft 1. Feb. 2008.
- [71] S. Glisic and B. Vucetic *Spread spectrum CDMA systems for wireless communications*. Artech House Publishers, 1997.
- [72] J. Godet, J. C. deMateo, P. Erhard and O. Nouvel. Assessing the radio frequency compatibility between GPS and Galileo. In *Proceedings of ION GPS*. Portland, OR, US, Sep. 2002.
- [73] R. Hamila. *Synchronization and multipath delay estimation algorithms for digital receivers*. PhD thesis, Tampere University of Technology, Finland, Jun. 2002.
- [74] M. Z. Hasan Bhuiyan. *Analyzing code tracking algorithms for Galileo Open Service signal*. MSc thesis, Tampere University of Technology, Finland, Aug. 2006.
- [75] S. Haykin and M. Moher. *Modern wireless communications*. Prentice Hall, 2005.
- [76] C. Hegarty and M. Tran. Acquisition algorithms for the GPS L5 signal. In *Proceedings of ION GNSS*, pp. 165–177, 2003.

- [77] G. W. Hein, J. Godet, J. L. Issler, J. C. Martin and P. Erhard. Status of Galileo frequency and signal design. In *Proceedings of ION GPS*, Portland, OR, US, 2002.
- [78] G. W. Hein, M. Irsigler, J. A. Rodriguez and T. Pany. Performance of Galileo L1 signal candidates. In *Proceedings of The European Navigation Conference (ENC-GNSS)*, May 2004.
- [79] G. W. Hein, J. A. Rodriguez, S. Wallner, A. R. Pratt and J. Owen. MBOC: The new optimized spreading modulation recommended for Galileo L1 OS and GPS L1C. Available via <http://forschung.unibwmuennen.de>.
- [80] G. Heinrichs, R. Bischoff and T. Hesse. Receiver architecture synergies between future GPS/Galileo and UMTS/IMT-2000. In *Proceedings of IEEE 56th Vehicular Technology Conference (VTC)*, pp. 1602–1606, Fall 2002.
- [81] V. Heiries, D. Roviras, L. Ries and V. Calmettes. Analysis of non-ambiguous BOC signal acquisition performance. In *Proceedings of ION GNSS 17th International Meeting of the Satellite Division*, pp. 2611–2622, Long Beach, CA, US, Sep. 2004.
- [82] V. Heiries, J. A. Avila-Rodriguez, M. Irsigler, G. W. Hein and E. Rebeyrol. Acquisition performance analysis of composite signals for the L1 OS optimized signal. In *Proceedings of ION GNSS 18th International Meeting of the Satellite Division*, pp. 877–889, Long Beach, CA, US, Sep. 2005.
- [83] J. K. Holmes, S. H. Raghvan and S. Lazar. Acquisition and tracking performance of NRZ and square wave modulated symbols for use in GPS. In *Proceedings of ION GPS Meeting*. pp. 611–625, 1998.
- [84] W. Huan-Chun and S. Wern-Ho. Variable dwell time code acquisition for direct sequence spread spectrum systems on multipath fading channels. In *IEEE International Conference on Communications ICC*, vol. 3, pp. 1232–1236, Jun. 1998.
- [85] H. Hurskainen, E.S. Lohan, X. Hu, J. Raasakka and J. Nurmi. Multiple Gate Delay Tracking Structures for GNSS Signals and Their Evaluation with Simulink, SystemC, and VHDL. In *EURASIP International Journal of Navigation and Observation*, vol. 2008, Art. ID 785695, 17 pages, doi:10.1155/2008/785695.
- [86] J. Iinatti. *Matched filter code acquisition employing a median filter in direct sequence spread-spectrum with jamming*. PhD thesis, University of Oulu, Finland, 1997.

- [87] J. Iinatti. On the threshold setting principles in code acquisition of DS-SS signals. In *IEEE Journal on Selected Areas in Communications*, vol. 18, no. 1, pp. 579–583, 1999.
- [88] J. Iinatti and A. Pouttu. Differentially coherent code acquisition in Doppler. In *Proceedings of 50th IEEE International Vehicular Technology Conference VTC 1999-Fall*, vol. 2, pp. 703–707, The Netherlands, Sep. 1999.
- [89] Inside GNSS Magazine. Policies, Programs, Engineering and Advance Applications of the Global Navigation Satellite Systems. Available via <http://www.insidegnss.com>.
- [90] M. Irsigler and B. Eissfeller. Comparison of multipath mitigation techniques with consideration of future signal structures. In *CDROM Proceedings of International Technical Meeting of the Institute of Navigation ION-GPS/GNSS*, Portland, OR, US, Sep. 2003.
- [91] Y. K. Jeong, K. B. Lee and O. S. Shin. Differentially Coherent Combining for Slot Synchronization in Inter-Cell Asynchronous DS/SS Systems. In *Proceedings of IEEE International Symposium on Personal, Indoor and Mobile Radio Communications PIMRC 2000*, pp. 1405-1409, London, UK, Sep. 2000.
- [92] X. Jia, S. R. Babu, J. Barnes, and C. Rizos. Study on carrier phase tracking receivers in difficult GPS environments. In *Proceedings of International Symposium on GNSS/GPS*, Sydney, Australia, Dec. 2004.
- [93] J. Jones, P. Fenton and B. Smith. Theory and performance of the pulse aperture correlator. Technical Report, NovAtel, available via <http://www.novatel.com/Documents/Papers/PAC.pdf>, Calgary, Canada, Sep. 2004.
- [94] J. Joutsensalo. Algorithms for delay estimation and tracking in CDMA. In *Proceedings of IEEE International Conference on Communications (ICC)*, vol. 1, pp. 366–370, 1997.
- [95] V. M. Jovanovic. Analysis of strategies for serial-search spread-spectrum code acquisition-direct approach. In *IEEE Transactions on Communications*, vol. 36, no. 11, pp. 1208–1220, Nov. 1998.
- [96] O. Julien, C. Macabiau, G. Lachapelle, M. E. Cannon and C. Mongrédien. A new Unambiguous BOC(n,n) signal tracking technique. In *CD-ROM Proceedings of the European Navigation Conference GNSS*, Rotterdam, The Netherlands, May 2004.

- [97] O. Julien, C. Macabiau, M. E. Cannon and G. Lachapelle. BOC signal acquisition and tracking method and apparatus. *US Patent Application Publication, US 2005/0270997 A1*, Dec. 2005.
- [98] O. Julien. *Design of Galileo L1F receiver tracking loops*. PhD thesis, University of Calgary, Canada, Jul. 2005.
- [99] E. D. Kaplan. *Understanding GPS - Principles and applications*. Artech House Publishers, Boston, 1996.
- [100] M. Katz. *Code acquisition in advanced CDMA networks*. PhD thesis, University of Oulu, Finland, 2002.
- [101] S. M. Kay. *Fundamentals of statistical signal processing*. vol. 2: Detection Theory. Prentice Hall, 1993.
- [102] S. Kogure. QZSS/MSAS Status. CGSIC 47th Meeting, Fort Worth, TX, USA Available via [http://www.navcen.uscg.gov/cgsic/meetings/47thMeeting/\[24\]qzmsas.pdf](http://www.navcen.uscg.gov/cgsic/meetings/47thMeeting/[24]qzmsas.pdf). Sep. 2007.
- [103] K. Krumvieda, P. Madhani, C. Cloman, E. Olson, J. Thomas, P. Axelrad, and W. Kober. A complete if software gps receiver: A tutorial about the details. In *Proceedings of ION GPS*. 2001.
- [104] A. Lakhzouri, E. S. Lohan and M. Renfors. Hybrid search single and double-dwell acquisition architectures for Galileo signal. In *Proceedings of IEEE IST Mobile and Wireless Communications Summit*. Lyon, France, Jun. 2004.
- [105] A. Lakhzouri, E. S. Lohan and M. Renfors. Reduced complexity time-domain correlation for acquisition and tracking of BOC-modulated signals. In *CDROM Proceedings of 1st ESA Workshop on Satellite Navigation User Equipment Technologies (NAVITEC)*. Dec. 2004.
- [106] A. Lakhzouri. *Channel estimation and mobile phone positioning in CDMA based wireless communications systems*. PhD thesis, Tampere University of Technology, Finland, Jun. 2005.
- [107] A. Lakhzouri, E. S. Lohan and I. Saastamoinen and M. Renfors. Measurement and characterization of satellite-to-indoor radio wave propagation channel. In *Proceedings of European Navigation Conference (ENC-GNSS 2005)*. München, Germany, Jul. 2005.
- [108] A. Lakhzouri, E. S. Lohan and I. Saastamoinen and M. Renfors. Interference and indoor channel propagation modeling based on GPS satellite

- signal measurements. In *Proceedings of ION-GPS*. pp. 896–901, Portland, OR, US, Sep. 2005.
- [109] M. Latva-aho. *Advanced receivers for wideband CDMA systems*. PhD thesis, University of Oulu, Finland, Oct. 1998.
- [110] M. Laxton. Analysis and simulation of a new code tracking loop for GPS multipath mitigation. *MSc thesis*, Air Force Institute of Technology, Dayton, OH, US, 1996.
- [111] S. Lee and J. Kim. Effects of multiple threshold values for PN code acquisition in DS-CDMA systems. In *Electronics Letters*, vol. 37, no. 6, pp. 363–365, Mar. 2001.
- [112] C. Lee, S. Yoo, S. Yoon and S. Y. Kim. A novel multipath mitigation scheme based on slope differential of correlator output for Galileo system. In *Proceedings of 8th International Conference on Advanced Communication Technology (ICACT)*, vol. 2, pp. 1360–1363, Feb. 2006.
- [113] Y. Li, J. Chen and Z. Li. A Second-Order-BPSK-like (SOB) Method for the Acquisition of BOC(1,1). In *Proceedings of the 20th International Technical Meeting of the Institute of Navigation Satellite Division (ION GNSS 2007)*, Sep. 2007, Texas, US.
- [114] A. Leick. *GPS satellite surveying*. 2nd edition, Wiley, 1995.
- [115] H. Li and R. Wang. Filter bank-Based Blind Code Synchronization for DS-CDMA Systems in Multipath Fading Channels. In *IEEE Transactions on Signal Processing*, vol. 51, no. 1, Jan. 2003.
- [116] V. S. Lin, P. A. Dafesh, A. Wu and C. R. Cahn. Study of the impact of the false lock points on subcarrier modulated ranging signals and recommended mitigation approaches. In *Proceedings of the 59th ION Annual Meeting and CIGTF Guidance Test Symposium*, pp. 156–165, Albuquerque, NM, US, Jun. 2005.
- [117] J. Liu and J. Li. An Efficient Code-Timing Estimator for DS-CDMA Systems over Resolvable Multipath Channels. In *EURASIP Journal on Applied Signal Processing*, vol. 5, pp. 670–682, 2005.
- [118] E. S. Lohan. *Multipath delay estimators for fading channels with applications in CDMA receivers and mobile positioning*. PhD thesis, Tampere University of Technology, Finland, Oct. 2003.

- [119] E. S. Lohan, A. Lakhzouri and M. Renfors. Selection of the multiple-dwell hybrid-search strategy for the acquisition of Galileo signals in fading channels. In *Proceedings of Personal and Indoor Mobile Radio Communications (PIMRC)*, vol. 4, pp. 2352–2356, Barcelona, Spain, Sep. 2004.
- [120] E. S. Lohan, R. Hamila, A. Lakhzouri and M. Renfors. Highly efficient techniques for mitigating the effects of multipath propagation in DS-SS-CDMA delay estimation. In *IEEE Transactions on Wireless Communications*, vol. 4, no. 1, pp. 149–162, Jan. 2005.
- [121] E. S. Lohan, A. Lakhzouri and M. Renfors. Spectral shaping of Galileo signals in the presence of frequency offsets and multipath channels. In *CDROM Proceedings of IST Mobile and Wireless Communications Summit*, Dresden, Germany, Jun. 2005.
- [122] E. S. Lohan. Statistical analysis of BPSK-like techniques for the acquisition of Galileo signals. In *CDROM Proceedings of 23rd AIAA/IEEE International Communications Satellite Systems Conference (ISCC)*, Rome, Italy, Sep. 2005.
- [123] E. S. Lohan. Filter-bank based technique for fast acquisition of Galileo and GPS signals. In *17th Annual IEEE International Symposium on Personal, Indoor and Mobile Radio Communications (PIMRC'06)*, Helsinki, Finland, Sep. 2006.
- [124] E. S. Lohan, A. Lakhzouri and M. Renfors. Feedforward delay estimators in adverse multipath propagation for Galileo and modernized GPS signals. In *EURASIP Journal on Applied Signal Processing*, Article ID 50971, 19 pages, 2006.
- [125] E. S. Lohan, A. Lakhzouri and M. Renfors. Binary offset carrier modulation techniques with applications in satellite navigation systems. In *Wiley Journal of Wireless Communications and Mobile Computing*, vol. 7, pp. 767–779, Jul. 2006.
- [126] E. S. Lohan, A. Lakhzouri and M. Renfors. Complex double-binary-offset-carrier modulation for a unitary characterisation of Galileo and GPS signals. In *IEEE Proceedings - Radar, Sonar and Navigation*, vol. 153, no. 5, pp. 403–408, Oct. 2006.
- [127] E. S. Lohan and M. Renfors. Correlation properties of Multiplexed Binary Offset Carrier (MBOC) modulation. In *Proceedings of 13th European Wireless Conference* Paris, France, Apr. 2007.

- [128] E. S. Lohan. Analysis of filter bank-based methods for fast serial acquisition of boc-modulated signals. in *EURASIP Journal on Wireless Communications and Networking*. vol. 2007, Art. ID 25178, doi:10.1155/2007/25178.
- [129] N. Martin, V. Leblond, G. Guillotel and V. Heiries. BOC(x,y) signal acquisition techniques and performances. In *Proceedings of Institute of Navigation ION GPS/GNSS*, pp. 188–198, Sep. 2003.
- [130] G. A. McGraw and M. S. Braasch. GNSS multipath mitigation using gated and high resolution correlator concepts. In *Proceedings of the National Technical Meeting of the Insitute of Navigation ION NTM*, pp. 333–342, San Diego, CA, US, Jan. 1999.
- [131] S. Mirabbasi and K. Martin. IIR Digital Filter for Delta-Sigma Decimation, Channel Selection, and Square-Root Raised-Cosine Nyquist Filtering. In *Proceedings of the 2002 IEEE International Solid-State Circuits Conference*, vol. 1, pp. 430–452, Feb. 2002.
- [132] R. Misra and P. Enge. *Global Positioning Systems: Signals, measurements and performance*. Ganga-Jamuna Press, 1st edition, 2001.
- [133] A. F. Molisch. *Wideband wireless digital communications*. Prentice Hall, 2000.
- [134] D. Morgan. A general characterization of lowpass FIR frequency response in the transition band. In *IEEE Transaction on Signal Processing*, vol. 43, Jun. 1995.
- [135] J. Z. Mou. Minimal structures for symmetric FIR filters of arbitrary length. In *IEEE Transaction on Signal Processing*, vol. 41, pp. 1790–1808, Jun. 1993.
- [136] M. Nakagami. The m-distribution - A General Formula of Intensity Distribution of Rapid Fading. In W.C. Hoffman, *Statistical Methods of Radio Wave Propagation*, pp. 3–36, Oxford, UK, 1960.
- [137] Navstar Global Positioning System. Interface Specification (IS-GPS-200) Revision D. Navstar GPS Space Segment/Navigation User Interfaces. Dec. 2004
- [138] M. O'Donnell, T. Watson, J. Fisher, D. Walsh and G. Brodin. Galileo Performance. GPS Interoperability and Discriminators for Urban and Indoor Environments. In *GPS World*, Jun. 2003.

- [139] T. Ojanperä and R. Prasad. *Wideband CDMA for third generation mobile communications*. Artech House Publishers, 1998.
- [140] E. Pajala. *Code-frequency acquisition algorithms for BOC modulated CDMA signals with Applications in Galileo and GPS Systems*. MSc thesis, Tampere University of Technology, Finland, Aug. 2005.
- [141] E. Pajala, E. S. Lohan and M. Renfors. On the choice of the parameters for fast hybrid-search acquisition architectures of GPS and Galileo signals. In *Proceedings of FWCW/NRS*, Oulu, Finland, Aug. 2004.
- [142] E. Pajala, E. S. Lohan, T. Huovinen and M. Renfors. Enhanced Differential Correlation Method for the Acquisition of Galileo Signals. In *Proceedings of 10th IEEE Singapore International Conference on Communication systems (ICCS'06)*, Singapore, Oct. 2006.
- [143] S. M. Pan, D. Madill and D. Dodds. A unified time-domain analysis of serial search with applications to spread spectrum receivers. In *IEEE Transaction of Communications*, vol. 43, no. 12, pp. 3046–3054, 1995.
- [144] T. Pany, B. Eissfeller and J. Winkel. Tracking of High Bandwidth GPS/Galileo Signals with a Low Sample Rate Software Receiver. In *Proceedings of GNSS*, Graz, 2002.
- [145] T. Pany and B. Eissfeller. Code and Phase Tracking of Generic PRN Signals with Sub-Nyquist Sample Rates. In *Journal of Navigation*, vol. 51, pp. 143–159, 2004.
- [146] T. Pany, S.W. Moon, M. Irsigler, B. Eissfeller and K. Furlinger. Performance Assessment of an Under Sampling SWC Receiver for Simulated High-Bandwidth GPS/Galileo Signals and Real Signals. In *Proceedings of ION GPS/GNSS 2003*, Portland, OR, US, Sep. 2003.
- [147] H.R. Park, Y. S. Yang, S. Sik. Performance analysis of the hybrid search code acquisition technique for cellular CDMA systems. In *IEEE International Conference on Communications Systems*, vol. 1, pp. 475–479, Nov. 2002.
- [148] T. W. Parks and C. S. Burrus. *Digital filter design*. Wiley-Interscience Publication, 1987.
- [149] B. W. Parkinson and J. J. Spilker. *Global Positioning System: Theory and Applications*. vol. 1: Progress in Astronautics and Aeronautics. American Institute of Aeronautics and Astronautics, 1996.

- [150] J. D. Parsons. *The mobile radio propagation channel*. Pentech Press Ltd, 1992.
- [151] R. L. Peterson, R. E. Ziemer and D. E. Borth. *Introduction to spread spectrum communications*. Prentice Hall, 1995.
- [152] R. E. Phelts and P. Enge. The Case for Narrowband Receivers. In *Proceedings of the National Technical Meeting of the Institute of Navigation (ION NTM)* pp. 511–520, Anaheim, CA, US, 2000.
- [153] A. Polydoros and C. L. Weber. A unified approach to serial search spread-spectrum code acquisition - Parts I: General Theory. In *IEEE Transactions on Communications*, vol. 32, no. 5, pp. 542–560, May 1984.
- [154] A. Polydoros and C. L. Weber. A unified approach to serial search spread-spectrum code acquisition - Parts II: A matched-filter receiver. In *IEEE Transactions on Communications*, vol. 32, no. 5, pp. 542–560, May 1984.
- [155] A. Polydoros and C. L. Weber. Generalized serial search code acquisition: The equivalent circular state diagram approach. In *IEEE Transactions on Communications*, vol. 32, no. 12, pp. 1260–1268, Dec. 1984.
- [156] G. J. Povey. Spread spectrum PN code acquisition using hybrid correlators architectures. In *Wireless Personal Communications*, vol. 8, pp. 151–164, 1998.
- [157] R. Prasad and M. Ruggieri. *Applied satellite navigation using GPS, Galileo and augmentation systems*. Artech House, 2005.
- [158] J. Proakis. *Digital communications*. McGraw-Hill, NY, 1995.
- [159] H. Puska. *Code Acquisition in Direct Sequence Spread Spectrum Systems using Smart Antennas*. PhD thesis, Faculty of Technology, Department of Electrical and Information Engineering, University of Oulu, Finland, Apr. 2009.
- [160] S. U. Qaisar, N. C. Shivaramaiah and A. G. Dempster. Exploiting the Spectrum Envelope for GPS L2C Signal Acquisition. In *CD Proceedings of European Navigation Conference GNSS 2008*. Apr. 2008, Toulouse, France.
- [161] S. H. Raghavan and J. K. Holmes. Modeling and simulation of mixed modulation formats for improved CDMA bandwidth efficiency. In *Proceedings of IEEE Vehicular Technology Conference (VTC)*. vol. 6, pp. 4290–4295, Sep. 2004.

- [162] S. H. Raghavan and J. Jameson. Bandwidth Criteria for GNSS Signals - Impact on Code Tracking Performance. In *CDROM Proceedings of 23rd AIAA International Communications Satellite Systems Conference (ICSSC)*. Sep. 2005.
- [163] T. S. Rappaport. *Wireless communications: principles and practice*. Prentice Hall, 1996.
- [164] J. Ray. *Mitigation of GPS code and carrier phase multipath effects using an multi-antenna system*. PhD thesis, University of Calgary, Canada, Mar. 2000.
- [165] K. Ravi and R. Ormondroyd. Simulation performance of a quantized log-likelihood sequential detector for PN code acquisition in the presence of data modulation and doppler shift. In *IEEE Military Communications Conference*, vol. 2, pp. 798–803, Nov. 1991.
- [166] E. Rebeyrol, C. Macabiau, L. Lestarquit, L. Ries and J. L. Issler. BOC power spectrum densities. In *CDROM Proceedings of ION National Technical Meeting*, San Diego, CA, US, Jan. 2005.
- [167] E. Rebeyrol, O. Julien, C. Macabiau, L. Ries, A. Delatour and L. Lestarquit. Galileo civil signal modulations. In *Springer Link GPS Solutions Journal*, vol. 11, no. 3, pp. 159-171, Jul. 2007.
- [168] S. Revnivykh. GLONASS Status Update. 46-th CGSIC Meeting, Fort Worth, TX, US, Sep. 2006 Available via http://www.fig.net/pub/fig2006/ppt/ts55/ts55_02_revnivykh_ppt_0995.pdf,
- [169] L. Ries, F. Legrand, L. Lestarquit, W. Vigneau and J. Issler. Tracking and multipath performance assessments of BOC signals using an bit-level signal processing simulator. In *Proceedings of ION GPS Meeting*, pp. 1996–2009, Portland, OR, US, Sep. 2003.
- [170] T. Ristaniemi and J. Joutsensalo. Code timing acquisition for DS-CDMA in fading channels by differential correlations. In *IEEE Transactions on Communications*, vol. 49, no. 5, pp. 899–910, May 2001.
- [171] M. F. Samad and E. S. Lohan. MBOC Performance in Unambiguous Acquisition. In *CDROM Proceedings of ENC-GNSS 2009*, 3-6 May 2009, Naples, Italy.
- [172] T. Saramäki, Y. Neuvo and S. K. Mitra. Design of computationally efficient interpolated FIR filters. In *IEEE Transactions on Circuits and Systems*, vol. 35, no. 1, pp. 70–88, Jan. 1988.

- [173] A. Schmid and A. Neubauer. Differential correlation for Galileo/GPS receivers. In *Proceedings of IEEE International Conference on Acoustics, Speech and Signal Processing (ICASSP)*, vol. 3, pp. 953–956, Mar. 2005.
- [174] J. Selva. *Efficient multipath mitigation in navigation systems*. PhD thesis, Department of Signal Theory and Communications, Universitat Politècnica de Catalunya, Spain, 2004.
- [175] O. S. Shin and K. B. Lee. Differentially Coherent Combining for Double-Dwell Code Acquisition in DS-CDMA Systems, In *IEEE Transaction on Communications*, vol. 51, no. 7, Jul. 2003.
- [176] N. C. Shivaramaiah and A. G. Dempster. An Analysis of Galileo E5 Signal Acquisition Strategies, In *Proceedings of European Navigation Conference ENC-GNSS '08*, Toulouse, France, Apr. 2008.
- [177] N. C. Shivaramaiah and A. G. Dempster. Galileo E5 Signal Acquisition Strategies, In *Coordinates Magazine on Positioning, Navigation and Associated Technologies*, Aug. 2008, pp. 12–16.
- [178] M. K. Simon and M. S. Alouini. *Digital communication over fading channels*, John Wiley and Sons, 2000.
- [179] M. K. Simon, J. K. Omura, R. A. Scholtz and B. K. Levitt. *Spread spectrum communication handbook*. McGraw-Hill Inc, NY, revised edition, 1994.
- [180] J. M. Sleewaegen, W. De Wilde and M. Hollreiser. Galileo AltBOC receiver. In *Proceedings of the European Navigation Conference GNSS*. 2004.
- [181] E. A. Sourour and S. C. Gupta. Direct-sequence spread-spectrum parallel acquisition in a fading mobile channel. *IEEE Transactions on Communications*, vol. 38, no. 7, pp.992–998, Jul. 1990.
- [182] E. A. Sourour and S. C. Gupta. Direct-sequence spread-spectrum parallel acquisition in nonselective and frequency-selective Rician fading channels. *IEEE Journal on Selected Areas in Communications*, vol. 10, no. 3, pp. 535–544, Apr. 1992.
- [183] C. L. Spillard, S. M. Spangenberg and G. J.R. Povey. A serial-parallel FFT correlator for PN code acquisition from LEO satellites. In *IEEE International Symposium on Spread Spectrum Techniques and Applications*, vol. 2, pp. 446–448, 1998.
- [184] M. Srinivasan, D. V. Sarwate. Simple schemes for parallel acquisition of spreading sequences in DS/SS systems. In *IEEE Transactions on Vehicular Technology*, vol. 45, no. 3, pp.593–598, 1996.

- [185] T. Stansell, J. Maenpa. ClearTrack - optimized GPS receiver technology. Optimized L2 Tracking. True Multipath Mitigation. Interference Protection. Future Signal Compatibility. *Leica document*, Mar. 1999.
- [186] T. Stansell, P. Fenton, L. Garin, R. Hatch, J. Knight, D. Rowitch, L. Sheynblat, A. Stratton, J. Studenny and L. Weill. BOC or MBOC ? The common GPS/Galileo Civil Signal Design. A manufacturers dialog. Parts I and II. In *Inside GNSS Magazine*, vol. 1, no. 5 and 6 Jul./Aug., Sep. 2006.
- [187] J. Thor and D. Akos. A direct RF sampling multifrequency GPS receiver. In *IEEE Position Location and Navigation Symposium*, pp. 44–51, Apr. 2002.
- [188] B. R. Townsend and P. C. Fenton. A Practical Approach to the Reduction of Pseudorange Multipath Errors in a L1 GPS Receiver. In *Institute of Navigation GPS 1994*, Salt Lake City, UT, US, Sep. 1994.
- [189] B. R. Townsend, R. D.J. Van Nee , P. C. Fenton and D. J.V. Dierendonck. Performance evaluation of the multipath estimating delay lock loop. In *Institute of Navigation National Technical Meeting*, Anaheim, CA, Jan. 1995.
- [190] B. R. Townsend, P. C. Fenton, D. J.V. Dierendonck and R. D.J. Van Nee. L1 Carrier Phase Multipath Error Reduction Using MEDLL Technology. In *Proceedings of 8th International Technical Meeting of the Satellite Division of the Insitute of Navigation*, vol. 1, Palm Springs, CA, US, Sep. 1995.
- [191] United Kingdom Parliament. House of Commons. Transport Committee. Galileo: Recent Developments. First Report of Session 2007-08. Available via <http://www.publications.parliament.uk/pa/cm200708/cmselect/cmtran/53/53.pdf>.
- [192] U. S. Department of Defense. *Global Positioning System Standard Positioning Service Performance Standard*. Oct. 2001.
- [193] A. J. Van Dierendonck, P. C. Fenton and T. Ford. Theory and performance of narrow correlator spacing in a GPS receiver. In *Journal of Institute of Navigation*, vol. 39, no. 3, pp. 265–283, 1992.
- [194] A. J. Van Dierendonck and M. Braasch. Evaluation of GNSS receiver correlation processing techniques for multipath and noise mitigation. In *Proceedings of the National Technical Meeting of the Institute of Navigation (ION NTM)*, pp. 207–215, Santa Monica, CA, US, Jan. 1997.

- [195] R.D.J. Van Nee. The Multipath Estimating Delay Lock Loop. In *Proceedings of IEEE Second International Symposium on Spread Spectrum Techniques and Applications*, pp. 39–42, Yokohama, Japan, Nov. 29 - Dec. 02, 1992.
- [196] R.D.J. Van Nee. *Multipath and multi-transmitter interference in spread-spectrum communication and navigation systems*. PhD thesis, Delft University, 1995.
- [197] R.D.J. Van Nee, J. Sierveld, P. C. Fenton and B. R. Townsend. The Multipath Estimating Delay Lock Loop: Approaching Theoretical Accuracy Limits. In *Proceedings of IEEE Position Location and Navigation Symposium*, vol. 1, pp. 246–251, Las Vegas, Nevada, Apr. 1994.
- [198] R. D.J. Van Nee. Method of Estimating a Line of Sight Signal Propagation Time Using a Reduced Multipath Correlation Function. *US Patent no. 5615232*, Mar. 1997.
- [199] A. J. Viterbi. *CDMA: Principles of Spread Spectrum Communication*. Addison-Wesley, 1995.
- [200] H. C. Wang and W. H. Sheen. Variable dwell-time code acquisition for direct-sequence spread-spectrum systems on time-variant Rayleigh fading channels. In *IEEE Transactions on Communications*, vol. 48, no. 6, pp. 1037–1046, Jun. 2000.
- [201] P. Ward. A Design Technique to Remove the Correlation Ambiguity in Binary Offset Carrier (BOC) Spread Spectrum Signals. In *Proceedings of the US Institute of Navigation NTM Conference*, pp. 886–896, San Diego, CA, Jan. 2004.
- [202] L. R. Weill. Multipath mitigation: How good can it get with new signals ? In *GPS World*, vol. 16, no. 6, pp. 106–113, 2003.
- [203] J. Wu and A. G. Dempester. Galileo GIOVE-A Acquisition and Tracking Analysis with a New Unambiguous Discriminator. In *Proceedings of International Global Navigation Satellite Systems Society IGNSS Symposium '07*, Sydney, Australia, Dec. 2007.
- [204] C. Yang. FFT Acquisition of Periodic, Aperiodic, Puncture and Overlaid Code Sequences in GPS. In *Proceedings of ION GPS Meeting*, pp. 137–146, 2001.
- [205] L. Yang and X. XiaoLi. Combining FFT and Circular Convolution Method for High Dynamic GPS Signal Acquisition. In *Proceedings of IEEE*

Eighth International Conference on Electronic Measurement and Instruments (ICEMI Š07), vol. 2, pp. 159–162, 2007.

- [206] L. Yang, C. Jiapin, L. Zhenbo and C. Nongji. A Second Order BPSK-like (SOB) Method for the Acquisition of BOC(1,1). In *Proceedings of ION GNSS 2007*, Texas, Sept. 25-28, 2007.
- [207] J. Yli-Kaakinen. *Optimization of Digital Filters for Practical Implementations*. PhD Thesis, Tampere University of Technology, Jun., 2002.
- [208] W. Yu, B. Zheng, R. Watson and G. Lachapelle. Differential combining for acquiring weak GPS signals. In *Science Direct, Signal Processing*, vol. 87, issue 5, pp. 824–840, May 2007.
- [209] W. Zhuang. Noncoherent hybrid parallel PN code acquisition for CDMA mobile communications. *IEEE Transactions on Vehicular Technology*, vol. 45, no. 4, pp. 643–656, Nov. 1996.
- [210] Z. Zhu, F. Van Graas and J. Starzyk . GPS signal acquisition using the repeatability of successive code phase measurements. *Springer-Verlag*, DOI 10.1007, Apr. 2007.
- [211] N. I. Ziedan. *GNSS Receivers for Weak Signals*. Artech House, 2006.